INTENSITY MEASUREMENTS OF THE LYMAN-BIRGE-HOPFIELD SYSTEM OF NITROGEN

by

Donald James McEwen

Submitted in partial fulfillment

of the requirements for the degree of

Doctor of Philosophy

Faculty of Graduate Studies

The University of Western Ontario

London, Canada

1965

INTENSITY MEASUREMENTS OF THE LYMAN-BIRGE-HOPFIELD SYSTEM OF NITROGEN

by

Donald James McEwen

Submitted in partial fulfillment
of the requirements for the degree of
Doctor of Philosophy

Faculty of Graduate Studies
The University of Western Ontario
London, Canada

1965

Approved for the

Department of Physics

by the Advisory Committee

R W Nichols

P J Fraunfelder

H S Ferguson

Approved for the

Department of Physics

by the Examining Committee

[illegible]

[illegible]

Pete A. Franken

Date: 5 March 1965

ABSTRACT

The current interest in the vacuum ultraviolet radiation emitted by the sun, the aurora and other sources has shown the need for development of techniques for measuring radiation intensities and for laboratory measurements of band intensities of molecular band systems in this spectral region. The present work is directed towards this end.

Studies of the Lyman-Birge-Hopfield system of N_2 and the Fourth Positive system of CO, excited in laboratory discharges, are made and a number of new bands reported. Modifications to the vacuum spectrograph to permit photoelectric recording are described and a number of methods of calibrating the instrument are investigated. Using a combination of techniques the spectral sensitivity of the instrument is determined over the region 1000 to 3000 A.

This instrument is used to measure the relative intensities of bands of the Lyman-Birge-Hopfield system. The results show that the electronic transition moment is constant over the band system. The band strengths are thus directly proportional to the calculated Franck-Condon factors for the system.

ACKNOWLEDGEMENTS

The author expresses his appreciation to Dr. P. A. Forsyth, Head of the Department of Physics, for making available the facilities of the department.

The author conveys his thanks to Dr. R. W. Nicholls for his supervision and encouragement. Thanks are also extended to Dr. H. I. S. Ferguson and Dr. P. A. Fraser for helpful discussions.

The assistance of Mr. V. Sells in operating the microtron and providing an electron beam for Cerenkov radiation studies is gratefully acknowledged.

The assistance of the technical staff of the Physics Department is acknowledged. The careful work of Mr. J. Radema in the preparation of diagrams and Mr. T. Davidson in providing photographs is much appreciated.

The generosity of the Defence Research Board in granting the author educational leave for the entire period of study at the University of Western Ontario is gratefully acknowledged.

This research has been supported by a research contract from the Department of Defence Production, and by research grants from the National Research Council of Canada, the National Aeronautics and

N5G -

Space Administration (N5G-349), the United States Air Force Office of Scientific Research (AF-AFOSR62-236) and the United States Air Force Cambridge Research Center (AF 19(628)-2820). This support is gratefully acknowledged.

TABLE OF CONTENTS

LIST OF FIGURES

LIST OF TABLES

CHAPTER I

INTRODUCTION

1.1 Historical Review

Investigations of the region of the spectrum below 2000 Angstroms began nearly a century ago, largely as a result of the contributions of Victor Schumann in the course of his researches from 1885 to 1903. First realizing that quartz ceased to transmit below about 2000 Angstoms, he began using fluorite for prisms and lenses and thus was able to record spectra down to 1820 A. He soon discovered that the gelatine normally used in photographic emulsions strongly absorbed ultraviolet radiation, and developed the Schumann plate containing almost no gelatine and sensitive all the way through the extreme ultraviolet. These were of such a high quality that it is only very recently that they have been improved upon.

Schumann recognized also that air appeared to become opaque below about 1850 A and thus constructed the first vacuum spectrograph. With this spectrograph he was able to photograph the spectrum from a hydrogen discharge tube down to 1267 A. It is due to the opacity of air that the region of the ultraviolet spectrum below 2000 Angstroms has since become known as the vacuum ultraviolet.

Lyman (1928), another pioneer in the field of ultraviolet spectroscopy, began his researches in the extreme ultraviolet about the end of Schumann's period of productivity. He recognized the value of concave gratings (first built by Rowland in 1882) and used one to build the first vacuum grating spectrograph in 1904. With this spectrograph he discovered in 1914 the hydrogen series which now bears his name and provided confirmation of the Bohr theory of the atom, enunciated one year before. Continuing his work with helium, Lyman discovered the principal series of HeI converging to a series limit at 504 A.

This lower limit was extended through the use of a vacuum spark as a light source thus exciting materials to high degrees of ionization, and spectral lines were observed to below 200 A. The region between this and X-ray wavelengths was investigated by Osgood (1927) who built the first grazing incidence concave grating spectrograph and photographed atomic lines down to 44 A.

During the next two decades considerable definitive work was done in the study of line spectra and molecular spectra both in emission and absorption. Various continuous sources were developed by means of which much quantitative absorption spectroscopy was begun. Investigation of optical properties of solids in the vacuum ultraviolet was initiated as well as photoelectric and photoionization effects.

Excellent reviews of this period of the beginning and the development of vacuum ultraviolet spectroscopy are given by Boyce (1941), Price (1951) and Tousey (1961, 1962).

A strong hint of the scope of ultraviolet spectroscopy and the impact it was to have upon other fields such as astronomy, astrophysics and plasma physics was given by the work of Edlén (1942), who showed that the corona of the sun is at a temperature of the order of one million degrees. This evidence was obtained by identification of a coronal emission line which Edlén showed was produced from Fe XIV. A temperature of the above magnitude is required to produce atoms in such a high degree of ionization.

This raised questions concerning the nature of the mechanism producing such a high temperature, the ultraviolet spectrum of the sun, and the photochemical processes going on in planetary atmospheres under the influence of such radiation. A large number of workers became actively engaged in studies of the extreme ultraviolet spectrum of the sun in 1946 when a number of captured V-2 rockets became available for scientific research.

The first ultraviolet spectrum obtained from a rocket borne spectrograph was reported by Baum et al (1946). In the ensuing years steadily improving instrumentation and techniques have permitted the recording of the sun's spectrum with high resolution both photographically and photoelectrically down to below 200 A. The vast amount of information obtained is reviewed by Tousey (1962), one of the foremost workers in the field.

Research programs involving studies of the solar ultraviolet spectrum have provided a great stimulus to vacuum ultraviolet spectroscopy in general. Firstly, the great improvements in instrumentation

and vacuum techniques have made experiment much simpler and secondly the information obtained as well as the technological advances in rocketry has aroused interest in a number of associated fields, all of which require greater knowledge of the extreme ultraviolet region of the spectrum. Some of these fields include physics of the aurora and airglow, studies of other planetary atmospheres, studies of high-temperature plasmas, and solid state phenomena.

1.2 Molecular Band Intensities

While much of the above review has dealt specifically with atomic spectra, considerable new data on molecular spectra have been obtained, especially since 1950. With the building of larger spectrographs and the use of higher diffraction orders it has been possible to resolve rotational structure of diatomic molecular bands; a large number of monochromators employing photoelectric detection have been built and have contributed greatly to intensity studies of molecular spectra.

To date these intensity measurements have been a result of absorption spectra where the chief requirements are a stable continuous source and a detector whose response is proportional to intensity. Because of a lack of intensity standards it has so far been impossible to measure either relative or absolute intensities of atomic or molecular emission spectra extending over any appreciable portion of the ultraviolet spectrum with any degree of accuracy or reliability. Considerable effort is being directed towards the development of intensity standards which have either a reproducible or a calculable spectral output and which thus can provide means of calibrating ultraviolet spectrographs

for measurement of intensities. As rocket and satellite spectroscopy progress spectral features observed from many astrophysical sources will require identification and intensity measurements and it is therefore important that intensity distributions of the predominant systems of the more abundant gases be known, especially those present in our own atmosphere.

One such important system is the Lyman-Birge-Hopfield ($a^1\Pi_g - X^1\Sigma_g^+$) system of nitrogen which extends roughly from 2600 Angstroms down to 1200 Angstroms. It was first identified by Birge and Hopfield (1928) and has since been studied under high resolution by Loftus (1956) and Wilkinson (1957). The only intensities available have been eye estimates of density of photographic spectra. It has recently (Crosswhite et al, 1962) been observed in rocket spectra of the aurora and appears to be a major component of the auroral spectrum in the vacuum ultraviolet.

It was considered worthwhile therefore to attempt to measure the relative intensities of the bands of the Lyman-Birge-Hopfield system of N_2 when excited in laboratory sources and this was the objective of the present research. The work of this thesis has involved the development of equipment for exciting and recording the spectra, the development of methods for obtaining intensity calibrations in the vacuum ultraviolet region, and finally the intensity measurements themselves and their interpretation.

CHAPTER II

INSTRUMENTATION

2.1 Introduction

Studies in the extreme ultraviolet require special types of spectrographs and the use of uncommon experimental techniques. The increasing opacity of air below 2000 Angstroms, due to absorption by its various constituents, makes it essential that the spectrograph be operated at a very low pressure; the maximum pressure permissible naturally depends on the type of measurement being made and on the length of light path but is in general considerably less than 10^{-3} mm Hg.

Spectrograph mounts employing a concave reflecting grating as the only optical element have been used almost exclusively to avoid light losses. There are two mounts of this type, the Paschen mount and the Eagle mount. Large spectrographs of the Eagle type have been described by Wilkinson (1957a) and Douglas and Potter (1962). Recently with development of techniques for making surfaces with high reflectivities it has become possible to consider the use of plane gratings, such as in the Ebert mounting, at least down to wavelengths of 1000 Angstroms.

Emulsions containing almost no gelatine, of the Schumann type, are normally used for recording spectra photographically. Great improvements in manufacturing, resulting in much improved sensitivity, have been brought about recently. While plates are excellent for qualitative studies, wavelength measurements and identifications, it is difficult to measure intensities from photographic spectra. Photoelectric detectors of various types have been developed recently and possess advantages in certain types of work.

In the following sections the vacuum spectrograph and associated equipment and materials used in this research are described. This is followed by a description of a photoelectric attachment and a scanning system which were added to the spectrograph, and a discussion of general performance of the instrument.

2.2 Spectrograph

The spectrograph is a Hilger 3 meter normal incidence vacuum spectrograph with a nominal spectral range of 3000 Angstroms. An external view of the instrument is shown in Figure 2.1. It is an in-plane Eagle type mount with the entrance slit, grating, and plate holder on the Rowland circle. The optical and mechanical configuration are shown in Figure 2.2.

A single external control operates the wavelength change by means of a link mechanism between the grating mount and the plate holder. The plate holder pivots around a vertical axis through the entrance slit which is fixed. Two arms (radii of the Rowland circle), one from the slit mount and the other from the grating mount, are linked at

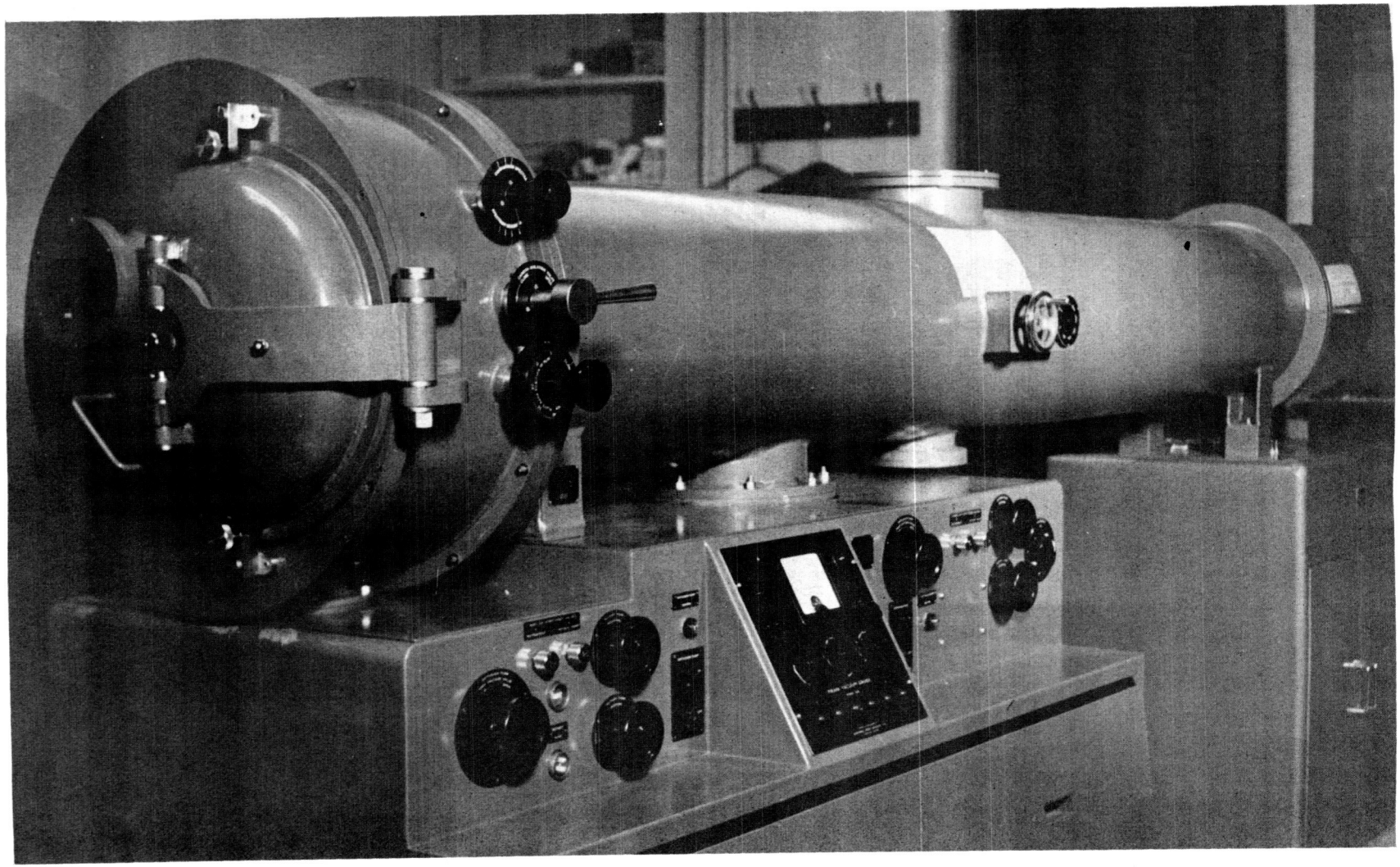

Figure 2.1

Figure 2.1 External View of Three Meter Vacuum Spectrograph

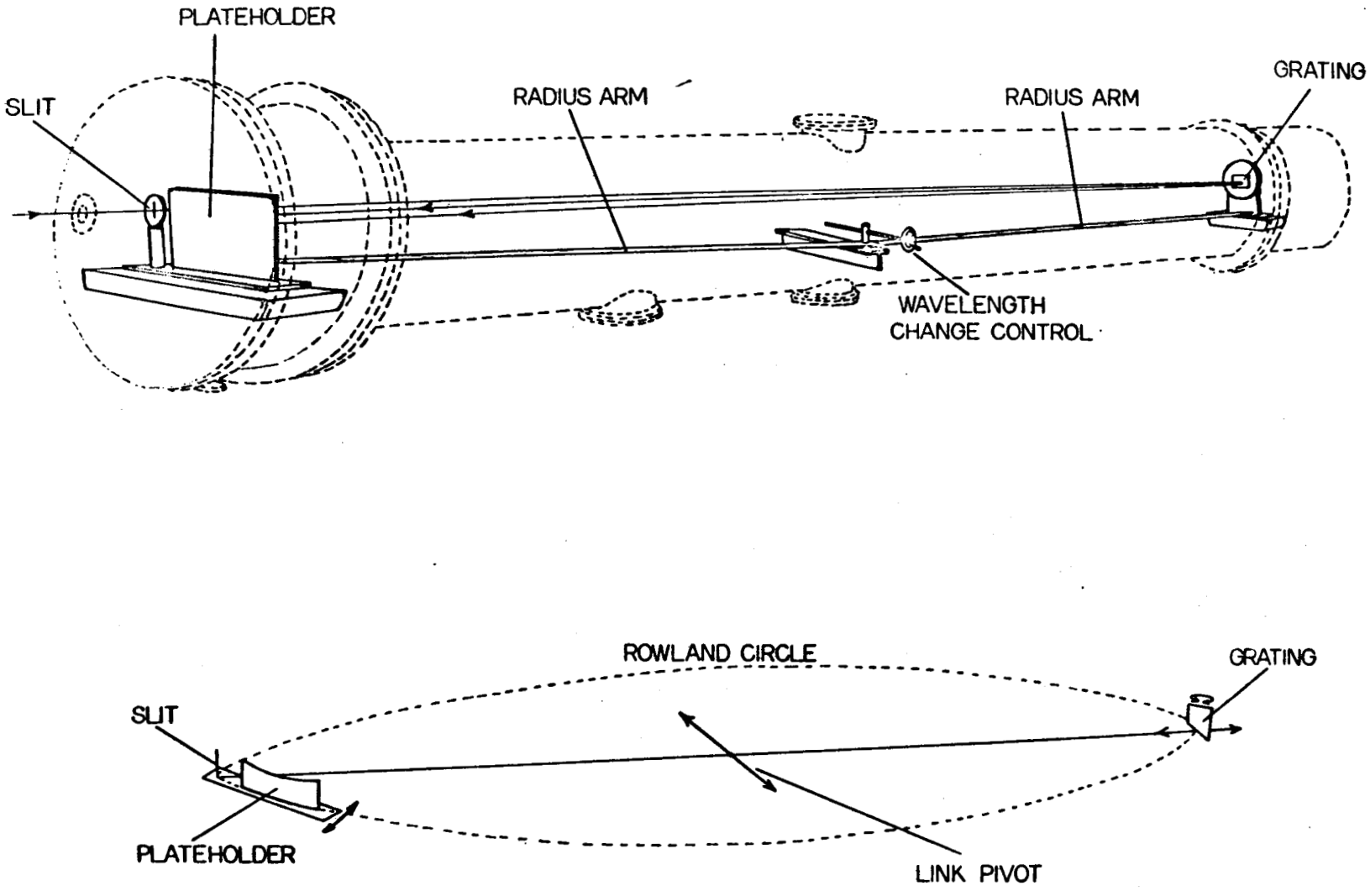

FIGURE 2-2 THREE METER VACUUM SPECTROGRAPH

their free ends by a pivot. The lateral movement (controlled by a screw) of this pivot causes wavelength change by moving the plateholder and grating. As they move, they both rotate slightly so as to remain on the circle; in addition the grating movement is constrained so that the mid-point of the grating surface can move only along the principal axis of the incident radiation. In this way correct conditions for focus are always maintained.

The grating is ruled aluminum on glass with a spacing of 14,600 lines per inch. The glass blank is circular, 11.43 cm in diameter and 1.27 cm thick. It is held in its cell by a retaining flange which is screwed down to the grating cell. A three-leaf spring in the cell behind the grating holds the grating against the retaining flange with enough pressure to prevent its shaking in the cell. The grating has a ruled area of 8 x 4 cm and is concave with a radius of curvature of 3 metres. The theoretical resolving power is thus 46,000 and the reciprocal dispersion is about 5.8 A/mm in first order.

The plateholder takes 2 x 10 inch plates. Two external controls determine the position and height of the spectrum recorded on the plate. The first racks the plateholder up or down to allow successive spectra to be taken on the same plate. The second operates a metal plate in front of the plateholder to mask the photographic plate, thus allowing successive spectra to be taken one above the other without moving the photographic plate, and controlling the height of the spectrum photographed between 1 mm and 4 mm.

A flap valve in front of the plateholder permits the camera compartment to be sealed off, so that the end cover can be opened without

the main vacuum being lost. This feature greatly facilitates the changing of plates or of spectral sources, since it requires only that the small volume of air in the camera compartment be evacuated before the valve is opened again.

2.3 Vacuum System for Spectrograph

The vacuum system and controls are shown schematically in Figure 2.3. There are two independent pumping systems - one for the main body of the spectrograph, and a smaller one for the camera compartment. Specifications are as follows:

Backing pumps (single stage)

(Speedivac) 1SC150 - 1/3 hp motor, 144 litres/min displacement.
1SC450 - 1 hp motor, 450 litres/min displacement.

Diffusion pumps (three stage) - with silicone oil

(Speedivac) F203 - 350 watt heater, speed 50 litres/sec.
F603 - 1300 watt heater, speed 300 litres/sec.

The diffusion pumps are each provided with a thermal switch. This protects the pump against damage in the event that the water cooling fails. Magnetic valves are located in the vacuum lines between each backing pump and the spectrograph proper thus precluding the possibility of any pump fluid backing up in the vacuum lines in the event of a power failure. All starter switches are of the reset type which require manual resetting in case of any power interruption. It is thus seen that the spectrograph and vacuum system are adequately protected against any possible damage resulting from interruption of either power or water.

As indicated in Figure 2.3, the diffusion pumps are both hung on the spectrograph while the mechanical pumps are connected by flexible

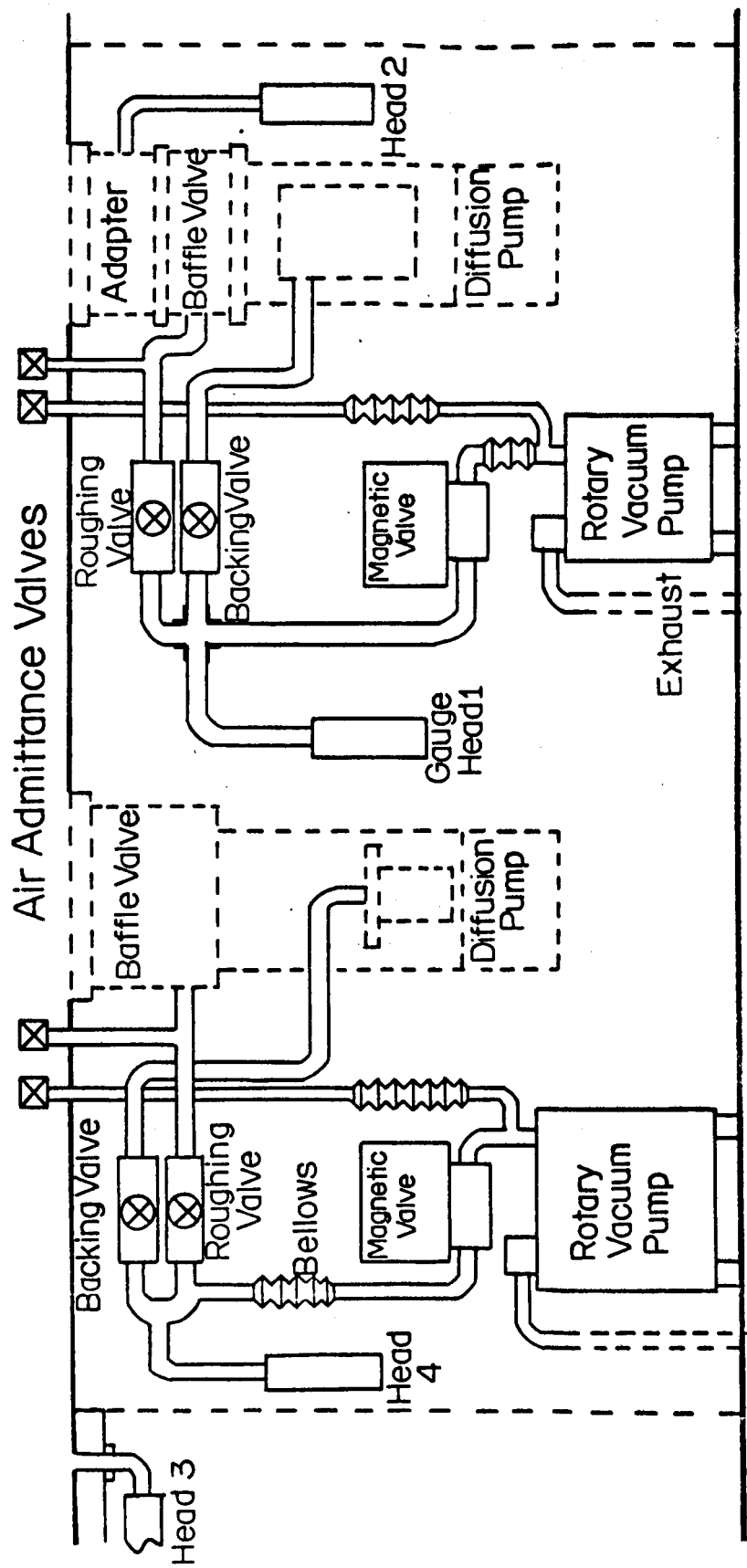

Figure 2.3 Schematic Diagram of Vacuum System

bellows. In addition the backing pumps are supported on anti-vibration mounting feet. These two features are intended to minimize possible vibration of the spectrograph due to the operation of the mechanical pumps.

The instrument is fitted with four Pirani type pressure gauge heads, one connected ahead of each backing pump, one to the camera compartment, and one to the main instrument body. These allow the measurement of pressure in the range of 1 to 10^{-4} mm Hg.

The spectrograph entrance slit is connected to the front plate of the spectrograph by means of a bellows. There are also adjustable baffle slits located both in front and behind the main slit. These features impede the flow of gases from the light source into the spectrograph when there is no window between. The front plate is machine faced to allow the fixing of spectral sources directly on the front of the spectrograph, making a vacuum tight connection by means of an O-ring.

2.4 Windows for the Vacuum Ultraviolet

It is advantageous to use a window to separate the spectral source from the spectrograph whenever possible. It avoids possible damage to the slit and the grating by particle bombardment or discharge products, and it allows the spectrograph to be kept at a lower pressure thus avoiding possible errors due to absorption.

There are few materials which will transmit light below 2000 **A**. One such material is lithium fluoride which has good transmission down to about 1200 **A**. Its surface and transmission properties however are

very adversely affected by both ultraviolet radiation and electron bombardment. Thus it is necessary either to clean and polish the windows periodically or to replace them regularly with new ones. The possibility of obtaining LiF crystals and making windows locally was considered due to the high cost of purchasing windows commercially. A further advantage was that cleaved crystals are reputed to have better transmission properties than polished windows.

Lithium fluoride crystals are vacuum grown by Harshaw Chemical Company. They can be cleaved in any desired plane to make windows because of the cubic nature of the lithium fluoride lattice. The optical crystals are usually mechanically so soft that they suffer plastic deformation and tend to split on more than one plane. This results in a non-uniform surface which will not allow a good vacuum seal.

A technique developed by Nadeau and Johnston (1963) was used to harden the LiF crystal to permit cleaving of thin flat windows. The LiF was hardened by irradiating it with Co^{60} gamma rays for approximately 48 hours. This resulted in a hardened crystal which was easily cleaved with a knife edge and hammer to produce windows of any desired thickness, without introducing any new dislocations or slip planes. The windows, which had turned a yellowish colour when irradiated, were returned to their normal condition by annealing them in an oven at $450^{o}C$ for two hours.

The results were very gratifying in that windows with better transmission properties than those commercially available were obtained,

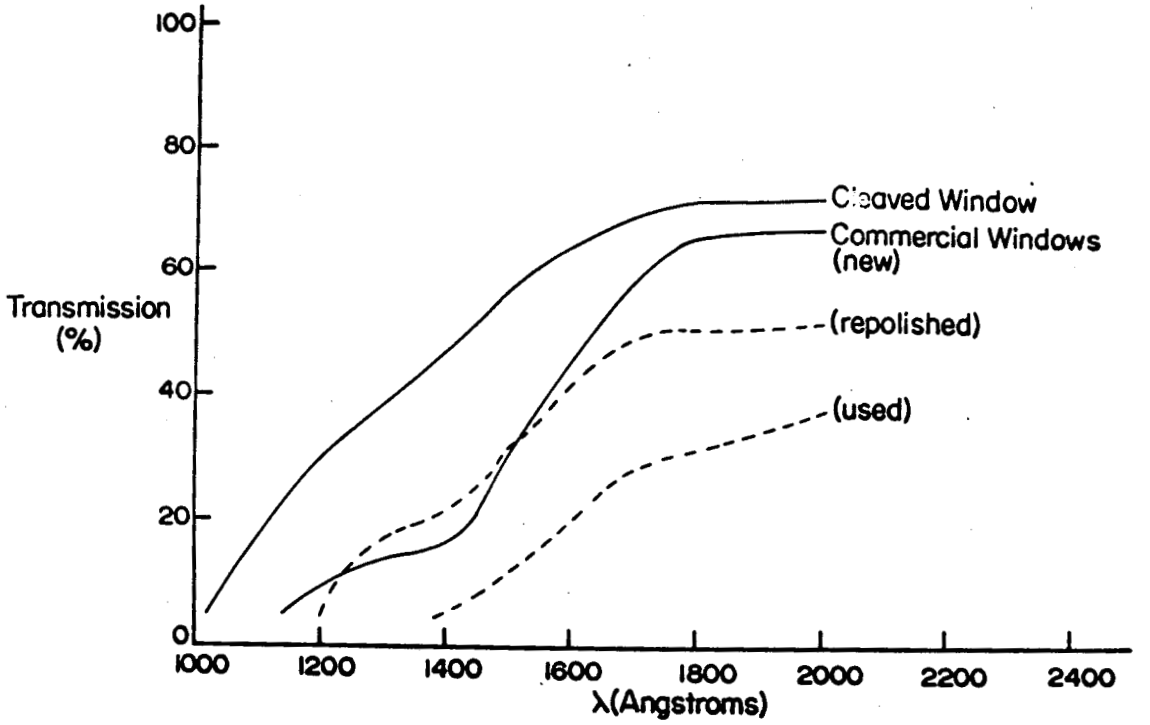

Figure 2-4 Transmission Properties of Lithium Fluoride Windows

and at a very nominal cost, by use of this method. Transmission characteristics of four LiF windows are illustrated in Figure 2.4. They include a thin cleaved window, an unused commercial window, and two commercial windows which had deteriorated through use. One of the latter was repolished with jewellers' rouge. These characteristics are not necessarily typical but are meant to show the wide variation in transmission of windows of various types and condition. Another significant point, noted by Patterson and Vaughan (1963), is that window transmission deteriorates with time after cleavage due to surface effects upon exposure to air. It is evident that the transmission properties of any window used between source and detector must be accurately known when making any intensity measurements.

2.5 Photographic Emulsions for the Vacuum Ultraviolet

The ordinary types of emulsions are of little value below about 2300 A since the gelatin strongly absorbs shorter wavelengths. For many years emulsions of the type developed by Schumann (1893) containing a large amount of silver halide and a minimum of gelatin have been the best material for use in the vacuum ultraviolet. In recent years however there have been marked improvements in methods of manufacture to meet the increasing demands of spectroscopists.

There are now three distinctly different types of plates readily available - Kodak 103-0 UV sensitized plates, Kodak SWR plates, and Ilford Q plates. In addition there are two emulsions, SC-5 and SC-7, which have been developed recently by Kodak Pathé (Paris). They are still at an experimental stage and are not yet readily available. The choice of plates is in general largely determined by the type of spectra being recorded and the specific spectral region of the ultraviolet. It is of value to outline briefly the particular qualities of the various types of plates and some points pertaining to their proper use.

A very useful and reliable plate is obtained by coating a Kodak 103-0 plate with Kodak ultraviolet sensitizer, a fluorescing material. This is done by dissolving the sensitizer in cyclohexane and coating the emulsion with a thin layer of the solution. After exposure it must be rinsed in cyclohexane and thoroughly dried before developing. This treatment is necessary to remove the sensitized overcoat so that the emulsion develops properly. The plate can then be developed in a

normal way. There is no indication of deterioration of sensitized plates hence they can be sensitized in quantity and stored, at least for a reasonable period, before use.

Kodak Short Wave Radiation emulsion (abbreviated SWR) was developed about 1950 initially on a film base but is now available in plate form. This emulsion is very sensitive to abrasion and must be handled with care. There are variations in quality from plate to plate, but the emulsion has high sensitivity and resolution. It requires a development time of two minutes in developer diluted 1:1. Even slight over-development may cause fogging.

Ilford Q plates have been available for some years. They contain an intermediate amount of gelatin, but have a high density of silver bromide grains at the top of the emulsion. They are commercially available in three grades, Q_1, Q_2 and Q_3, listed in order of increasing speed and grain size. A development time of two minutes with similarly reduced fixing and washing times is recommended.

Schoen and Hodge (1950) have found an increase in sensitivity of the SWR emulsion over 103-0 UV sensitized emulsion below about 1500 A, and markedly superior below 1000 A. Ilford emulsions appear somewhat less sensitive than either of the others. The SWR plates have a much higher contrast than is usually desirable, while Ilford plates show low contrast. The SWR plates are capable of resolving more than 100 lines per millimeter and in this respect are somewhat superior to the other plates; excellent resolution is obtained with Q_1 and Q_2 Ilford plates, but this is at the expense of sensitivity. The new SC-7 emulsion is reported by Madden (1964) to have rather similar characteristics

to SWR emulsion but is more than 10 times as sensitive at 200 A and markedly faster through the spectral range below 600 A.

It has been found in this work that SWR plates are ideal for survey work, identification of spectral features, wavelength measurements and recording of atomic spectra, where high contrast and sensitivity are advantageous. The UV sensitized plates are somewhat more suitable for recording of molecular spectra since they have a more reasonable contrast. Ilford plates may be preferred when quality and uniformity of emulsion rather than speed is important. The combination of low light gathering power and poor spectrograph efficiency in most vacuum instruments, and certainly in the present instrument, dictate speed as an important factor however, and for this reason Kodak SWR and 103-0 UV sensitized plates were used almost exclusively.

2.6 Photoelectric Detection

The use of photographic emulsions for the measurement of intensities requires that a standard source be available for determining the spectral response and the characteristic curve of the emulsion. The lack of such a source in the vacuum ultraviolet makes photographic plates of little value for making accurate intensity measurements in the ultraviolet.

The quantum efficiency of photographic emulsions has been estimated by Fellgett (1958) at somewhat less than 1% even for optimum exposure, and much less (because of reciprocity failure) for long exposures. Photocells are now readily available with quantum efficiencies of 20-30%. The photocathodes have a high photoelectric efficiency in the ultraviolet and are available with quartz windows. Photomultipliers with windows

transparent down to 1000 Angstroms are in the process of development, but are not yet commercially available. There are many materials however which fluoresce strongly under ultraviolet radiation and it has been shown that with a fluorescent coating a photomultiplier can perform well.

A useful coating is sodium salicylate (HOC_6H_4COONa) which has been shown to have very good properties. Watanabe and Inn (1953), among the first to evaluate this material, reported that it gave excellent response over the spectral range from 500 to 3000 Angstroms, and also that its response was linear with intensity at least over an intensity range of 50 and with intensities up to 2×10^{13} quanta/cm^2 sec. They further reported that it was very stable both under vacuum and over long periods of time. The quantum efficiency of sodium salicylate was measured by Johnson et al (1951) and found to be constant between 900 and 2300 Angstroms. It appeared to be superior to most other fluorescent materials in several respects, including stability, sensitivity and ease of handling.

With this information to hand it was decided to investigate the feasibility of converting the spectrograph to a photoelectric instrument to facilitate the measurement of intensities in the vacuum ultraviolet. Two questions had to be answered before proceeding too far: a) was the light gathering power of the instrument (f/50) sufficient so that adequate signal could be recorded photoelectrically, and b) was the wavelength control screw and the grating table designed sufficiently well that the grating would rotate in a smooth and uniform manner.

Preliminary tests showed that photoelectric recording was possible and the grating drive was at least acceptable for scanning. Hence complete adaptations were begun so that the 3 meter instrument could be used conveniently and interchangeably as either a photographic or a photoelectric instrument. This involved the building of a grating drive mechanism, a photomultiplier mount, and an exit slit arrangement.

2.6.1 Photomultiplier Mount and Exit Slit

An exit slit was constructed as shown in Figure 2.5, to replace the photographic plate holder. A rectangular hole was cut from the $\frac{1}{4}$ inch aluminum plate to allow an exit slit assembly to be mounted.

It was found that razor blades would make adequate slits if the edges were honed lightly with a fine emery stone to remove slight irregularities in the edge contours. Four sets of blades were mounted on a $\frac{1}{4}$ inch brass plate with screws which allowed adjustments in slit position and alignment. The brass plate was provided with slotted holes to allow it to be rotated to align the slits with the image of the entrance slit.

Slit widths of 25, 50, 100 and 200 microns were chosen as a reasonable range and the slits were set at those widths by means of a microscope to an accuracy of about 5%. The slits were located at the same distance from the grating as the photographic plate would be in its holder so that no extra focussing would be required.

It was decided to mount the photomultiplier outside the spectrograph for two reasons - firstly, for ease of construction and demounting, secondly, to utilize more of the sensitive area of the photomultiplier

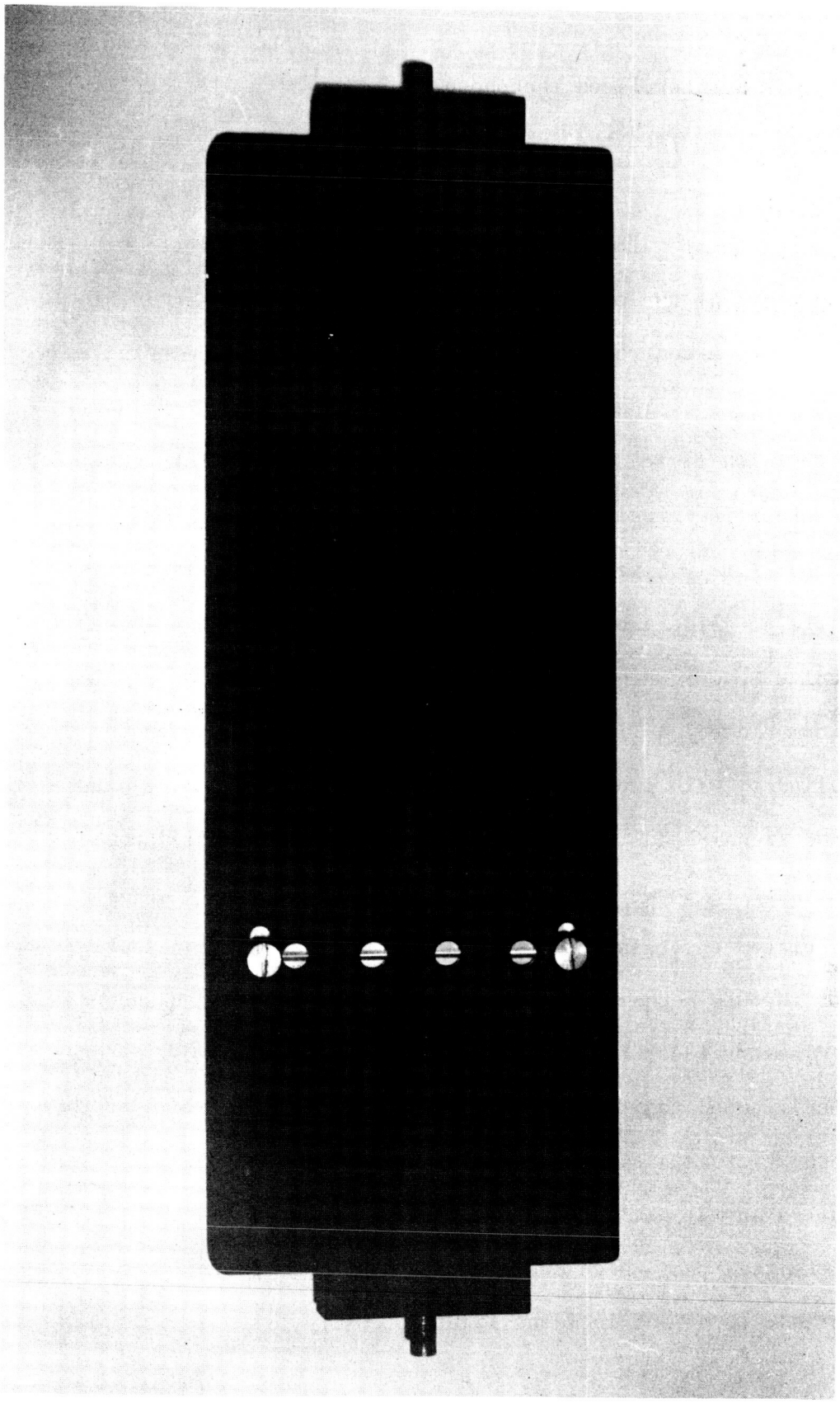

Figure 2.5 Exit Slit Plate

cathode. This design placed the photomultiplier at a distance of approximately 21 cm from the exit slit, where the image size was about 7 mm square.

An end plate of $\frac{1}{2}$ inch aluminum was machined to replace the standard inspection plate at the end of the camera compartment. A $\frac{1}{2}$ inch hole was drilled at the centre. The photomultiplier tube was mounted as shown in Figure 2.6. The tube was supported in its socket on a disc of bakelite which fitted into a $2\frac{1}{4}$ inch inside diameter fiber cylinder. A second supporting ring was located near the end of the tube. The tube was thus firmly fixed in the centre of the hollow cylinder and yet was free to slide along to allow the tube end to make a vacuum seal with a lucite spacer which in turn was seated against an O-ring in the aluminum plate. A light-tight cap was fitted snugly over the end of the cylinder, with two small holes for running through the high voltage and signal leads. An external view of the assembled photomultiplier unit is shown in Figure 2.7.

A regulated power supply provided high voltage for the photomultiplier through a chain of 1 megohm resistors connecting succeeding dynodes. These values were chosen rather than the much smaller ones conventionally used to limit the current which could be drawn by the tube and thus act as a safety device. Currents drawn from the photomultiplier in normal use were 10^{-8} amperes or less, a factor of 100 or more less than that which could be drawn without losing linearity between signal level and incident light intensity.

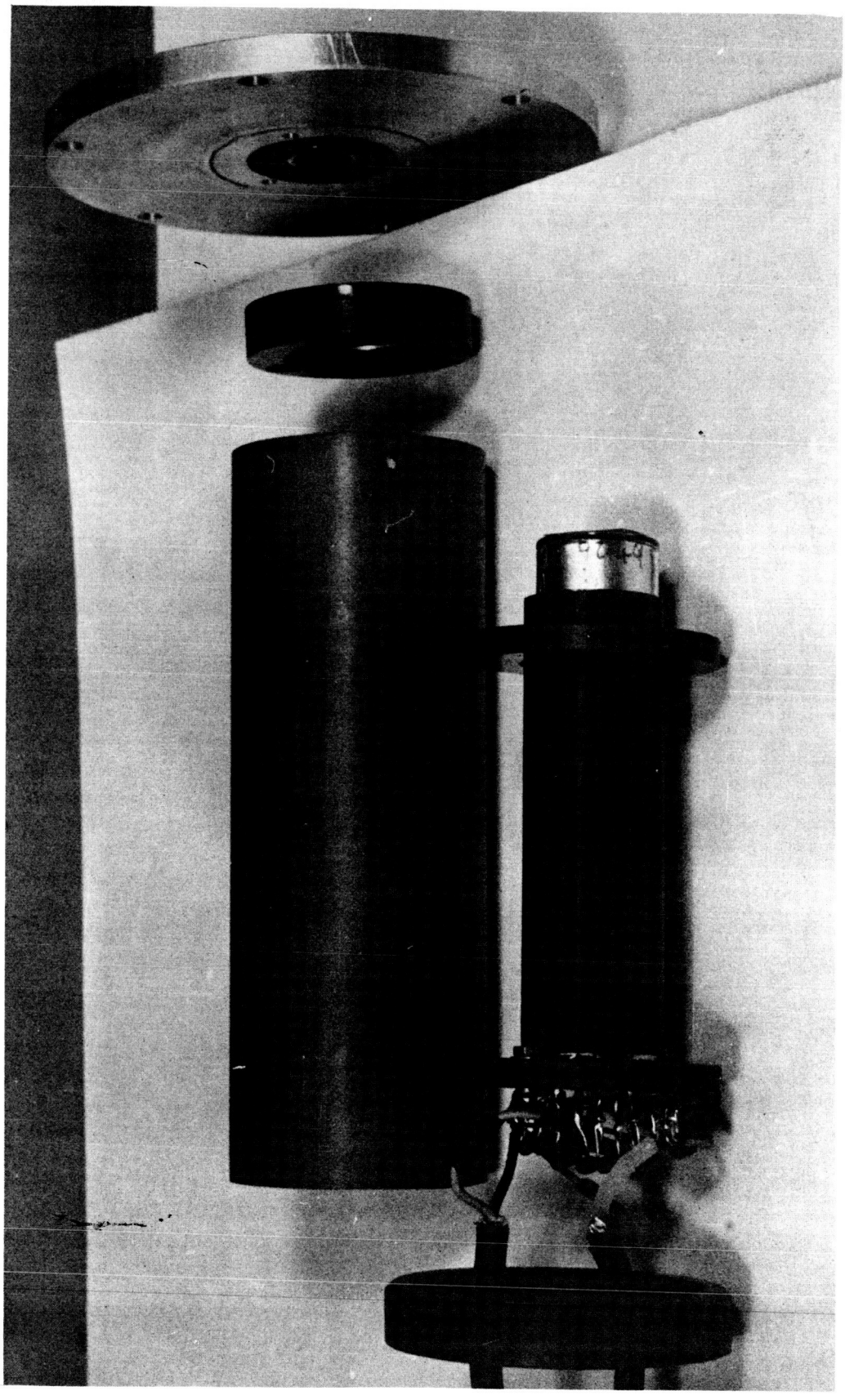

Figure 2.6 Photomultiplier Unit Assembly

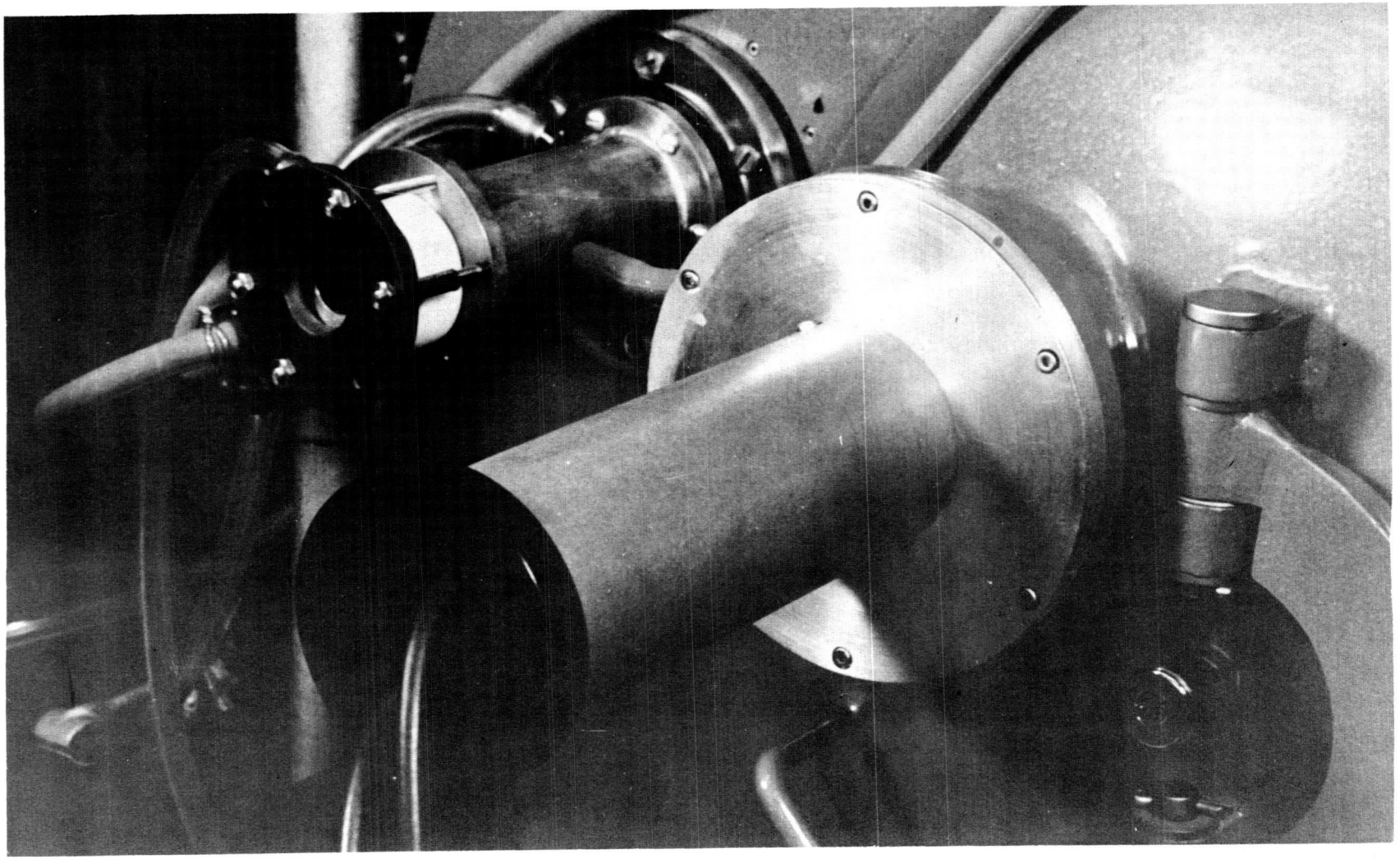

Figure 2.7 External View of Photomultiplier Unit

A range of voltages from 500 to 1300 volts was available from the power supply with a stability of 0.1%. A by-pass resistance of 1.3 megohms was added to the dynode resistance chain since the power supply was of a type which required a current of 1 milliampere or more to be drawn for proper voltage regulation.

The signal from the photomultiplier was fed through a shielded cable to a Leeds and Northrup DC amplifier and a Speedomax recorder. A block diagram of the circuitry is shown in Figure 2.8.

Since the entrance and exit slits of the spectrometer are close together the photomultiplier is of necessity mounted close to the spectral source being used. It was therefore necessary to shield the photomultiplier from any electrical noise or magnetic fields generated by such sources. AC condensed discharges in particular caused extremely high noise levels. The photomultiplier was therefore enclosed in a mu-metal shield placed at cathode potential, and the signal cable shield was grounded at both ends. In addition, it was necessary to enclose the whole photomultiplier unit in a grounded cylindrical screen.

Two E.M.I. photomultipliers, a 9526B and a 9524B, were obtained for use with the spectrometer. Both had similar cathodes of SbCsO with peak sensitivity about 4000 Angstroms. Typical curves of quantum efficiency versus wavelength are shown in Figure 2.9. The 9526B is satisfactory down to the quartz window cut-off at about 1600 Angstroms while the 9524B, with a glass window, requires a fluorescent coating for use in the ultraviolet.

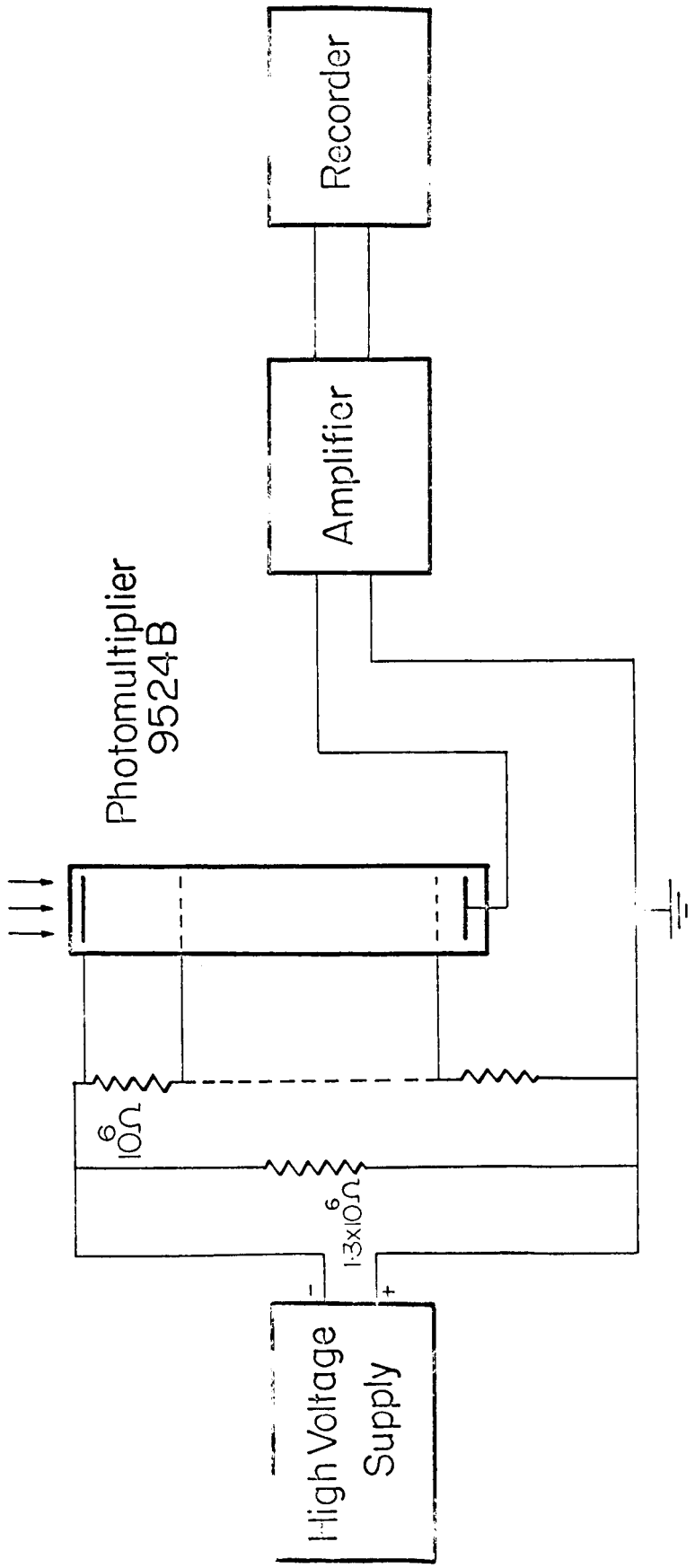

Figure 2.8 Block Diagram of Electronics

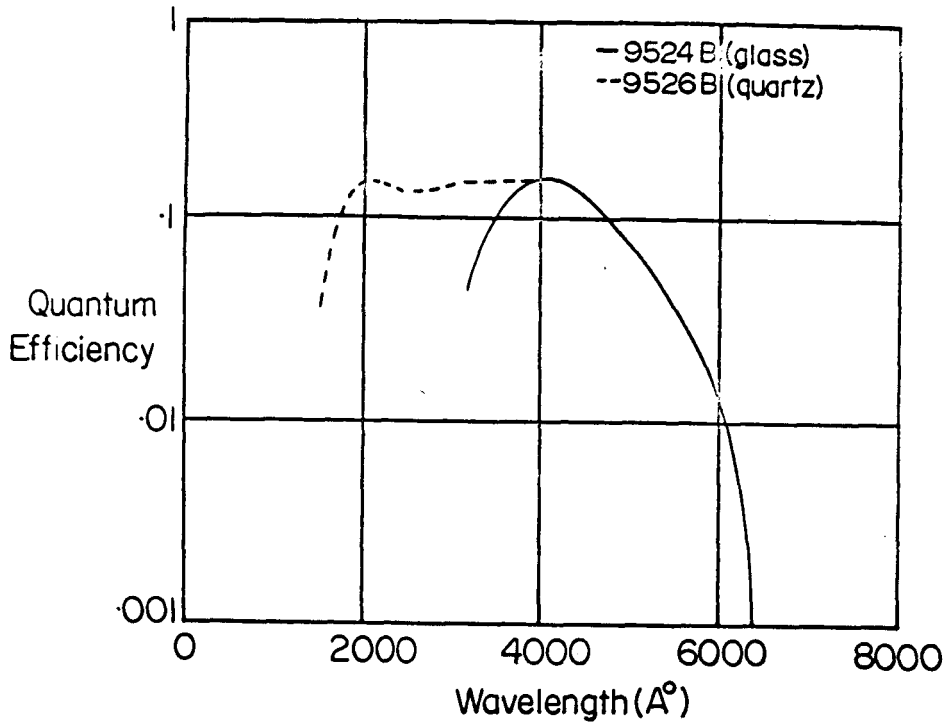

Figure 2·9 Quantum Efficiency of Photomultipliers

A solution of sodium salicylate and ethyl alcohol was prepared and applied to the 9524B window with a fine brush. Tests made on various types of coatings indicated that the most efficient fluorescent coating was a fairly thin semi-transparent coating. Such a coating gave a measured efficiency of 14%, while thicker opaque coatings gave efficiencies of about 10%.

More recently it was found that a much improved surface could be obtained by using an atomizer containing a saturated solution of sodium salicylate and ethyl alcohol. By spraying on the solution from a distance of 8-10 inches, a fine mist reaches the window surface and dries immediately, resulting in a uniform surface with no holes or large crystals. Any desired thickness can be readily obtained. This method

of application has been suggested by Knapp (1964) and Allison et al (1964). A quantum efficiency of approximately 25% was obtained by this means. This compared reasonably well with an effective quantum yield in the forward direction of 32% measured by Kristianpoller (1964).

2.6.2 Grating Drive Assembly

With the exit slit mounted in the focal plane and behind it a photoelectric detector, it remained to provide for rotation of the grating at a uniform and controlled speed to scan the spectrum across the slit. It was observed that an interval of 150 Angstroms was covered per revolution of the wavelength control shaft and that a torque of 50 in.-oz. was needed to turn it. A Bodine 1 rpm synchronous reversible motor with a torque of 110 in.-oz. was obtained to provide the necessary power.

A gear system was designed, as shown in Figure 2.10, which consisted of a 5 inch drive gear on the wavelength control shaft, a 2/3 inch diameter drive gear on an idler shaft (thus getting a 7.5 to 1 reduction), and the motor mounted with a separation of $1\frac{1}{2}$ inches from its drive shaft to the idler shaft. It was thus possible to connect the motor to the wavelength control shaft with any pair of gears having a combined diameter of 3 inches.

Two pairs of gears of 1 and 2 inches diameter, and $\frac{1}{2}$ and $2\frac{1}{2}$ inches diameter were obtained, thus providing possible scanning speeds of 4, 10, 40 or 100 Angstroms per minute. Combined with the fixed recorder chart speed of 2 inches per minute, these would provide integral numbers of divisions per Angstrom. This range of speeds appeared satisfactory

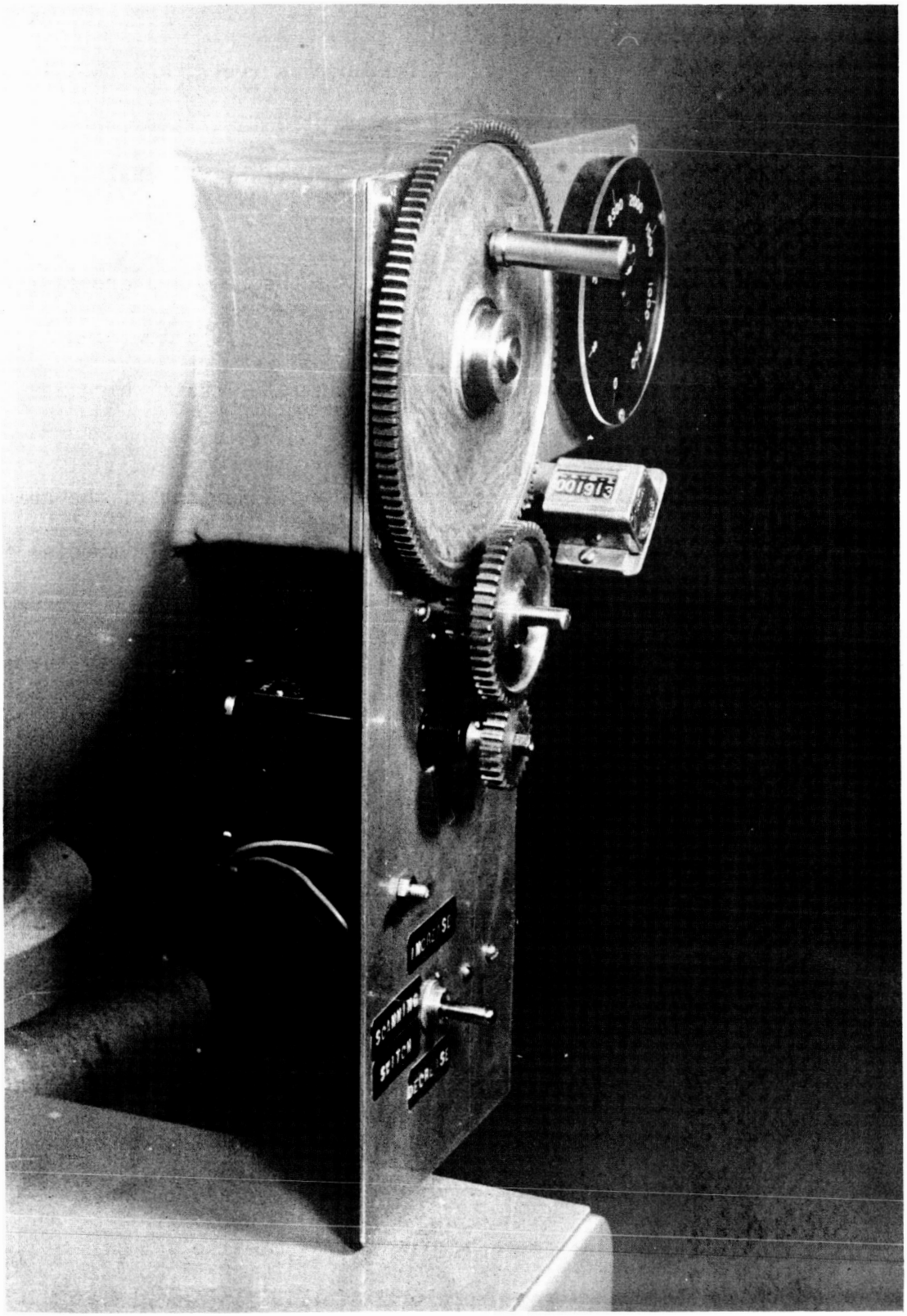

Figure 2.10 Grating Drive Assembly

as the upper speed would be suitable for quick surveys, and the slower ones adequate for making intensity measurements. A greater selection of intermediate speeds could be obtained if desirable by choosing other pairs of gears of appropriate size.

The gears are fixed to the shafts with set-screws and are easily removable. It is possible to disengage the gears, to allow manual setting of the wavelength, by pulling out the idler shaft which is spring loaded.

The existing dial which indicated wavelength setting of the grating was adequate for photographic work but was not sufficiently precise for photometric work as it could be read only to within about 100 Angstroms. A one-tenth revolution counter was obtained and by fixing it to the main wavelength drive gear with a gear ratio of 15:1, wavelengths could be read to an accuracy of 1 Angstrom for uni-directional scans. While the scanning is reasonably linear over the centre of the range, it deviates towards the upper and lower ends of the spectral range. This non-linearity is due to the combined effect of the sine terms in the grating equation and the Rowland circle mounting. Figure 2.11 shows the error in wavelength reading, as a function of wavelength, when the counter is set to read correctly at 1500 Angstroms.

It should be pointed out that the wavelength counter, and error graph are simply for ease of locating desired spectral regions or features. The graph illustrates however that while the wavelength scan between 1000 and 2500 Angstroms is satisfactorily linear, above 2500 Angstroms the scanning rate is changing slightly and this may need to

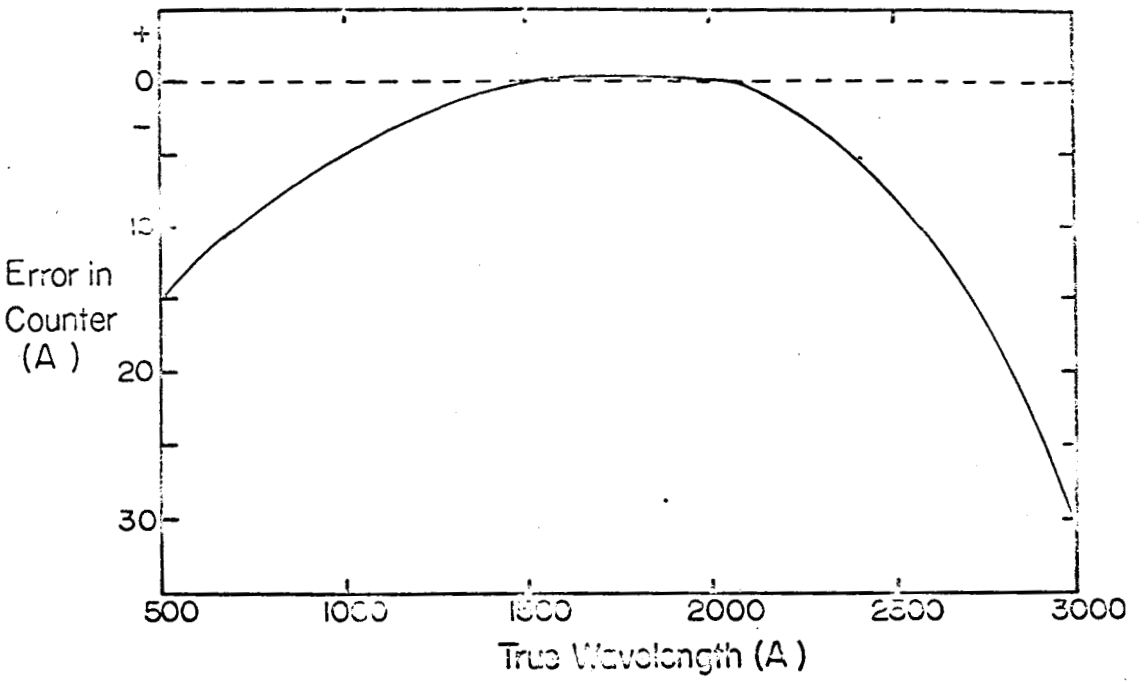

Figure 2-11 Wavelength Counter Error

be taken into account in measuring areas under spectral features (bands) in arriving at intensities.

2.7 Discussion of Performance

Following are a few general comments on the performance of the instrument, pertaining to its use as a spectrograph and as a spectrometer.

2.7.1 Spectrograph

The pumping system is quite adequate for evacuating the spectrograph. It is possible to reach 2×10^{-5} mm Hg in the main compartment after a few hours of pumping. Evacuation from atmospheric pressure to 10^{-3} mm Hg requires approximately 30 minutes. It is not usually possible to evacuate the camera compartment beyond 10^{-4} mm Hg, but this is undoubtedly due to small leaks in the camera compartment door.

With a spectral source connected to the spectrograph it is a different situation. When pumping discharge products through the entrance slit it is impossible to maintain the spectrograph pressure much below 10^{-3} mm Hg. To improve this would require a more effective arrangement of baffle slits and differential pumping.

Spectra obtained are usually sharp when exposure time is short (< 1 hour). It is seldom that exposures of longer than about 2 hours give sharp spectral lines. This was attributed to two main causes - temperature changes in the spectrograph, and unsuitable spectrograph mounting. The former was alleviated by the installation of an air conditioner which would hold the room at a reasonably constant temperature.

Spectral lines are broadened somewhat because of poor quality of the grating rulings. This is not noticeable above 2000 A but at shorter wavelengths it becomes progressively more noticeable.

2.7.2 Spectrometer

The grating drive mechanism shows no evidence of uneveness of motion. There is however a backlash in the wavelength control screw which results in about a 15 A lag when reversing the direction of scan. This presents no problem for use at present; if desired it could be eliminated by spring loading the grating drive arm.

Spectral resolution of the photoelectric instrument is satisfactory for present use. A representative scan is shown in Figure 2.12. This is a chart recording of the signal obtained from the $2p^3\ ^4S_o - 3s\ ^4P$ nitrogen multiplet at 1200 A covered at the slowest scanning speed (4 A/min) with 25μ slits, in both the first and second order. The nitrogen lines are approximately 0.5 A apart and are completely resolved

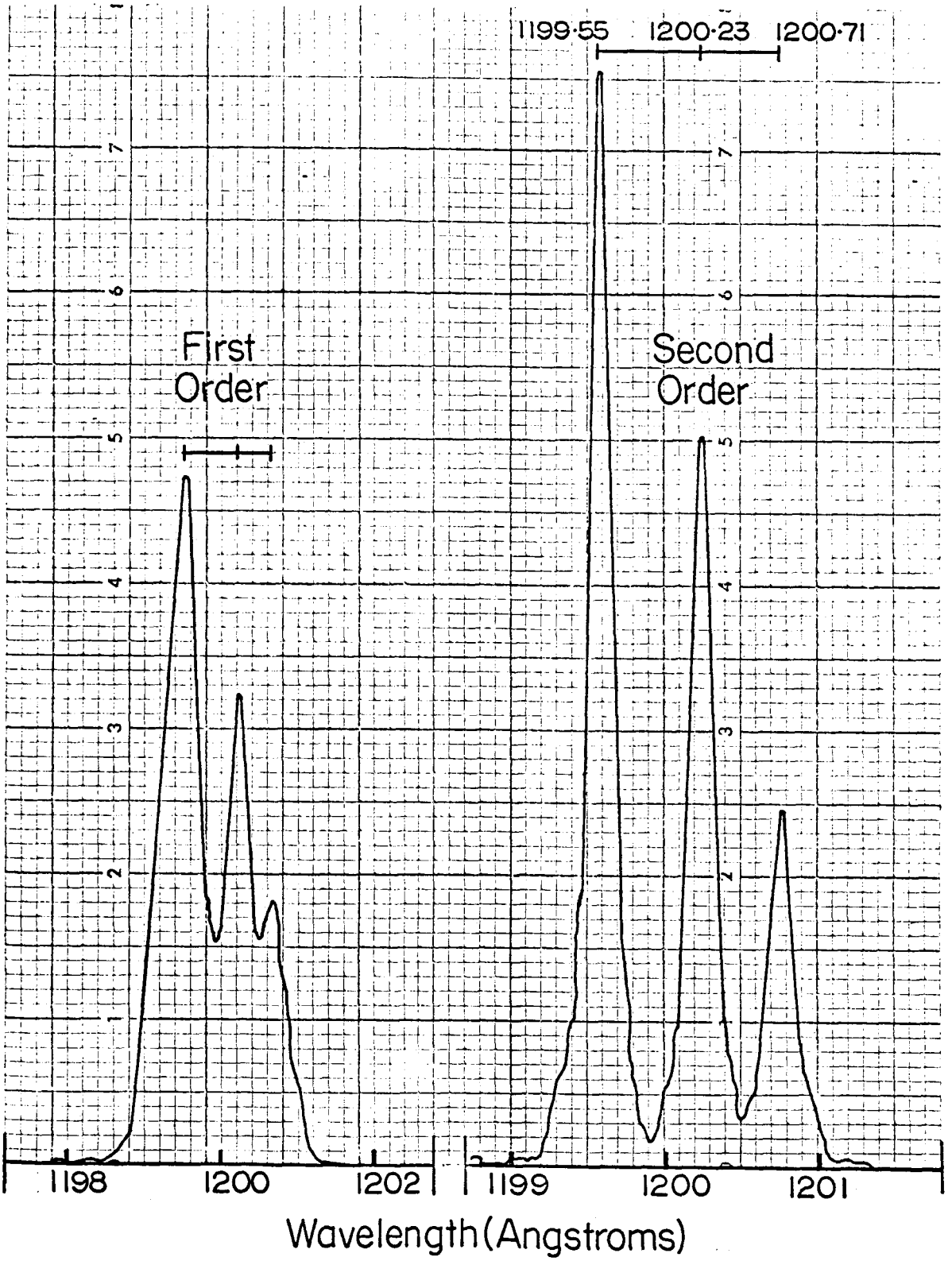

Figure 2·12 Spectrometer Scan of NI Multiplet

in second order. Wavelengths can be read reliably from the chart paper to an accuracy of 0.1 A.

The scan shows present rather than optimum performance. Resolution could be improved by an order of magnitude by using narrower slits and a higher quality exit slit, and by using an amplifier and recorder with good time response (the ones in present use have a response time of 2 seconds).

The detector response is considered excellent; it is possible to record photoelectrically any spectral features that can be recorded photographically in a two hour exposure. This is possible largely as a result of using wider slits, and hence is at the expense of some resolution.

The lower limit of response is determined largely by the dark current of the photomultiplier which is approximately 10^{-9} amperes at a cathode potential of -1000 volts and at room temperature. This could be markedly improved by cooling the photomultiplier although this would present a few other problems.

CHAPTER III

MOLECULAR BAND SYSTEMS IN THE VACUUM ULTRAVIOLET

3.1 Introduction

There are many molecular band systems in the vacuum ultraviolet region. Molecules with a closed shell of electrons (such as N_2 and CO) in particular have some of their most intense band systems in this region. While much of the groundwork in studies of molecular spectra in the vacuum ultraviolet was laid a few decades ago, there has recently been a revival of interest in the field and intensive studies have been carried out on the spectra of an increasing number of diatomic and polyatomic molecules. A comprehensive review of band systems which have been studied since 1950 and the information obtained is given by Wilkinson (1961). The present study was centred primarily on the Lyman-Birge-Hopfield (LBH) system.

Preliminary to measurement of relative intensities of the bands of the LBH system it was necessary to develop a light source which would provide this system with reasonable brightness and with a minimum of contamination from other nitrogen band systems or foreign species. It was necessary also to examine the band system in detail to identify all the detectable bands and to be aware of overlapped

bands or atomic lines which would interfere with intensity measurements. For this survey work photographic techniques are preferable to photoelectric recordings, hence most of the preliminary studies were photographic in nature.

It is worthwhile to describe briefly here the various light sources which were built for exciting molecular spectra and to present a historical review of the LBH system along with an identification spectrum of the system. Factors pertaining to relative intensities of these bands will be discussed in a later chapter.

In the course of this survey a number of other band systems were observed and studied briefly. To dwell at any length on these would be extraneous, however two of them merit mention because of their relation to the LBH system. These are the CO Fourth Positive system, completely analagous to the LBH system, in the same region and readily excited, and the N_2^+ Second Negative system, also in the same spectral region and excited to a certain extent along with the LBH system.

3.2 Light Sources for Excitation of Molecular Spectra

Light sources for investigations of molecular spectra do not differ markedly from those suitable for use at longer wavelengths. The principal differences are that they must be so designed as to fit on the end of the spectrograph with a vacuum tight seal, and self-absorption of their radiation must be avoided.

The first source built was a π-shaped discharge tube 12 inches in length and 1 inch in diameter, with two cylindrical nickel electrodes

5/8 inch in diameter. The diameter of the glass envelope between the electrodes was drawn down to 5/8 inch to constrict the discharge somewhat and thus to increase the current density. The discharge tube was secured to the entrance flange of the spectrograph by means of a retaining ring and an O-ring seal and was viewed end-on by the instrument.

An AC condensed discharge was produced by a 15 kv, 0.45 kva transformer combined with a .005μf condenser and an external spark gap. The tube was air cooled with a fan.

A second source was the hollow cathode discharge tube described in section 4.3.4.2. It was found to be a reasonable one for excitation of certain molecular band spectra. However some of the material of the cathode was vaporized by heating and ion bombardment during operation and this resulted in unwanted atomic lines appearing in the spectrum. A second disadvantage of this tube as a source for the LBH system was that the degree of ionization and dissociation of the nitrogen molecule in the discharge was higher than desirable.

A third source was an electrodeless discharge excited by a Microtherm power generator (2450 megacycles, 100 watts). The discharge lamp consisted of a $\frac{1}{2}$ inch diameter quartz tube with two side arms. One end was sealed while the other was flanged to fit into an aluminum plate with a $\frac{1}{2}$ inch hole at the centre. It was secured there with sealing wax and the plate was machined to fit on the entrance flange of the spectrograph.

Each source was built with a gas inlet and also an outlet so that it could be evacuated independently. In general however the window was removed between the source and spectrograph, and the discharge

products were pumped through the entrance slit by the spectrograph vacuum system.

3.3 N_2 Lyman-Birge-Hopfield System $a^1\Pi_g - X\ ^1\Sigma_g^+$

The LBH band system is the most intense of all the nitrogen systems appearing in the region below 2700 A. It consists mainly of about 75 bands extending from 1200 A up to 2150 A; in addition there are some 40 weaker bands extending up to about 2600 A. The system is excited in any discharge in nitrogen. There have been numerous investigations of this band system since it provides the most reliable data available on both the ground state of N_2 and the important $a^1\Pi$ state.

It was first studied by Lyman (1911) who observed and measured the wavelengths of twenty-one of the strongest bands excited in a high voltage discharge through nitrogen at low pressure. Birge and Hopfield (1928) made an extensive study of the system, reporting more than sixty bands and analyzing the vibrational structure in detail.

The rotational structure of the system was first studied by Appleyard (1932) and he concluded that the transition was between a a $^1\Pi$ state and the ground state X $^1\Sigma_g^+$ of nitrogen. Further rotational analyses were made by Watson and Koontz (1934) and later by Spinks (1942).

Several new bands up to vibrational levels of the ground state of $v'' = 27$ were observed in the region 2100 - 2600 A by Herman and Herman (1942). A predissociation in the $a^1\Pi$ state above $v' = 6$ was also observed.

While it was initially believed that the $a \rightarrow X$ transition was allowed and thus a $u \rightarrow g$ transition, on the basis of indirect evidence Herzberg

(1946) concluded that the transition was in fact a $^1\Pi_g - X\ ^1\Sigma_g^+$ and thus forbidden as an electric dipole transition. It is however allowed as a magnetic dipole transition. The two types of transitions cannot be distinguished experimentally unless quadrupole lines are observed (electric quadrupole transitions are allowed concurrently with magnetic dipole transitions). High resolution absorption spectra obtained by Wilkinson and Mulliken (1957) showed the presence of the quadrupole lines (S and O branches) and removed any doubt concerning the assignment of the LBH bands as a $a\ ^1\Pi_g - X\ ^1\Sigma_g^+$ transition. The electric quadrupole contribution to the intensity of the bands was estimated to be about 13% of the total.

A partial energy level diagram of the nitrogen molecule is shown in Figure 3.1. The $a\ ^1\Pi_g - X\ ^1\Sigma_g^+$ electronic transition of the LBH system is shown and also a number of other prominent transitions for the N_2 and N_2^+ molecule.

Further high resolution measurements were carried out on the LBH system in absorption and in emission by Wilkinson and Houk (1956), Loftus (1956) and Wilkinson (1957). Accurate molecular constants were derived from these studies for both the $a\ ^1\Pi_g$ and the $X\ ^1\Sigma_g^+$ states. These have been compiled by Loftus (1960) and pertinent ones are listed in Table 3.1.

Table 3.1

Molecular Constants for the $X\ ^1\Sigma_g^+$ and $a\ ^1\Pi_g$ States of N_2

State	T_{oo}	ω_e	$\omega_e x_e$	$\omega_e y_e$
$X\ ^1\Sigma_g^+$	0	2358.07	14.188	- 0.0124
$a\ ^1\Pi_g$	68951.21	1694.06	13.86	

Nomenclature as used by Herzberg (1950)

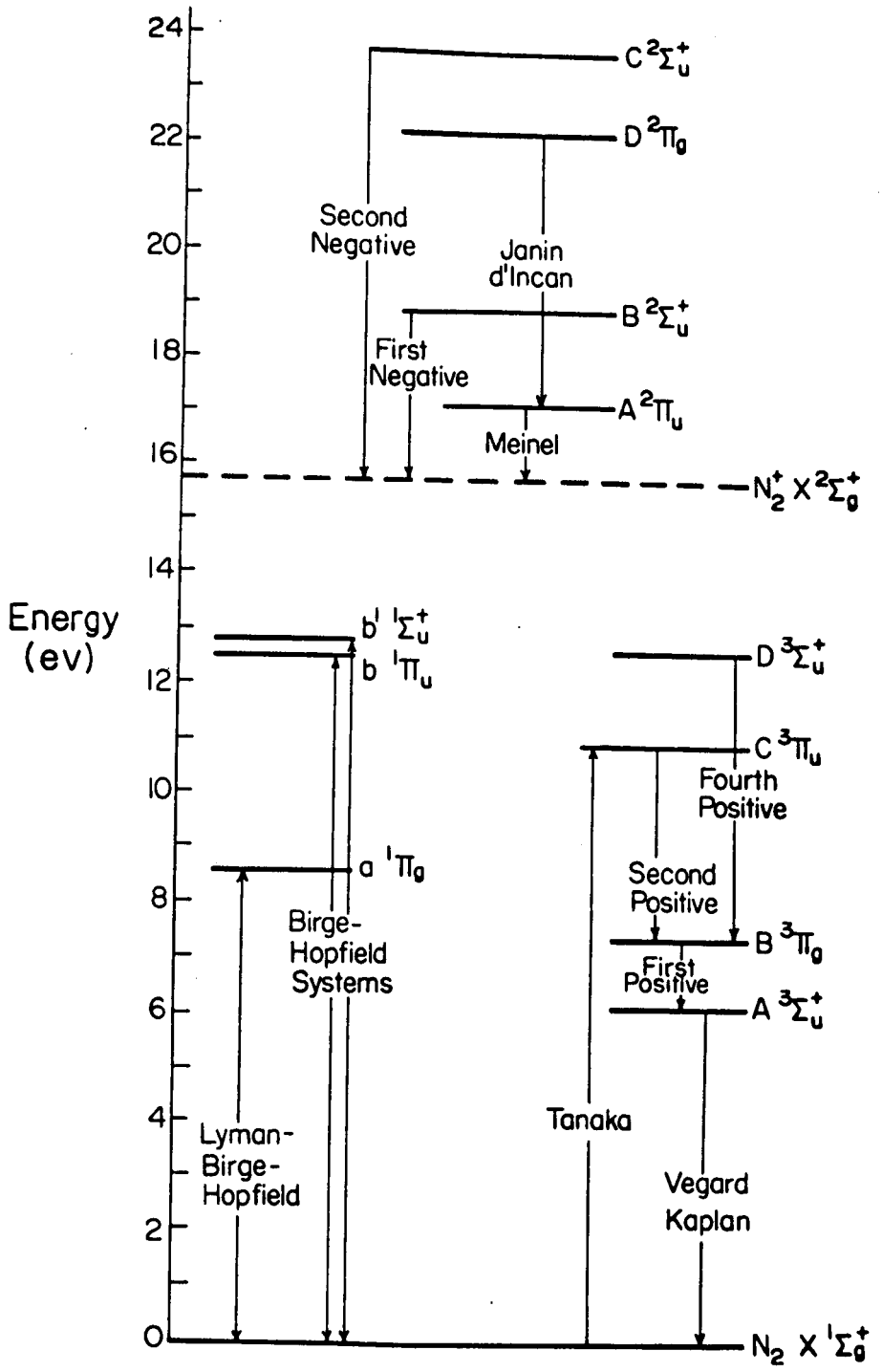

Figure 3-1 Partial Energy Level Diagram for N_2 and N_2^+

A Deslandres array of band head wavelengths of all observed emission bands of the LBH system lying below 2150 A is displayed in Table 3.2. The wavelengths are calculated from the molecular constants of Table 3.1 and agree in general with the observed wavelengths to within 0.1 A. The vast majority of the bands listed were observed and identified by Birge and Hopfield (1928).

Four additional bands, previously unreported, were observed by the author. They are the (0, 7), (0, 8), (3, 1) and (7, 1) bands. They can be seen in the spectrum of the LBH system shown in Figure 3.2. The bands in the spectrum are identified by the vibrational levels of the upper and lower states, v' and v''.

The spectrum was obtained from an AC condensed discharge through nitrogen at 0.5 mm pressure. It was recorded on a Kodak 103-0 UV sensitized plate with a three hour exposure. Slit width was .01 mm.

A number of atomic nitrogen lines appear prominently in the spectrum. There are as well a number of bands of the Birge-Hopfield system seen at the lower end of the spectrum and some bands of the N_2^+ Second Negative system appear weakly in the region 1800-2000 A. These features are too numerous for individual designation.

As seen in the spectrum of Figure 3.2 the bands are single headed and degraded to longer wavelengths. Under high resolution (e.g. Wilkinson (1957)) they are seen to consist of single P, Q and R branches, arising from magnetic dipole and electric quadrupole transitions, and weaker S and O branches arising from electric quadrupole transitions. There is an intensity alternation in the rotational structure, with the odd numbered rotational lines being weak.

Table 3.2 Deslandres Table of Band Head Wavelengths of Lyman-Birge-Hopfield System of N_2

v' \ v''	0	1	2	3	4	5	6	7	8	9	10	11	12	13	14	15
0	1450.1	1500.8	1554.5	1611.4	1671.9	1736.1	1804.6	1877.7	1955.9							
1	1415.9	1464.2	1515.3		1626.6	1687.4	1752.0	1820.8	1894.2	1972.6						
2	1383.8	1429.9	1478.6	1530.0	1584.4		1703.1	1768.1	1837.2	1910.9	1989.6	2073.8				
3	1353.6	1397.7	1444.2		1544.9	1599.7	1657.6		1784.4	1853.8	1927.8	2006.8	2091.2			
4	1325.3	1367.5	1411.9		1508.0	1560.2					1870.8	1945.0	2024.2	2108.8		
5	1298.5	1339.0	1381.6	1426.3	1473.5	1523.2	1575.7		.			1887.9	1962.4	2041.9	2126.7	
6	1273.2	1312.2		1395.9		1488.6		1591.5	1647.3			1835.0		1980.1	2059.8	2144.8
7	1249.3	1286.9														
8		1262.9														

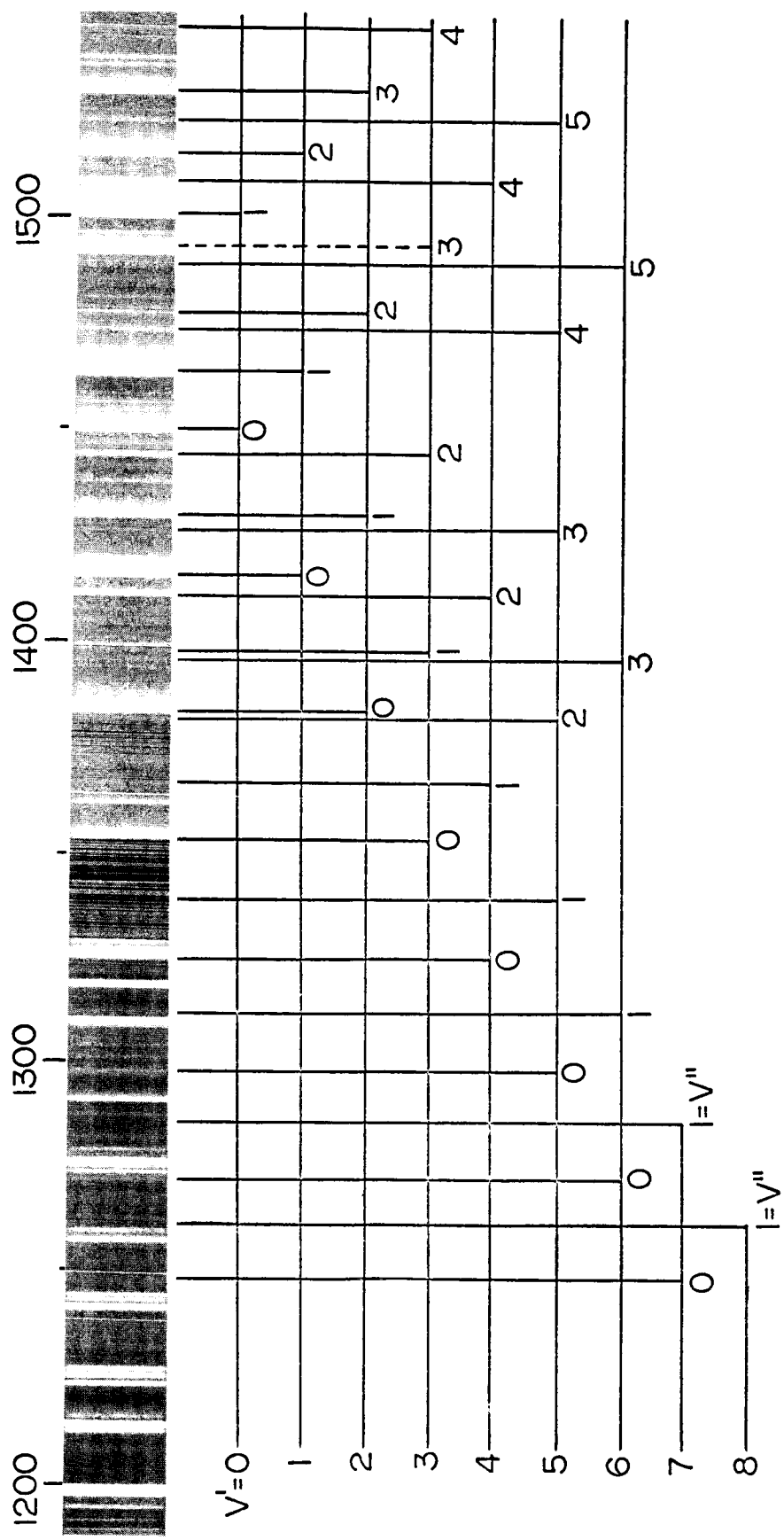

Figure 3.2 N_2 Lyman Birge Hopfield System $a\,{}^1\Pi_g - X\,{}^1\Sigma_g^+$

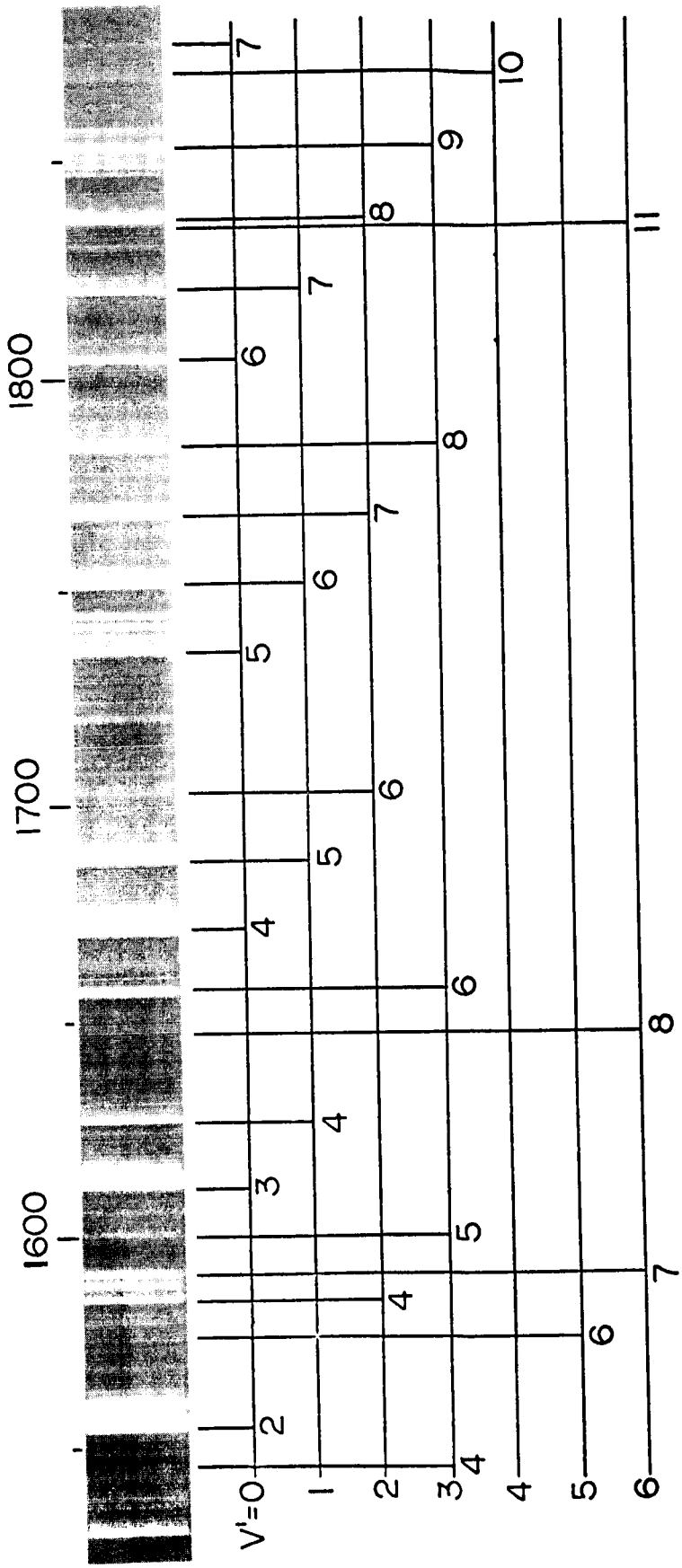

Figure 3·2 (continued)

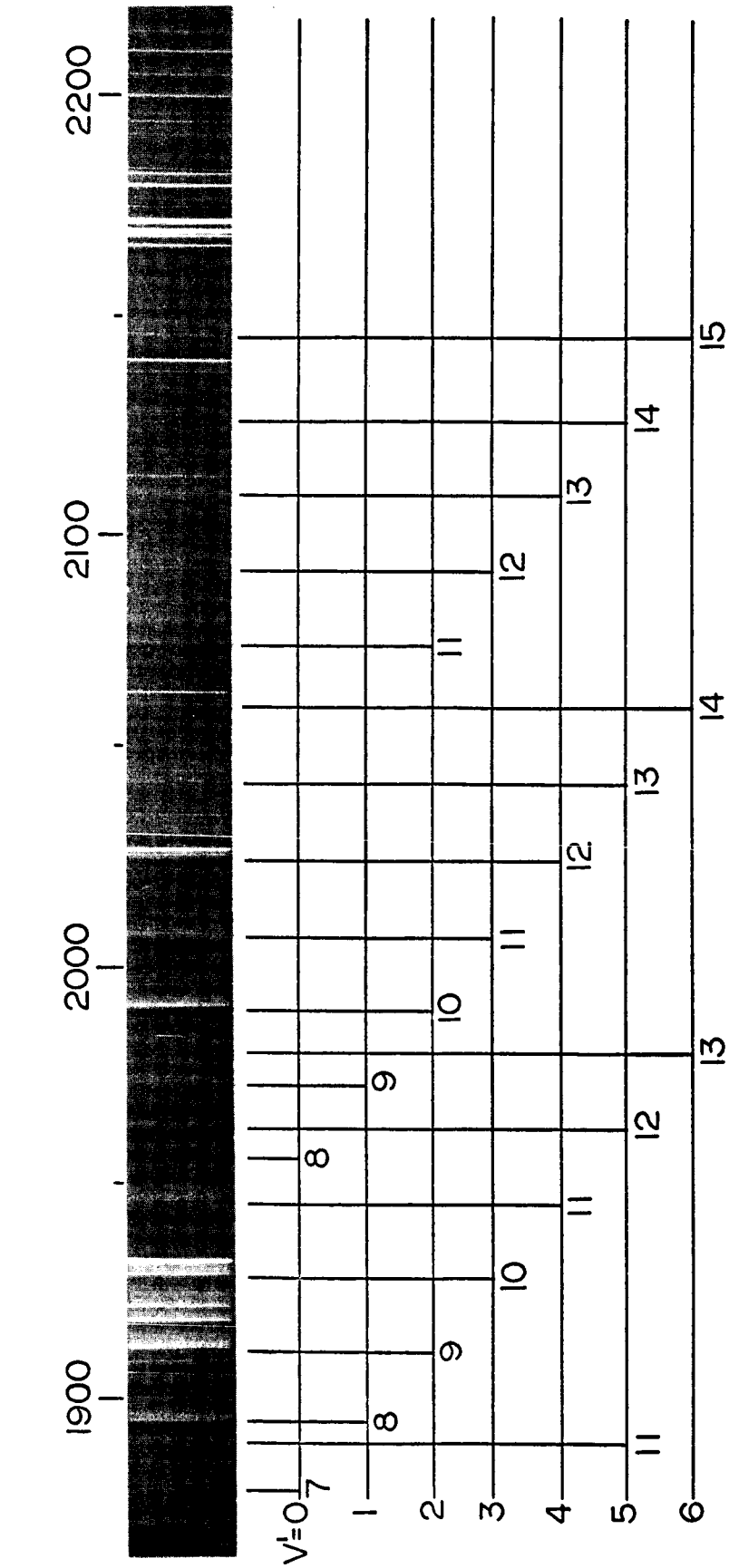

Figure 3:2(continued)

3.4 CO Fourth Positive System $A\,^1\Pi - X\,^1\Sigma^+$

The Fourth Positive bands are the most prominent part of the spectrum of carbon monoxide. The band system extends from about 2800 A down to 1140 A. It arises from the transition between the $X\,^1\Sigma^+$ ground state and the $A\,^1\Pi$ upper state of the CO molecule as shown in the partial energy level diagram in Figure 3.3.

The bands are very easily excited and occur in any discharge through CO or CO_2. They occur also as impurity bands in many discharge tubes, particularly if there is stop-cock grease or carbon present. They were first observed by Deslandres (1888) who measured some 40 band heads in the region above 2000 A. Lyman (1906) observed about 100 bands and made measurements down to 1300 A.

Birge (1926) first identified the band system as belonging to the carbon monoxide molecule. Wavelength measurements of band heads are reported by Headrick and Fox (1930) for 68 bands lying between 2200 and 1280 A, and by Estey (1930) for bands between 2000 and 2800 A. Read (1934) determined the rotational constants of the upper state from a rotational analysis and from these determined the vibrational constants accurately.

The system is also readily observed in absorption. Tanaka et al (1957) investigated the absorption spectrum of CO and observed band heads up to an upper vibrational level $v' = 20$ from the ground level $v'' = 0$ and up to $v' = 13$ from the $v'' = 1$ level.

A spectrum of the band system up to 2300 A is shown in Figure 3.4. Beyond that wavelength the bands are very weak and CO^+ bands predominated

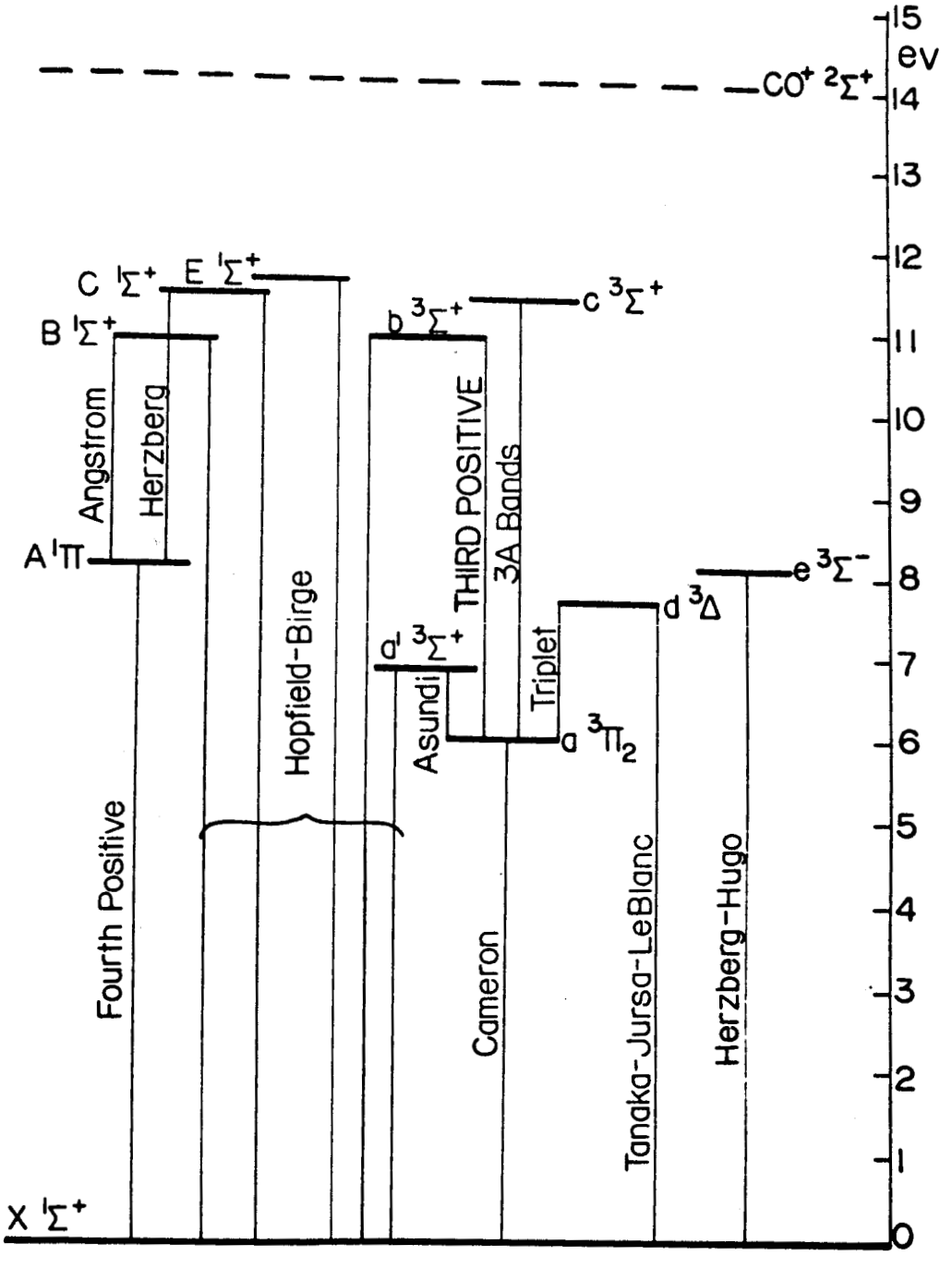

Figure 3.3 Energy Levels and Band Systems of CO

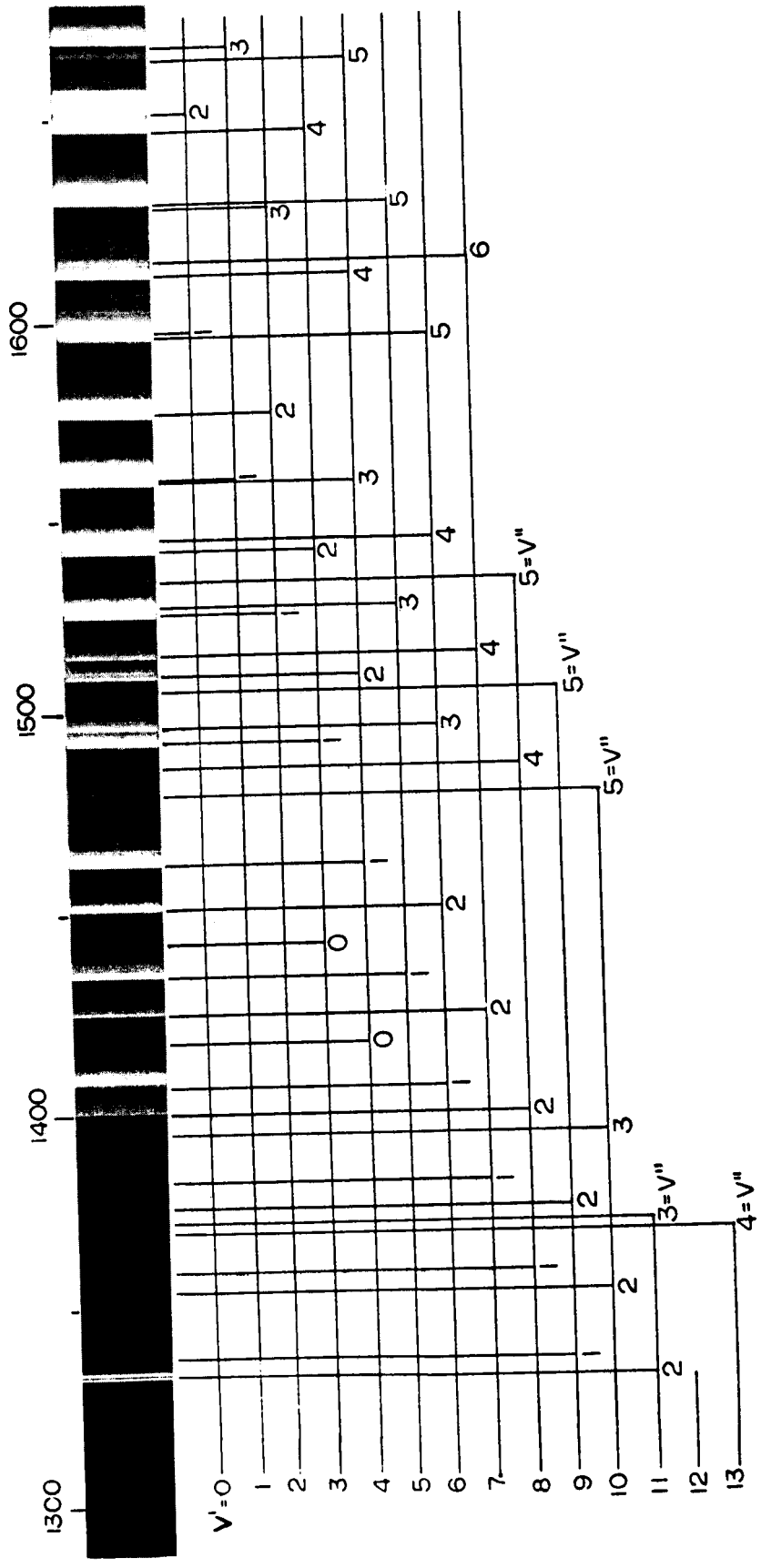

Figure 3·4 CO Fourth Positive System $A\,^1\Pi\text{-}X\,^1\Sigma^+$

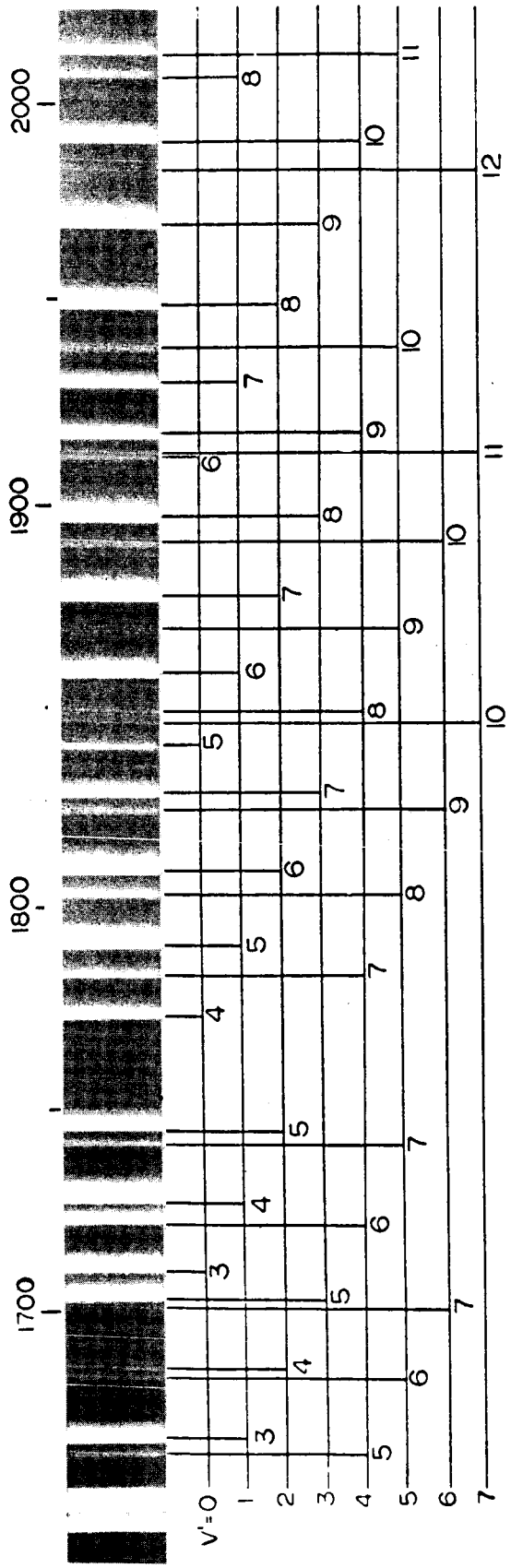

Figure 3.4 (continued)

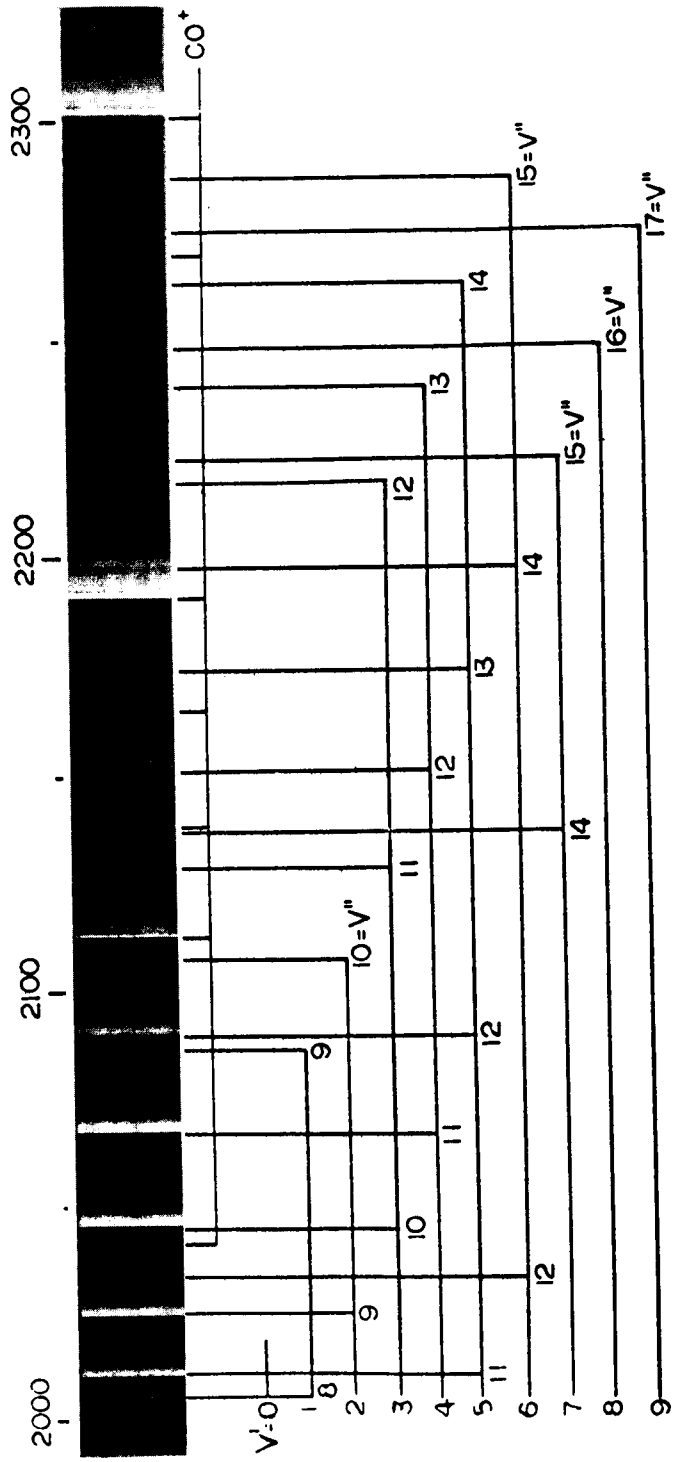

Figure 3·4 (continued)

in the AC condensed discharge used to excite the spectrum. Pressure in the discharge was approximately 0.2 mm Hg, while the spectrograph pressure was 10^{-3} mm Hg. Exposure time was 30 minutes and slit width was .01 mm.

Included in the spectrum of the CO Fourth Positive system are 13 bands which have not previously been observed. They are included in the Deslandres table of wavelengths of all observed bands below 2300 A (Table 3.3) and are underlined for reference. The wavelengths listed for those bands are as calculated from the molecular constants determined by Read (1934).

3.5 N_2^+ Second Negative System $C\ ^2\Sigma_u^+ - X\ ^2\Sigma_g^+$

The Second Negative system consists of some fifty bands in the region 2100 A to 1370 A. It was first observed by Hopfield (1930) in emission in a helium-nitrogen mixture. The system was further investigated by Watson and Kuntz (1934) who identified it as a N_2^+ transition with the same lower state as the First Negative system. They made a tentative vibrational assignment, but a further investigation of their plates by Setlow (1948) suggested a renumbering of the upper levels. The latter was confirmed by Baer and Miescher (1952) who observed the isotope shifts in these bands and obtained vibrational constants for the upper state. High resolution measurements have been made more recently on the Second Negative system by Douglas (1952), Wilkinson (1956) and Carroll (1959).

The system is most strongly excited in a helium-nitrogen mixture in either a condensed discharge or a hollow cathode discharge. It is

Table 3.3 Deslandres Table of Band Head Wavelengths of Fourth Positive System of CO

$v'v''$	0	1	2	3	4	5	6	7	8	9	10	11	12	13	14	15	16	17
0	1545.3	1597.1	1653.0	1712.2	1774.9	1841.5	1912.8											
1	1509.7	1560.1		1669.7	1729.3	1792.4	1859.4	1930.7	2006.6	2087.6								
2	1477.5	1525.8	1576.7	1630.4	1687.2	1747.2	1810.8	1878.8	1950.1	2026.4	2107.9							
3	1447.3	1493.6	1542.3		1647.9	1705.2		1829.8	1897.8	1970.1	2047.0	2129.0						
4	1418.9	1463.5	1510.4	1559.5	1611.3		1723.8	1784.9	1850.1	1918.1	1990.9	2068.4	2150.9	2239.0				
5	1392.0	1435.3	1480.2	1527.5		1629.6	1684.9	1743.1	1804.7		1939.1	2012.5	2090.6	2173.8	2262.4			
6	1367.7	1408.9	1452.2	1497.6	1545.4	1595.6		1704.3		1825.4	1891.2		2035.0		2197.4	2286.8		
7		1384.0	1425.8		1515.7		1614.6				1846.7	1913.1	1983.6		2138.1	2222.1		
8		1360.8	1401.0			1534.1											2247.9	
9		1338.8	1377.8			1506.2												2274.6
10			1355.8	1395.4		1480.1												
11			1335.3	1373.7														
12																		
13					1371.7													

also excited in a pure nitrogen discharge, but not as strongly and with a markedly different intensity distribution. This was originally attributed to resonance excitation of the $v' = 3$ level by He^+ (ionization potential 24.58 ev). It was suggested by Douglas (1952) that this effect was more probably a case of inverse predissociation - a nitrogen ion and a nitrogen atom coming together and undergoing a radiationless transition into the $v' = 3$ level. A normal intensity distribution is obtained when neon is used instead of helium with nitrogen.

Spectra of the Second Negative system are illustrated by Tanaka et al (1961) and Wilkinson (1961). They show the marked differences in intensity distribution under various excitation conditions.

CHAPTER IV

INTENSITY CALIBRATION TECHNIQUES IN THE VACUUM ULTRAVIOLET

4.1 Introduction

For the measurement of radiation intensities it is necessary that some form of intensity standard be available to determine the relation between the response of the spectrometer and the true intensity distribution of the radiation incident on the spectrometer. The solution is straightforward in the visible and near ultraviolet regions where black body radiation can be employed as a radiation standard, but in the vacuum ultraviolet no completely satisfactory techniques have been developed to date.

The electromagnetic radiation from centripetally accelerated high energy electrons has been suggested as a radiation standard by Tomboulian and Hartman (1956). It possesses the advantages that it is continuous, of high intensity, and covers a wide spectral range. The radiation extends from the soft x-ray region through to the visible; the relative intensity distribution and the position of the maximum can be calculated from the energy of the beam. Unfortunately there are many instrumental difficulties and to date its only application has been as a background

continuum for absorption studies. The continuum radiation of a 180 Mev electron synchrotron has been utilized for such work by Madden and Codling (1964).

Another means of determining absolute intensities is based on the photoionization of the rare gases. The photoionization yield of such gases is approximately unity for photons whose energy is greater than the ionization potential of the gas. Thus an absorption cell containing one of the rare gases, such as xenon with ionization potential 12.13 ev (λ = 1022 A), and a plate to collect the photo-electrons can be used to measure incoming radiation absolutely up to about 1000 A. Samson (1964) has used such a device to measure the quantum yield of sodium salicylate as a function of wavelength from 400 to 1000 A.

While this technique is useful for measuring detector response it cannot be used directly to determine grating response;thus it is not an adequate means of calibrating a complete instrument. Moreover it is limited to the shorter wavelengths - even filling the absorption cell with nitric oxide, which has an ionization potential of just 9.25 ev, would extend its useful range up to only 1343 A.

Various other techniques have been employed including measurements of continua emitted by discharges in hydrogen and certain of the inert gases. These continua however usually extend over limited spectral regions and are not adequately reproducible.

4.2 Analysis of Problem

Before discussing calibration techniques attempted in the present study it is worthwhile to consider individually the various parameters

which will determine the overall efficiency of the spectrometer. It is possible with this approach to determine, at least qualitatively, the response of the spectrometer as a function of wavelength. The three parameters in this case are:

(1) the grating reflectivity,

(2) the detector response,

(3) the grating efficiency.

4.2.1 Grating Reflectivity

The reflection coefficient of aluminum, the grating surface, is essentially constant through the visible region and down to about 2000 A. Below that it falls off rather linearly to nearly zero at 1000 A. This is due to the oxide layer that forms on the aluminum surface shortly after being exposed to air.

Hass and Tousey (1959) observed that when a fresh aluminum surface is coated with magnesium fluoride a large increase in reflectance in the extreme ultraviolet is obtained. This coating not only prevents oxidation of the aluminum surface but somewhat enhances the reflectance of the surface through interference effects. The reflectances of day old and year old aluminum surfaces and of a fresh aluminum surface to which MgF_2 has been added, as measured by Hass and Tousey over the wavelength interval 2000 to 1000 A, are shown in Figure 4.1. The marked enhancement of reflectance of the MgF_2 coated aluminum surface is apparent below 1600 A. The exact shape of the curve above that wavelength is somewhat dependent on the thickness of the magnesium fluoride layer.

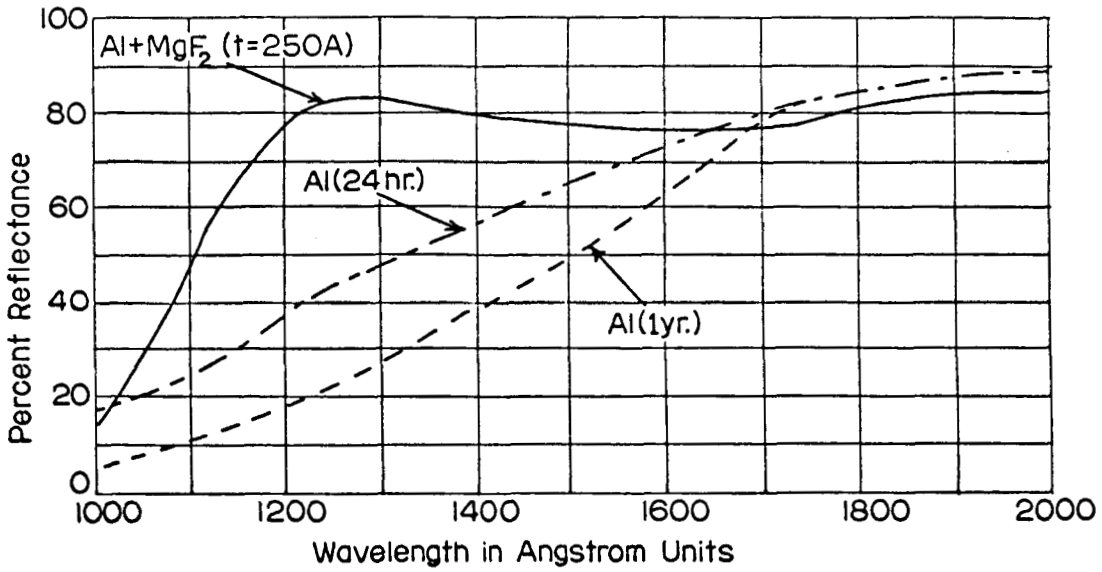

Figure 4-1 Reflectivity of Aluminum Surfaces

Due to extremely poor performance of the original grating, noticed especially below 1500 A, two measures were taken. A new grating coated with MgF_2 was ordered from Bausch and Lomb, and an attempt was made to improve the original grating by adding a MgF_2 coating.

The grating was taken to Bausch and Lomb by the author where it was cleaned, a fresh coat of aluminum deposited on the surface, and a MgF_2 coating added. The reflectance at 1215 A was measured at 71% following this treatment. The success of this venture was due largely to the assistance and advice provided by Mr. D. Richardson of Bausch and Lomb.

On returning the grating to the spectrograph an increase in efficiency over previous performance of 15 times was measured at 1215 A and 40 times at 1026 A. Response at 584 A and above 1600 A was approximately the same as before, while response at 304 A and below was somewhat poorer.

These observations are rather comparable to measurements by Wilkinson and Angel (1962) on a similarly coated grating; they reported an improvement of 20 times at 1215 A.

It would appear safe to conclude that the reflectivity of the MgF_2 coated grating is of the form shown in Figure 4.1, that is, relatively constant down to about 1200 A.

4.2.2 Detector Response

Photomultipliers with a sodium salicylate film added to the window surface have become widely used as detectors for the ultraviolet region, as discussed in section 2.6. The sodium salicylate fluorescence occurs in a wavelength region centred about 4400 A that matches the wavelength of maximum sensitivity of most photomultipliers.

It has generally been considered that the relative quantum yield of sodium salicylate is constant over a wide spectral range. Recent measurements however, by a number of workers, have indicated that this is only approximately so and under certain conditions the quantum yield may decrease markedly.

The relative quantum yield of freshly prepared samples of sodium salicylate of thickness 1.5 - 7 mg/cm^2 in the spectral region 900 to 2200 A, obtained from measurements by Kristianpoller and Knapp (1964) and Knapp and Smith (1964), are shown in Figure 4.2. The yield of a 20 day old sample is also shown. This aging effect is quite pronounced below 1600 A and may continue until the yield at 900 A is only one-third of that at 1600 A [Samson (1964)].

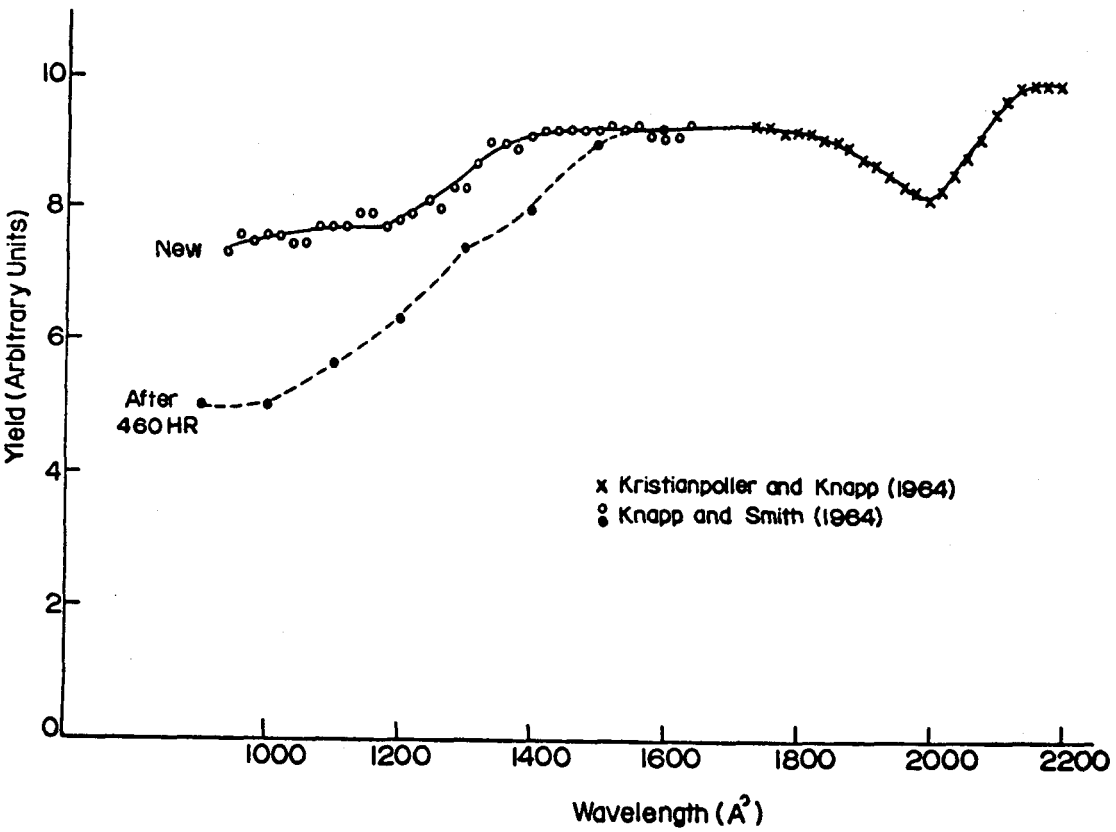

Figure 4·2 Relative Quantum Yield of Sodium Salicylate

The other feature noted is the decrease in yield between 2200 A and 2000 A. This decrease amounts to about 20% for the thickness of coating required for maximum efficiency (>1.5 mg/cm^2). Thinner films do not show the same decrease, but their efficiency is lower and they are more subject to fatigue effects when subject to high levels of radiation [Knapp and Smith (1964)] .

More recently Allison et al (1964) suggest that this apparent loss in efficiency is due to contamination by diffusion pump oil, since the yield of sodium salicylate is found to be stable for long periods in dry air or a clean vacuum. The only way to remedy this would be to use liquid nitrogen traps to reduce oil contamination of the interior of the spectrometer.

It is thus seen that detector response can be maintained reasonably constant only if age and fatigue effects and/or contamination effects are avoided, and even then one must expect deviations of up to 25% at 2000 **A** and below 1400 **A**.

4.2.3 Grating Efficiency

The efficiency of a grating changes greatly with wavelength since gratings are ordinarily blazed to concentrate the spectral energy into a desired angular region. This is accomplished by controlling the face angle of the ruled grooves of the grating. The groove face angle with respect to the grating normal is called the blaze angle. The wavelength of the light for which the angle of reflection from the groove face and the angle of diffraction from the grating are the same is the blaze wavelength, λ_b. This value is usually specified as the first order wavelength; the blaze wavelength for higher orders is determined by the blaze wavelength divided by the order number. A grating is most efficient at its blaze wavelength, and in high quality gratings this efficiency may be as high as 80 - 90%.

Richardson (1964) has found that as a general rule grating efficiency has dropped to about one-half the peak efficiency at 3/2 λ_b and 2/3 λ_b. Thus if one has definite information or measurement which defines the blaze wavelength it is possible to predict qualitatively how the grating should perform at any wavelength.

The manufacturer's specification of the present grating was a 2^o blaze angle, corresponding to a blaze wavelength of 1200 **A** in the first order.

4.2.4 Combined Effect

The above three parameters will together determine the overall response of the spectrometer. From this discussion of the wavelength dependence of each it is possible to picture their combined effect and thus to arrive at a good estimate of the relative sensitivity of the spectrometer as a function of wavelength. This can be of considerable value in assessing the reliability of calibration measurements. This point will be discussed further in section 4.4.

4.3 Calibration Methods and Results

Four different calibration techniques were investigated in the hope that one or more would prove of value and that individually or collectively they would provide a reliable measure of spectrometer sensitivity as a function of wavelength. The first two methods involved the use of Cerenkov radiation and a carbon arc as radiation standards. The third method involved observation of short wavelength atomic lines in higher diffraction orders, and the last method utilized a number of atomic lines whose relative intensities could be calculated.

4.3.1 Cerenkov Radiation

When a fast charged particle travels through a transparent medium with a velocity greater than the speed of light in the medium an optical "shock wave" known as Cerenkov radiation is generated. The number of photons dN emitted as Cerenkov radiation per unit path length per particle is given by

$$\frac{dN}{dl} = A \int \left[\beta\, n(\lambda) - 1\right] \frac{d\lambda}{\lambda^2} \quad , \tag{4.1}$$

where A is a constant, β is the ratio of the velocity of the particle to the velocity of light in the medium and $n(\lambda)$ is the index of refraction of the medium. The radiation is emitted in a cone of half angle θ to the original beam direction where

$$\cos \theta = \frac{1}{\beta n} \tag{4.2}$$

The theory is discussed fully by Jelley (1958). The significant point here is that the energy radiated is inversely proportional to λ^3, for constant β and n.

This radiation appears to have application to the vacuum ultraviolet region as a standard source since its intensity as a function of wavelength can be calculated and, contrary to most sources, its intensity rapidly increases towards shorter wavelengths. The requirements are readily seen - a source of electrons of sufficient energy and a medium which will transmit the short wavelength radiation generated.

It has been confirmed experimentally that the radiation is of the spectral form predicted. Rich et al (1953) measured the spectral distribution of the Cerenkov radiation induced in water by gamma rays from a Co^{60} source and found good agreement with theory between 6000 A and 3500 A. A similar experiment by Greenfield et al (1953) using a 300 mg radium source, and also 3 millicuries of P^{32} in water gave Cerenkov radiation of the expected spectral distribution from 5000 A to 3000 A.

While a choice of several materials is available as media above 3000 A, lithium fluoride is one of the few materials which will transmit

well down into the vacuum ultraviolet region. It does not fluoresce and its index of refraction has been measured down to 1200 A (Schneider (1936)).

For preliminary studies a 20 mc. St^{90} source, emitting mainly 2.2 Mev β rays, was used with LiF as a radiator. Sufficient thickness was used to stop the β rays. The source and LiF absorber were placed in the evacuated spectrograph immediately in front of the slit and attempts were made to record the Cerenkov radiation photographically. Nothing was recorded however, even with exposures up to 100 hours duration with a 2 mm wide slit.

The electron beam from a 6 Mev microtron was made available through the courtesy of Dr. E. Brannen and Mr. V. Sells and the study was pursued using a 9/16 inch thick LiF block as an absorber. The source was sufficiently strong (equivalent to several curies) that the Cerenkov radiation was clearly visible, having a bluish-white appearance. Spectra were obtained with a Hilger F4 quartz spectrograph; they showed a continuum extending down to about 2750 A where there appeared to be a sharp cut-off.

To examine the spectrum more carefully an Ebert $\frac{1}{2}$ meter scanning spectrometer was set up at about 45° from the beam axis and at a distance of about 50 cm from the LiF source. The spectral region from 3500 A to 2000 A (the end of the scanning range of the spectrometer) was scanned using a 2 mm slit width. A number of spectra were obtained, all showing a continuum gradually increasing in intensity down to about 3000 A and then dropping off rather sharply to zero by about 2600 A.

There was a small amount of radiation recorded below 2300 A. The average of four spectral scans each using different areas of the LiF block as absorber is shown in Figure 4.3a.

This raw data was converted to true relative intensity by measuring the spectral response of the spectrometer and the optical transmission of the LiF block both as functions of wavelength. The resulting data is plotted in Figure 4.3b. It is terminated at 2900 A because it was found that the transmission of the LiF block decreased sharply to zero beyond this point.

This was found to be due to the formation of F-centres in the LiF crystal which resulted in a broad absorption band peaked at about 2420 A. The formation of F-centres in LiF crystals exposed to x-ray or particle bombardment has been studied by Delbecq and Pringsheim (1953) and others.

The deviation of the Cerenkov spectrum above 3000 A from a $1/\lambda^3$ type distribution (also shown in Figure 4.3) may be explained in one or more of the following ways. The optical transmission of the LiF block was measured 24 hours after the radiation measurements and its properties may have changed somewhat in that time, since a secondary absorption band centred at 3450 A has been observed by Pringsheim and Yuster (1950) at lower temperatures. The angle of emission of radiation is dependent upon the index of refraction of LiF, as shown in equation 4.1, and n does change slowly with wavelength. Varying the viewing angle of the spectrometer a few degrees however did not appear to change substantially the spectral distribution. Noise pickup by the photo-multiplier was rather large when the microtron was operating and this

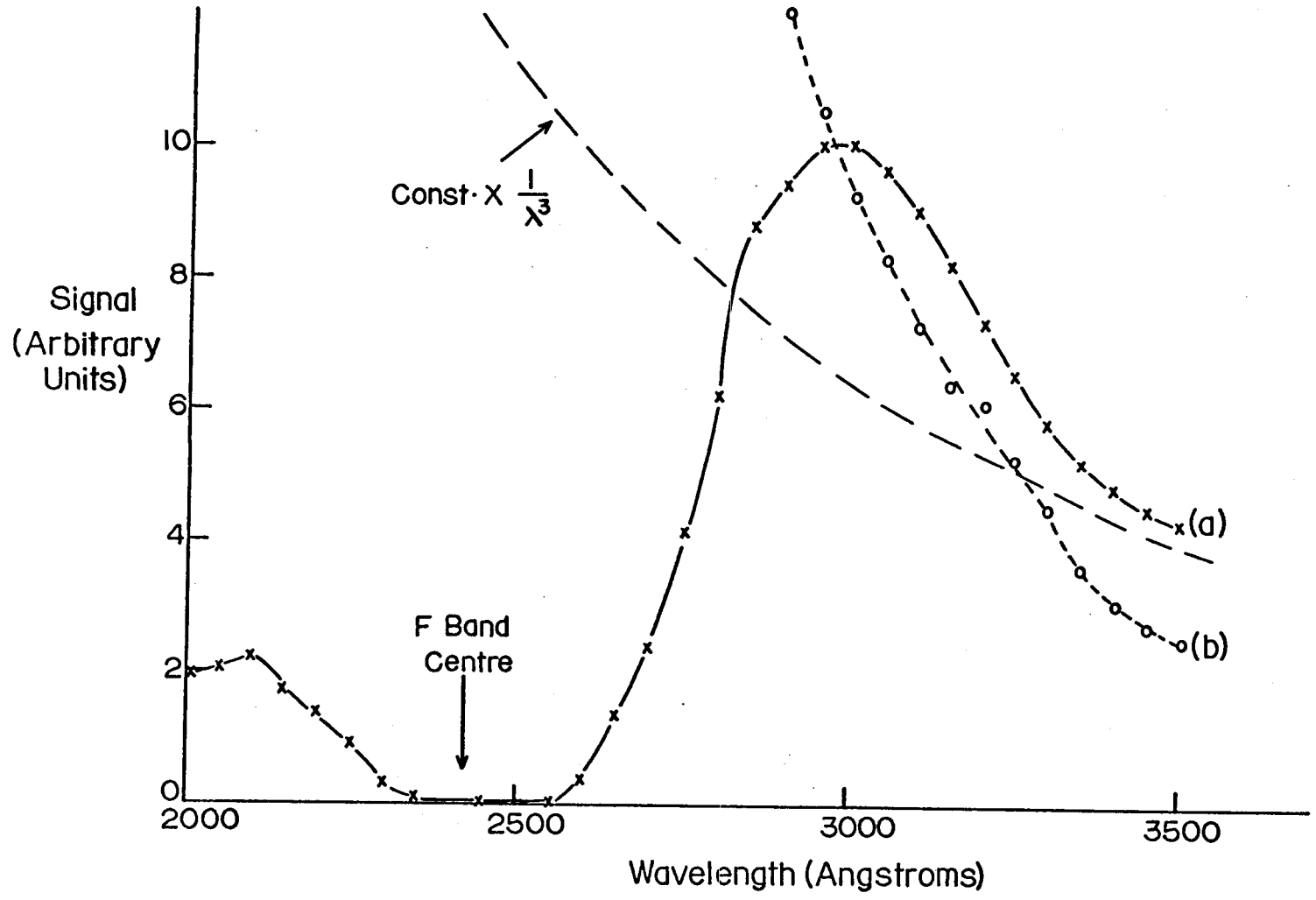

Figure 4·3 Spectral Distribution of Radiation Induced in LiF by 6 Mev Electrons
(a) Recorded Signal (b) Corrected for Spectrometer Response and LiF Transmission

resulted in a low signal to noise ratio at the two extremities of the spectral region.

These preliminary studies indicated that Cerenkov radiation with LiF as the medium was of no value as a radiation standard in the ultraviolet, due to the extreme sensitivity of LiF to radiation not only above 2000 A as shown in this study but also at shorter wavelengths as discussed in section 2.4.

Possible alternatives might be either magnesium fluoride or calcium fluoride which are normally transparent in the vacuum ultraviolet. This would require further studies of the optical properties of these crystals. It is doubtful that either would prove satisfactory however as all the alkali halides react somewhat similarly in the formation of colour centres when exposed to particle bombardment. The use of a cell of gas at high pressure as a Cerenkov chamber is a distinct possibility. It is interesting to note that Heddle et al (1963) used such a cell of nitrogen at pressures of 10 to 20 atmospheres in a similar experiment but with a different objective - to measure the index of refraction of N_2 at short wavelengths.

4.3.2 High Order Diffraction

A measure of the blaze wavelength and the grating response can be obtained relatively simply by observing short wavelength lines in higher orders and measuring their relative intensities in the various orders. In spectral regions where the reflectance of the grating and the sensitivity of the detector are constant such measurements will give a direct measure of spectrometer efficiency. There are naturally limitations to this technique and a number of precautions which must be taken.

An example of the application of this technique is measurement of the relative brightness of the HeI 584 A line in the first to fifth diffraction orders - corresponding to first order wavelengths of 584, 1169, 1753, 2337 and 2921 A respectively. It is necessary to take account of the constant quantum efficiency of the detector, to place these measurements on a meaningful scale. This necessity is illustrated by considering a photon of wavelength 2921 A; its energy is only 1/5 that of a photon of wavelength 584 A, and yet the detector cannot discriminate between the two photons. Thus from a standpoint of sensitivity the detector is really 5 times more sensitive at 2921 A than the higher order measurement suggests. This factor is most easily taken into account by multiplying each measured brightness by the order number n. The results will then be meaningful as measures of relative spectrometer efficiencies at the equivalent wavelengths of the higher order lines.

Such measurements can be used only when no other spectral lines or bands are present at higher order wavelengths and this in general will limit one to simple atomic lines. It is most effective using lines of very short wavelength such that they can be observed in many orders; one such line is the He II 304 A line, which unfortunately is not easily observable with the present grating.

A hollow cathode DC discharge (described in section 4.3.4.2) proved to be a satisfactory source for such measurements, using gases filtered by a liquid air trap. This type of discharge provided lines sufficiently stable and bright that relative intensity measurements could be made photoelectrically.

Atomic lines used were HeI 584 A, Ne II 736 A and H 1216 A, excited in helium, neon and hydrogen discharges respectively. Results are tabulated in Table 4.1; in each case measurements are relative to the first order intensity. The results are shown graphically in Figure 4.10.

Table 4.1

Higher Order Measurements of Atomic Lines

Order Number n	Atomic Line (A)	Equivalent Wavelength (A)	Relative Signal	Rel. Signal xn
1	HeI	584	1.00	1.00
2		1169	1.08	2.17
3		1753	1.42	4.26
4		2337	1.93	7.32
5		2921	2.02	10.10
1	NeII	736	1.00	1.00
2		1472	1.90	3.80
3		2208	2.71	8.13
4		2944	3.10	12.40
1	H	1216	1.00	1.00
2		2431	1.56	3.12

The figures in column 4 correspond to the relative efficiency of the grating at the wavelengths specified in column 3 while the data in column 5 should correspond approximately to the relative efficiency of the spectrometer as a whole, for all wavelengths for which the grating reflectivity is constant. The three sets of measurements are independent; to compare with one another it would be necessary to normalize them at some wavelength where the spectrometer response is known.

These measurements show conclusively that the grating efficiency is increasing to well above 2000 A. It is not possible to define the

blaze wavelength since measurements above 3000 A could not be made; it would seem however that the blaze wavelength is in the vicinity of 2900 A (or higher).

4.3.3 Carbon Arc

The radiation from the positive crater of a pure carbon arc has found many uses due to its high intensity, but also has proven to be very useful as a radiation standard because of the reproducibility of its spectral energy distribution. When the arc is burning steadily the crater radiates similarly to a black body at approximately 3800°K, except for cyanogen molecular radiation at certain wavelengths. Use of the carbon arc as an intensity standard has been suggested and discussed by Macpherson (1940) and more recently by Null and Lozier (1962).

The spectral region of interest in the present case of course is that below 3000 A. The carbon arc radiates essentially as a black body from 3000 to 2500 A; below this the radiation consists largely of cyanogen radiation from the arc stream. Johnson (1956) has investigated the emission from the arc stream and measured the spectral radiance of the carbon arc from 2500 A down to the air cut off at 1850 A, by using a grating monochromator with a diffraction grating previously calibrated by a double monochromator technique and a photomultiplier coated with sodium salicylate. His measurements were made by viewing the positive crater end on through a small aperture to eliminate contributions from the arc stream surrounding the crater. Spectral radiances obtained by him are shown in Figure 4.4. The relative contributions of the crater and the arc stream are shown. The carbon lines at 1931 and 2478 A appear prominently in the spectrum.

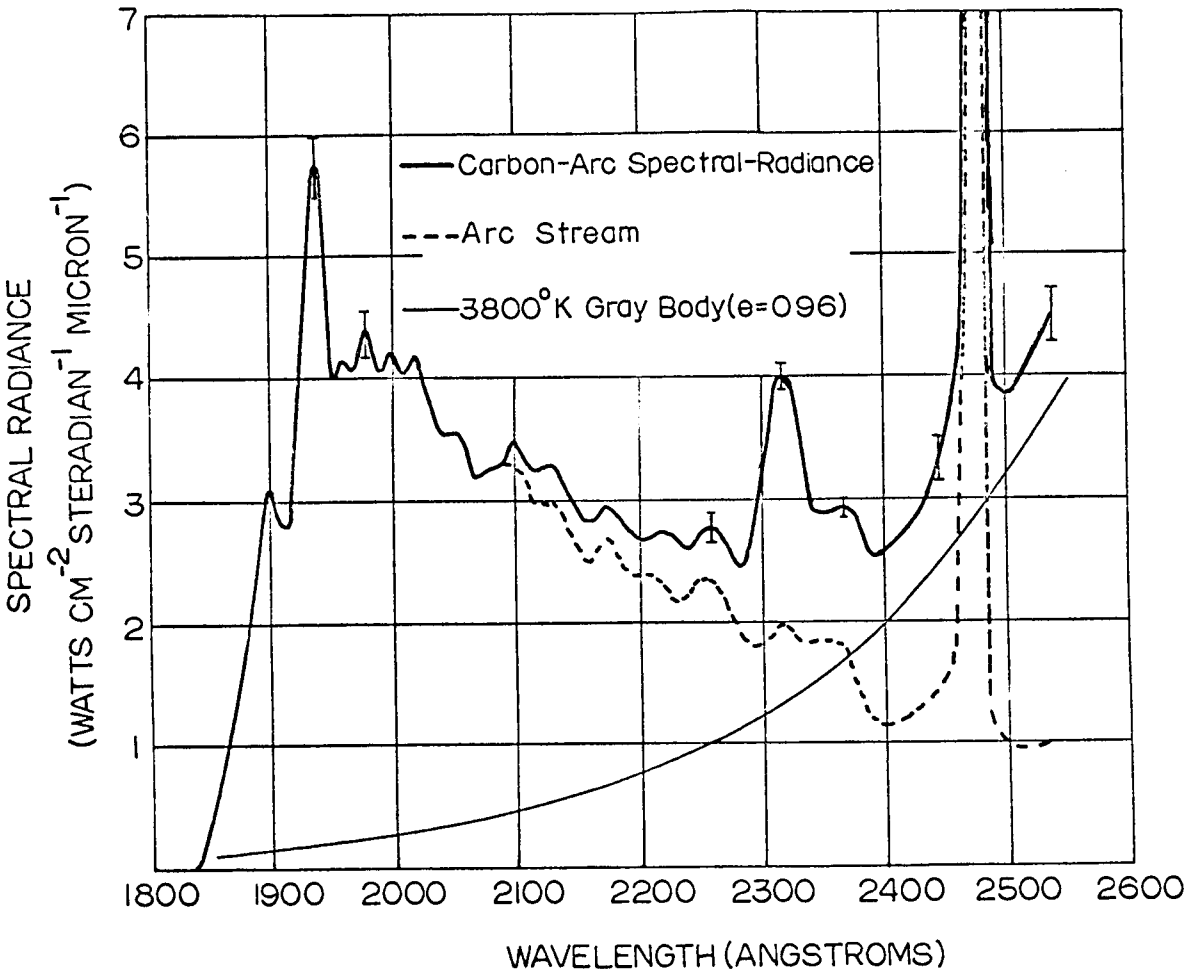

Figure 4·4 Spectral Radiance of Carbon Arc [Johnston (1956)]

Since a carbon arc designed for spectroscopic work was available it was decided to use it to measure overall spectrograph efficiency from 3000 A down to 1900 A.

No particular precautions were required for the upper region 3000 to 2500 A, other than proper illumination of the grating. As the arc is essentially a point source it illuminated only a vertical strip of the grating approximately 15 mm wide. Thus to obtain measurements applicable to the whole grating, calibrations were carried out with the center of the grating illuminated, then strips 20 mm on either side of the center and an average of the three was taken. While no appreciable differences were detected across the surface of the grating, the same techniques were employed for the lower region of the calibration 2500 - 1900 A.

In order to obtain reliable data from 2500 to 1900 A it was necessary to duplicate as closely as possible the operating conditions employed by Johnson (1956). Those measurements were obtained using a 5/16" carbon positive electrode and a 1/8" graphite negative electrode. The radiation was filtered by 120 cm of air and recorded with a spectral resolution of 11 A. The experimental arrangement to duplicate these conditions required some minor improvising so it is worthwhile to outline the techniques employed.

A nickel plate with a 2.4 mm diameter hole was mounted 2 cm in front of the carbon arc anode. This limited the region viewed to the center of the crater area. The carbon arc was placed 50 cm in front of the entrance slit of the spectrograph, as close as physically possible.

An equivalent air path of 120 cm between source and detector was obtained by evacuating the spectrograph to approximately 90 mm of Hg.

Slit widths of 1.93 mm were required to obtain a spectral resolution of 11 A. This necessitated the removal of the preslit which had a maximum opening of only 1 mm. A suitable exit slit was obtained by temporarily widening one of the fixed slits. This duplication was essential to avoid instrumental errors in measurements of spectral radiance below 2500 A.

The carbon arc was operated at a current of 12.0 ± 0.5 amperes and a voltage of approximately 70 volts. It was impossible to avoid minor fluctuations in the current, however observations indicated that as long as the current was maintained near the maximum level before unsteadiness and sputtering occurred, the temperature and output of the arc remained reasonably constant.

The spectrum was scanned at the rate of 100 A per minute, the maximum available speed. Very large light fluxes were incident on the photomultiplier, due to the combination of the wide slits and the high intensity source. The photomultiplier was therefore operated at a reduced voltage (approximately 700 volts); measured currents were of the order of 10^{-8} amperes.

Scattered light was naturally a serious problem using a source of this type. It was reduced somewhat by masking, but still amounted to about 1/3 of the total signal at the weakest part of the spectrum. The stray light level did not change with wavelength below the air cutoff at 1800 A. Its contribution through the spectral range to

3000 A was measured by placing a 0-54 Corning filter (which transmitted only above 3000 Å) in front of the source and scanning over the range. The stray light signal level was found to be approximately constant from 1700 A through to 3000 Å, except for a spurious signal caused by some sort of reflection at 2150 to 2200 A.

A representative scan is shown in Figure 4.5, with the total signal measured, and the contribution from scattered light. The true signal was obtained by subtracting the scattered light from the total signal.

It was originally assumed that the transmission of the LiF window in the spectrograph would be approximately constant from 3000 to 1900 Å. Transmission measurements showed this was true only down to 2500 Å. From 2500 to 1900 A the transmission of the particular window used during the calibration measurements decreased gradually from 53% to 45%. This factor had to be taken into account in arriving at spectrometer sensitivity values.

The upper spectral region from 2500 to 3000 A was covered with the same arc conditions, but with the spectrograph slits closed down to 0.1 mm. Spectral radiances for a black body at 3800°K were obtained from Pivovonsky and Nagel (1961).

To decrease the effect of random fluctuations in carbon arc intensity approximately 10 runs were made in each of the two spectral ranges, and the results averaged. For the region above 2500 Å deflections were measured every 50 A; below 2500 Å wavelengths for which spectral radiances were known were used, in general about every 50 A if possible. Dividing the measured signal at each wavelength by the spectral radiance and

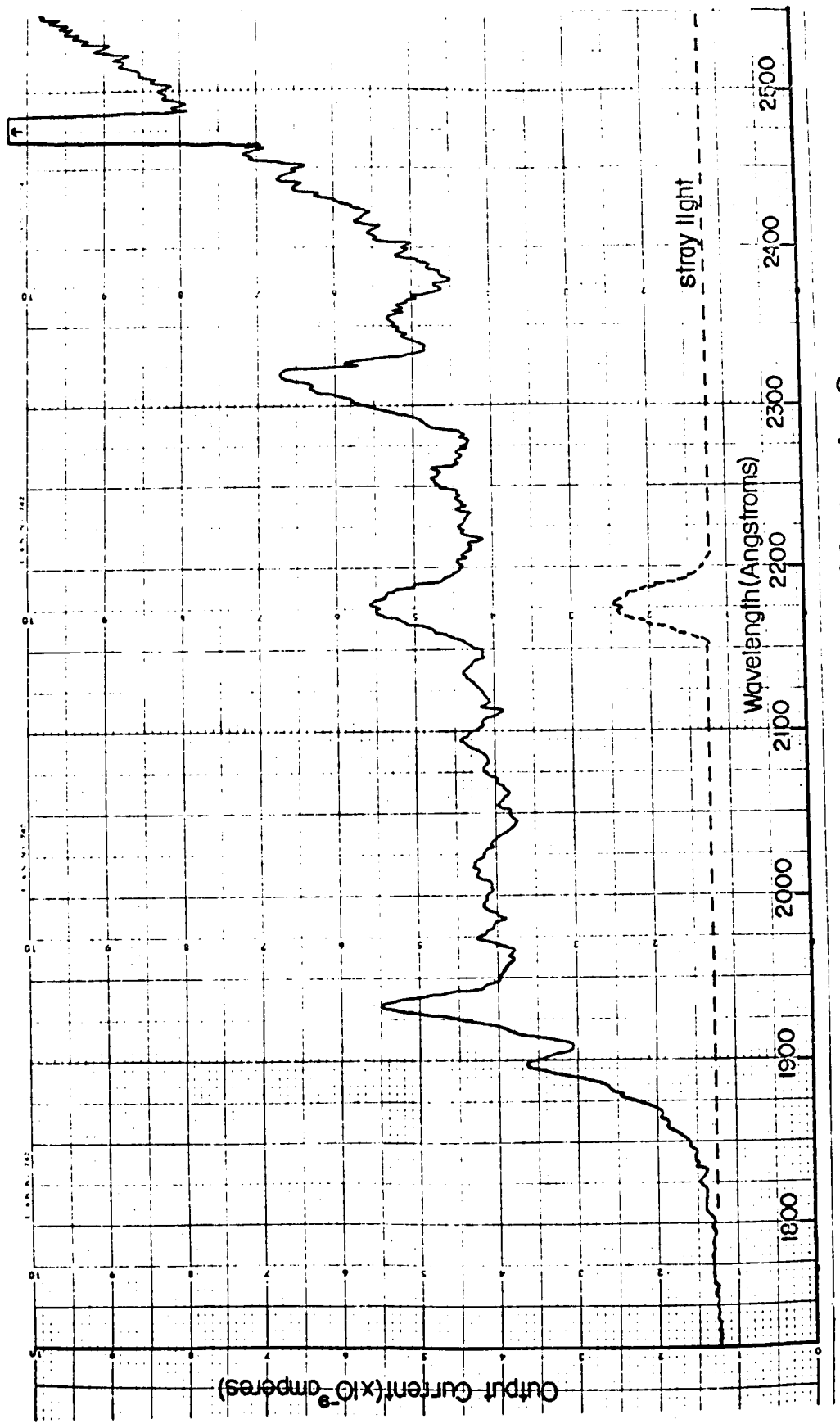

Figure 4·5 Typical Scan of Carbon Arc Source.
The stray light contribution to the total signal is also shown.

applying a transmission correction factor where applicable provided a measure of relative spectrometer efficiency at each wavelength. The values below 2500 Å were matched to those above by normalizing the scales to give equal sensitivities at 2500 A. Finally the values were normalized to a value of 100 at the wavelength of peak sensitivity, which was 2850 A.

The results are listed in Table 4.2 and shown graphically in Figure 4.10.

4.3.4 Atomic Line Intensities

4.3.4.1 Theory

The method is based on observations of pairs of spectral lines originating from a common upper energy level in an atom for which the atomic transition probabilities are accurately known. If one of the lines lies above about 3000 Å its absolute intensity can be measured by comparison with the radiation from a standard such as a tungsten ribbon lamp; the intensity of the other line lying in the vacuum ultraviolet region can then be calculated.

Such a pair of lines are the hydrogen lines Balmer α and Lyman β. The lines are produced in the hydrogen atom by transitions from the excited level having the principal quantum number n = 3 to the ground state (Lyman β, 1026 A) and to the state n = 2 (Balmer α, 6563 Å). These transitions are illustrated in Figure 4.6.

The theoretical calculations of transition probabilities can be carried out accurately for hydrogen and other one-electron systems (such as He II). They involve the evaluation of the integral

$$R_{nl}^{n'l'} = \int_0^\infty R_{nl}\, R_{n'l'}\, r\, dr\,, \qquad (4.3)$$

Table 4.2

Relative Sensitivity Measurements from Carbon Arc Source

Wavelength (Angstroms)	Spectral Radiance (Watts/cm^2 sterad micron)	Relative Spectrometer Sensitivity
3000	16.30	87
2950	14.31	92
2900	12.50	97
2850	10.84	100
2800	9.34	99
2750	8.00	97
2700	6.79	95
2650	6.00	95
2600	5.35	92
2550	4.53	87
2500	3.82	84
2452	3.49	74
2400	2.65	71
2358	2.89	67
2317	4.06	63
2252	2.78	60
2207	2.77	52
2129	3.25	46
2094	3.48	45
2051	3.60	40
2012	4.14	39
1977	4.38	38
1931	5.74	43
1898	3.08	43

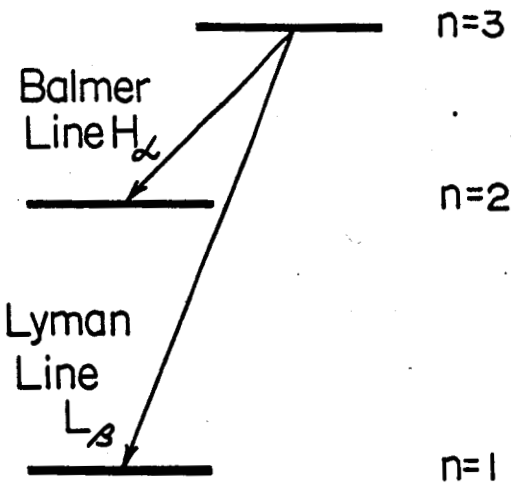

Figure 4-6 Simplified Energy Levels of Hydrogen

where R_{nl} and $R_{n'l'}$ are the normalized radial eigenfunctions and n and l correspond to the principal and azimuthal quantum numbers respectively. Both the calculations and the results are discussed fully by Bethe and Salpeter (1957) and Condon and Shortley (1935).

This method was investigated by Griffin and McWhirter (1961) who measured intensities of H_α and L_β in hydrogen discharges in the Zeta torus.

While in principle the method appears to be simple, there are two conditions which must be satisfied for the results to be reliable. The light source and the path to the detector must be optically thin to both lines, and, the population distribution of the various sub-levels of the upper level must be proportional to their statistical weights. This is important because some fine structure levels contribute to one line of the pair being observed and not the other, while the transition probabilities used are averages over all fine structure components, weighted by the statistical weight of each sublevel.

This situation is illustrated in Figure 4.7, an energy level diagram of hydrogen. Solid lines refer to allowed transitions while broken lines are forbidden transitions. It is seen that L_β is a 1s-3p transition while H_α includes not only 2s-3p but also 2p-3d and 2p-3s transitions. Thus if the s, p and d sublevels are not populated according to their statistical weights the L_β/H_α intensity ratio will differ from that calculated from their transition probabilities.

The effects of non statistical populations and the conditions necessary for statistical population of sublevels are discussed by Hinnov and Hofmann (1963) who used the Lyman series of hydrogen and the similar series of ionized helium to obtain a calibration from 231 **A** to 1026 **A** with an additional two points at 1085 A and 1640 **A** from the ionized helium Balmer series.

The calculation required for determining spectrometer sensitivity S_λ at a particular wavelength is straightforward. The intensity of an emission spectrum line for a given transition $n \rightarrow m$ is given by the expression

$$I_{nm} = N_n \, h\nu \, A_{nm} \quad , \tag{4.4}$$

where N_n is the number of atoms in the initial state and A_{nm} is the number of transitions per second per atom, the so-called Einstein transition probability, and $h\nu$ is the energy of the radiated quantum.

In general also the observed intensity of a spectral line may be expressed

$$I_\lambda = K \, D_\lambda / S_\lambda \tag{4.5}$$

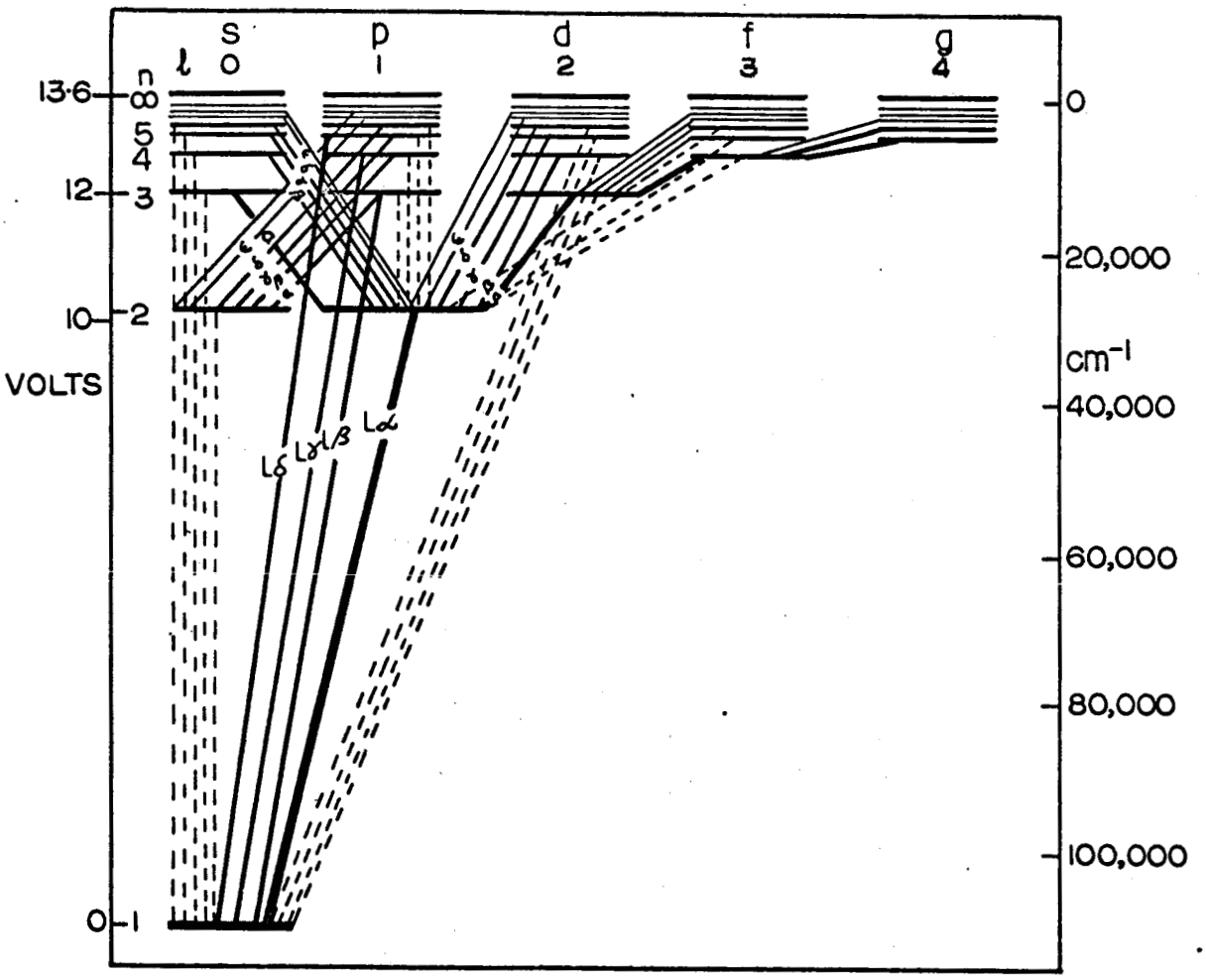

Figure 4·7 Energy Level Diagram for Hydrogen

for a spectrometer where D_λ is the measured photocurrent, S_λ is the instrument sensitivity and K is a constant including source and slit geometry.

Combining equations 4.4 and 4.5 it is easily shown that for any pair of spectral lines originating from the same upper level, and identifying the parameters pertaining to these lines by subscripts v and u signifying visible and ultraviolet respectively,

$$I_v \times \frac{S_u}{D_u} = C \frac{\upsilon_v A_v}{\upsilon_u A_u} \quad , \tag{4.6}$$

or, in a more useful form

$$S_u = C \frac{D_u}{I_v} \left[\frac{\lambda_u A_v}{\lambda_v A_u} \right] \quad . \tag{4.7}$$

Here C is a new constant including slit characteristics of the two monochromators, solid angles subtended by the source at the slits and transmission characteristics of any windows. Since only relative sensitivities are required it may be neglected, provided that it remain constant throughout the series of measurements. The quantities in the brackets for a selected pair of lines are constants and may be obtained from Allen (1963).

Thus the determination of spectrometer sensitivity, S_u, at the wavelength of the ultraviolet line involves only the recording of the spectrometer signal D_u for that line and the measurement of the intensity of the second line of the pair I_v using a second monochromator.

The only available lines of the one electron type in the region below 3000 A were found to be the hydrogen Lyman lines at 1026 and 972 A,

the ionized helium Balmer lines at 1640, 1215, and 1085 A and the Paschen lines at 2733, 2511 and 2386 A. These lines are identified in the spectra in Figure 4.8. They will be discussed in more detail in succeeding sections.

The Paschen series lines of ionized helium lie beyond the vacuum region of the ultraviolet but there are two important reasons for including them. They are in a spectral region where an independent calibration is possible (eg with carbon arc) and thus serve as a check on the reliability of the method, and secondly they provide an overlap so that the calibrations at the shorter wavelengths can be put on a proper relative scale.

4.3.4.2 Experimental Technique

Various gas discharges were tried as light sources; a hollow cathode discharge provided the He II and H lines with good intensity and stability. A cross-sectional view of the discharge tube built for this purpose is shown in Figure 4.9. It also appears mounted in front of the entrance slit of the spectrograph in Figure 2.7.

The hollow cathode was 5/8" in diameter and 4" long. A teflon spacer separated it from the concentric anode ring whose inner diameter was 3/4". Both cathode and anode were made of brass for ease of construction and both were water cooled. A quartz window was placed on the outer side of the anode and a bakelite plate secured these components to the cathode assembly which was in turn held against a lucite plate on the entrance flange of the spectrograph. O-rings were used to make vacuum seals between the various components of the discharge tube.

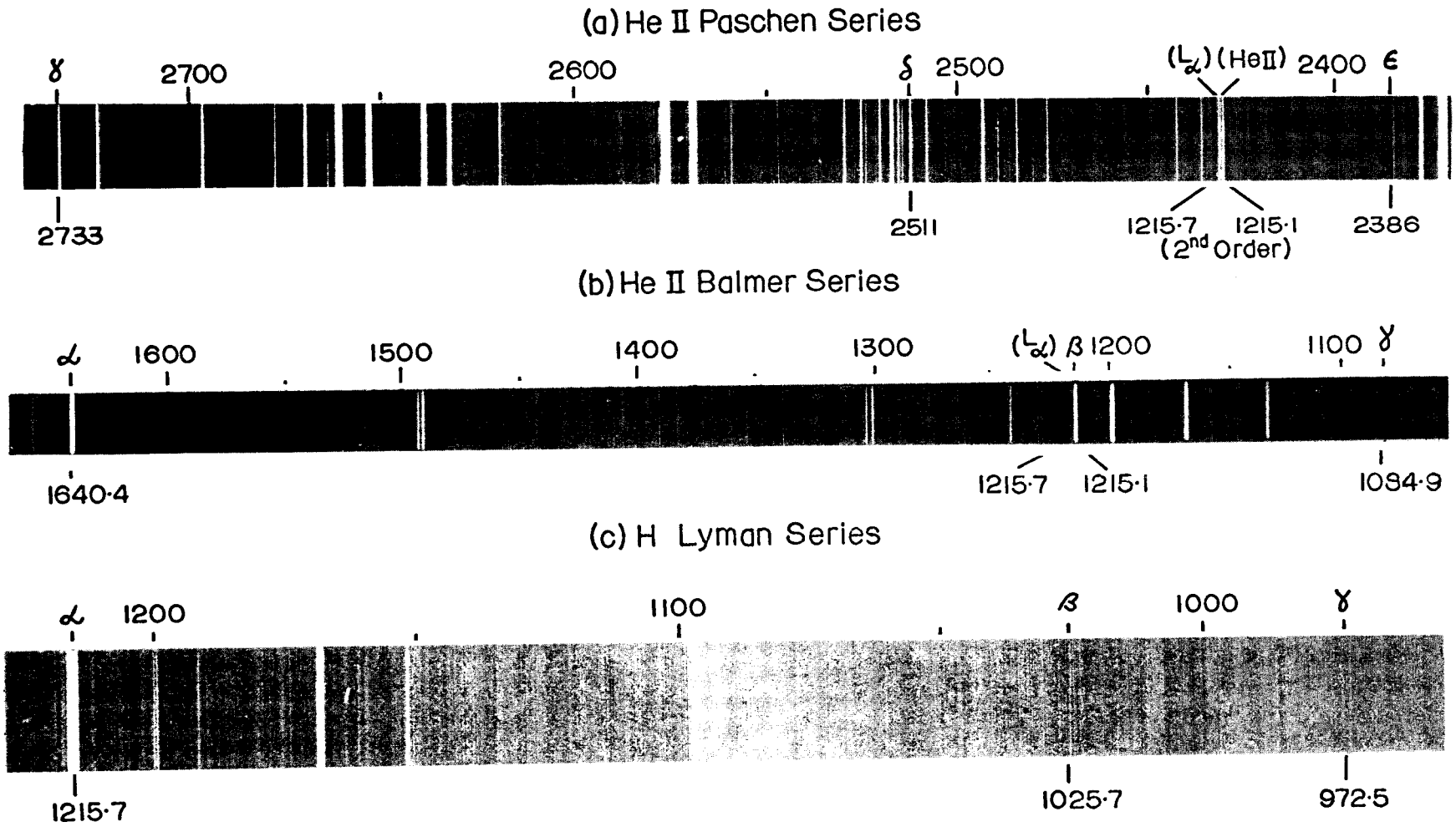

Figure 4·8 Helium and Hydrogen Series Spectra (Wavelengths in Angstroms)

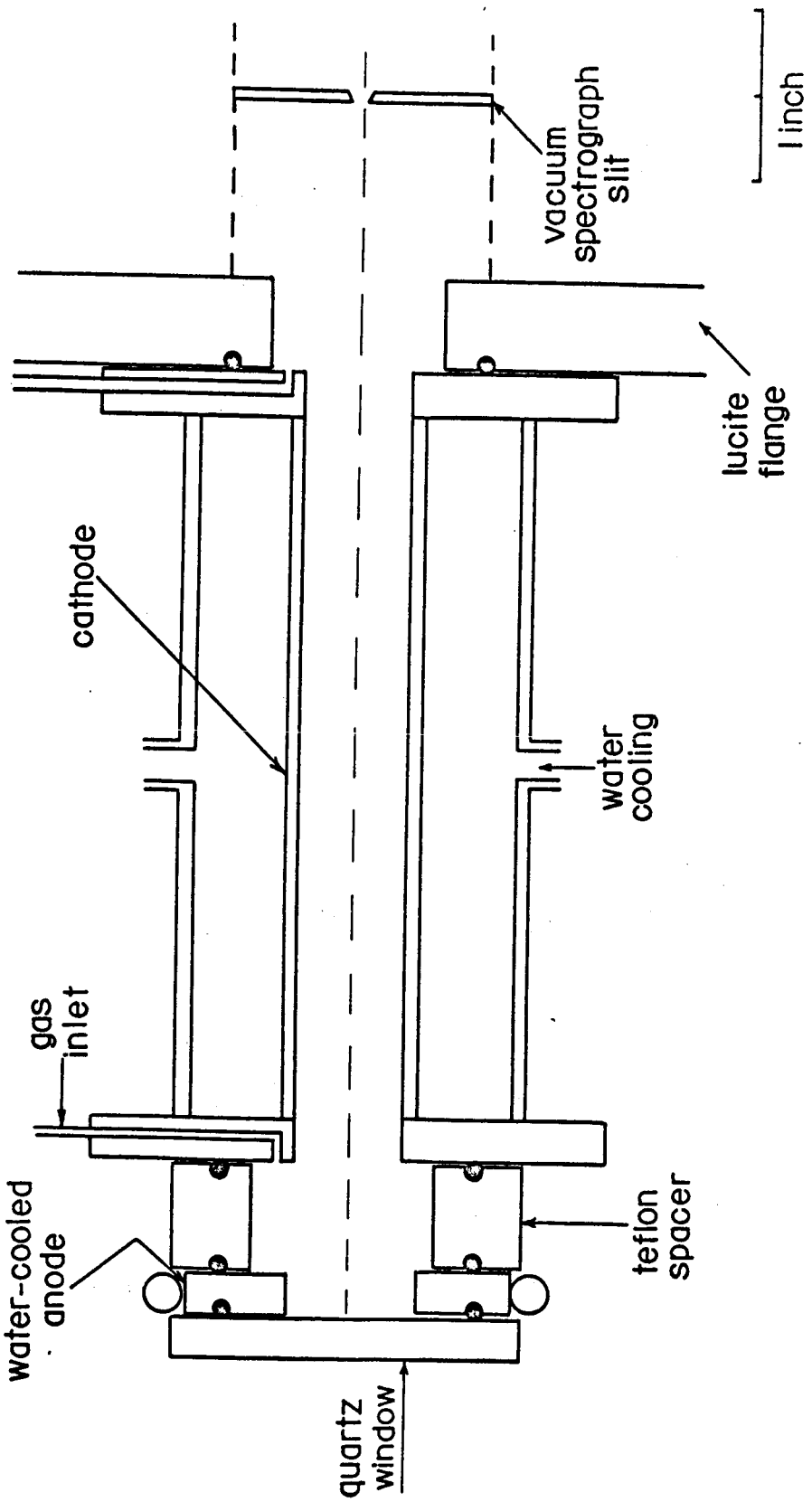

Figure 4.9 Cross-sectional View of Hollow Cathode Discharge Tube

A thin aluminum liner was later inserted in the hollow cathode when it was observed that the brass was eroding and depositing on the quartz window thus impairing its transmission. A thin quartz cylinder was also inserted inside the teflon spacer to protect it from surface heating.

Helium was flowed through the system at a controlled rate. A liquid nitrogen trap immediately before the discharge tube served to remove condensable impurities such as water vapour from the gas stream. The discharge was operated normally at a current of 250 ma and a voltage of about 250 volts. Power was provided by a 1000 volt DC supply with a suitable ballast resistor. The pressure in the discharge was about 0.3 mm Hg while the spectrometer pressure was approximately 2×10^{-3} mm Hg.

The discharge consisted of a tubular column extending the full length of the cathode. A coarse mesh screen was placed across the end of the cathode to prevent the discharge column from continuing on through to the entrance slit.

This discharge tube proved to be very useful, not only for calibration purposes, but also for exciting other atomic and molecular spectra. It provided a very stable and reproducible discharge of high intensity and could be operated over a wide range of pressures and currents.

The helium and hydrogen lines used for calibration measurements are illustrated in Figure 4.8. All were obtained with a .01 mm slit on Kodak 103-0 U.V. sensitized plates. The first was a 20 minute exposure while the latter two were 2 hour exposures. The strong

impurity lines are mainly Al II lines; a number of weaker N and O lines are also present.

The He II line at 1215.1 A is normally swamped by the H Lyman α line at 1215.7 A which is many times stronger. The hydrogen impurity evidently appeared as a result of dissociation of water vapour because after careful elimination of all leaks and several hours of outgassing with the discharge on and the liquid nitrogen trap in operation the Lyman α line intensity was reduced sufficiently to permit measurement of the nearby He II line. The Lyman α line is a very broad resonance line and this combined with its small separation from the helium line made accurate measurement of the helium line difficult. It was found very advantageous to make the measurement in the second order and convert it to an equivalent first order reading. The conversion factor was reliably determined to be 0.64 (see section 4.3.2). The two lines well resolved in second order may be seen in the first spectrum of Figure 4.8.

Line intensities in the spectral range 3200 to 6600 A were measured through the quartz window of the discharge tube with a $\frac{1}{2}$ meter Ebert type spectrometer, while the discharge was viewed simultaneously from the other end by the vacuum spectrometer.

A complete calibration was carried out by first recording photoelectrically the amplitudes of the hydrogen lines at 1026 and 972 A in the helium discharge with the liquid nitrogen trap removed (allowing the water vapour impurity through to provide a source of hydrogen) then inserting the trap again and continuing with the helium line

measurements after the helium discharge was sufficiently pure. The slit-width for all measurements was 200 microns, with the exception of the He II line where it was necessary to use 50 microns to resolve the line from Lyman α . The proper slit-width conversion factor was obtained by recording the He II 1640 A line at both slit-widths.

To avoid any errors due to either hyperfine structure or instrumental effects, areas under the line profiles were measured. The results were not noticeably different from simply recording peak amplitudes however.

4.3.4.3 Results

The results obtained are tabulated in Table 4.3. The signal strengths for the ultraviolet lines given in column 2 are in arbitrary units of photocurrent. The intensities of the comparison lines from 6560 to 3203 A given in column 6 are included since their relative values remained reasonably constant for the operating conditions outlined. The upper energy level from which each pair of lines originated is given by the principal quantum number n'. The spectrometer sensitivities (S_λ) given in column 3 were obtained by means of equation 4.7.

Intensity values for the hydrogen Balmer lines are omitted since their intensity ratio was strongly dependent upon the operating conditions and the source of hydrogen. Signal strengths of the hydrogen Lyman lines are omitted for the same reason. This does not affect the reliability of the S_λ values for those wavelengths however as they were obtained from simultaneous measurements.

Table 4.3

Spectrometer Sensitivity (S_λ) Data from Line Intensities

λ_u (A)	D_u (Arb. Units)	S_λ	n'	λ_v (A)	I_v (Arb. Units)	Source
2733	1.00	100	6	6560	10.3	He II
2511	.47	89	7	5411	5.6	He II
2386	.21	77	8	4859	3.3	He II
1640	13.0	29	3			He II
1215	1.31	11.4	4	4686	100	He II
1085	.12	2.1	5	3203	46.0	He II
1026		.73	3	6563		H
972		.96	4	4861		H

The He II 1640 A line could not be used directly as a calibration point, since the only other spectral line arising from the same upper level ($n' = 3$) is at 256 A and not observable with the present grating. Hinnov (1964) has measured the intensity ratio of the 1640 and 1085 A lines to be 8:1 in a similar type of discharge. Hence, lacking more direct means, this value was used in arriving at a sensitivity value at 1640 A, by utilizing the directly measured sensitivity at 1085 A.

It is necessary now to consider the validity of these results in view of the limitations stated in section 4.3.4.1. There should be no error due to absorption for any of the lines chosen. The major constituent both in the discharge and in the spectrograph was helium which is transparent down to nearly 500 A. The matter of statistical equilibrium requires more careful consideration.

As discussed by Hinnov and Hofmann (1963) the statistical redistribution of sublevel populations in light sources of this type is largely caused by electron collisions, although energy exchange atomic collisions may contribute as well. Thus if the lifetime with respect to collisional transitions $nP \rightarrow nD$ is small compared to the radiative lifetime of the nP state, the latter may be expected to be in equilibrium with the other states of the n^{th} level. Hinnov and Hofmann, by estimating the electron collisional transition rate, arrive at the following condition for statistical equilibrium at the n^{th} state

$$\frac{6 \times 10^6 \, (kT_e)^{\frac{1}{2}}}{n^4 \, N_e} < \tau_R(nP) \, , \tag{4.7}$$

where $\tau_R(nP)$ is the radiative lifetime of the nP state, kT_e is expressed in electron volts and N_e is the electron density.

Hirschberg et al (1963) have made detailed spectroscopic investigations of a helium hollow cathode discharge and report an electron density of about 10^{12} per cm^3 and an electron temperature in the neighbourhood of 0.3 ev. Substitution of these values in the above expression yields

$$\frac{3 \times 10^{-6}}{n^4} < \tau_R(nP) \tag{4.8}$$

as the condition for statistical equilibrium at the n^{th} state.

Lifetimes of states increase towards higher values of n; also for one-electron systems they are proportional to Z^{-4}. Evaluation of the above condition for each level of He II and H indicates that

there may not be statistical equilibrium for n = 3 and also n = 4 for He II. All higher levels would appear to have sufficient time to reach equilibrium before radiating.

This suggests that the sensitivity value at 1026 A may be in error. The effect of non-statistical population for non resonance lines such as He II 1640 and 1215 A is not nearly as serious however as in these cases the errors tend to cancel.

4.4 Consolidated Calibration Results and Discussion

The consolidated calibration results from 3000 to 1000 A are shown graphically in Figure 4.10. They include the data obtained from the carbon arc, the high diffraction order technique and the atomic line intensity method.

The relative spectral sensitivity measurements with the carbon arc standard taken from Table 4.2 are plotted from 3000 to 1900 A. The high order line measurements from Table 4.3 have been normalized to match the carbon arc curve at the long wavelength end and plotted on the same graph. The atomic line intensity measurements from Table 4.4 were normalized so that the sensitivity at 2733 A matched the carbon arc curve and added to the graph.

The overall pattern is very consistent with preliminary estimates of spectrometer response and individual measurements. The blaze wavelength of the grating is seen to be at 2850 A contrary to manufacturer's specification of 1200 A but in agreement with the high diffraction order measurements of section 4.3.2.

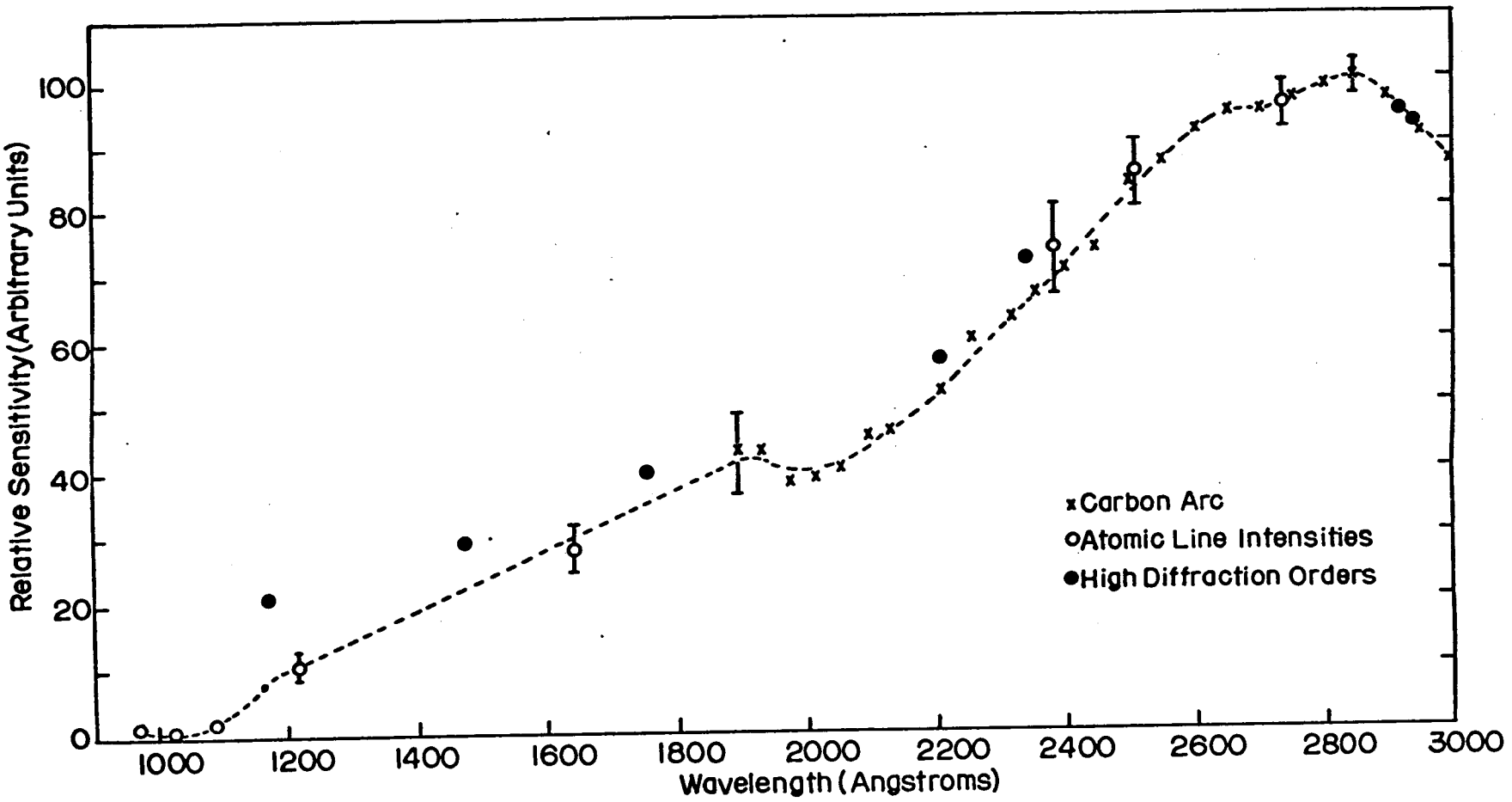

Figure 4·10 Relative Spectral Response of Vacuum Spectrometer

The decrease in spectrometer sensitivity below 2850 A is fairly linear and is well explained by the decrease in grating efficiency below its blaze wavelength. The sharp drop in spectrometer sensitivity below 1200 A is clearly due the decrease in reflectivity of the grating surface which was illustrated in Figure 4.1.

The high order measurements at the shorter wavelengths at first glance appear high, however they really represent an upper limit to the spectrometer sensitivity rather than its actual value since they assume constant grating reflectivity and constant quantum efficiency of the sodium salicylate. The grating reflectivity is actually somewhat lower below 1800 A than above 2000 A, and the sodium salicylate coating on the photomultiplier was approximately one month old at the time of the calibration measurements hence its efficiency undoubtedly was decreased at wavelengths below about 1600 A.

To investigate this point further, similar calibration measurements were made using a new sodium salicylate coating. The spectrometer sensitivity, relative to that at 2733 A, was increased by about 100% at 1085 and 1215 A and by 40% at 1640 A. Thus the high diffraction order measurements shown in Figure 4.10 really approximate the spectrometer sensitivity curve one would obtain when using a new sodium salicylate coating on the photomultiplier.

While the calibration curve of spectrometer sensitivity covers the spectral range from 3000 to 1000 A, it has its limitations and these must be recognized. The carbon arc data from 3000 to 2500 A are certainly accurate to within a few percent; the data from 2500

to 1900 A however is limited by the accuracy of the spectral radiances of the carbon arc measured by Johnson (1956). His estimate of possible error was $\pm$ 20%.

The calibration points at 1215 A and 1640 A could well be in error by 10 - 20%, in view of the inherent difficulties discussed in section 4.3.4. These were the only calibration points between 1900 and 1085 A. The fact that they lie in a reasonably straight line suggests that the spectrometer sensitivity is decreasing approximately linearly with wavelength in that region but it does not preclude the possibility of irregularities such as the one at 1900 A.

The relative sensitivity of the spectrometer down to perhaps 1600 A should be constant with time; below that wavelength the sensitivity is partially determined by the age and condition of the sodium salicylate surface on the detector. Hence when the instrument is used for measuring spectral intensities a calibration must be made at the same time to be applicable.

CHAPTER V

INTENSITY MEASUREMENTS

5.1 Introduction

This chapter begins with a discussion of some theoretical considerations in interpretation of band intensities and factors determining band intensities. The experimental methods used in determining relative band intensities of the LBH system are described and the band intensities obtained are tabulated.

These results are treated to determine properties of the electronic transition moment and of the discharge used to excite the LBH system. The intensities are discussed in relation to other information available on the LBH system.

5.2 Theory

5.2.1 Band Structure of the LBH system

It is necessary before discussing band intensities to investigate some details of the band structure of the LBH system, particularly as it is a forbidden transition and is a combination of magnetic dipole and electric quadrupole transitions. The LBH system was the first molecular band system observed which contains an electric quadrupole electronic transition. Douglas and Rao (1958) have since observed a similar band system of P_2.

The selection rule $\Delta J = 0, \pm 1$ holds for both magnetic dipole and electric quadrupole radiations. There are thus P, Q and R branches observed, typical of $^1\Pi - {}^1\Sigma$ transitions.

Evaluation of the Hönl-London line strength factors indicates that the intensities of the corresponding rotational lines of the three branches P, Q and R are in the ratio J', $2J' + 1$ and $J' + 1$ where J' is the quantum number of the upper rotational level. That is, in general the R branch lines are slightly stronger than those of the P branch, and the Q branch lines are about the same intensity as the P and R branch lines combined. There is of course a temperature dependence of these intensities but this effect only slightly changes the relative branch intensities.

In addition to these three branches, the selection rule $\Delta J = \pm 2$ holds for electric quadrupole radiation thus it is of interest to determine the relative intensities of the S and O branches arising from these transitions.

Electric quadrupole transitions in molecular spectra are very rare and hence very little theoretical work has been done. Quadrupole matrix elements have been evaluated by James and Coolidge (1938) for the infrared rotation vibration bands of OH and these show that the S branch intensity is about 1.5 times the intensity of either the O branch or the Q branch.

A microphotometer tracing of the (2, 0) LBH band at 1384 A in absorption is shown in Figure 5.1. This was obtained by Wilkinson and Mulliken (1957) with a 21 ft. concave grating spectrograph in fourth order with a reciprocal dispersion of 0.3 A/mm and shows the

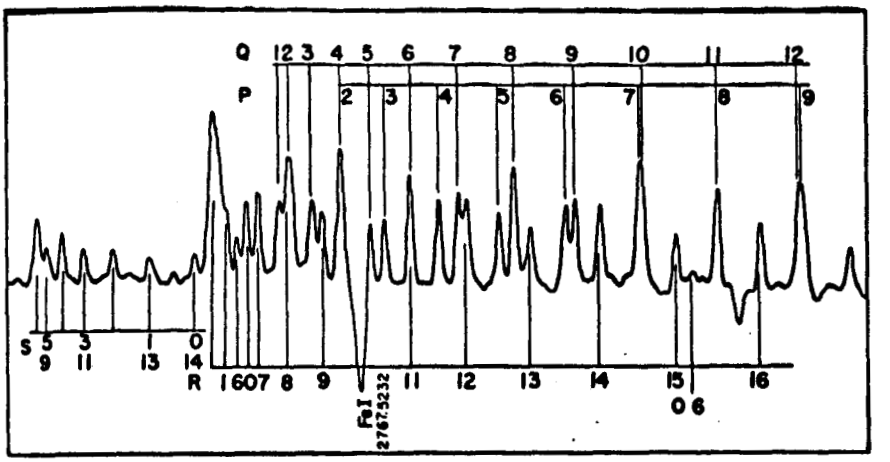

Figure 5.1 Microphotometer Tracing of the (2, 0) Absorption Band in the LBH System (Wilkinson and Mulliken (1957)).

branch structure in detail. Lines of all five branches are observed. The S and O branches are electric quadrupole transitions only while the P, Q and R branches are combined magnetic dipole and electric quadrupole transitions. By Comparing the observed intensity of the S branch with that of the Q branch Wilkinson (1961) has estimated that the electric quadrupole contribution to the total band intensity is about 13%.

5.2.2 Integrated Band Intensities

We can now consider integrated band intensities. The factors determining the intensity of a molecular band (v', v'') in emission and an expression for the intensity $I_{v'v''}$ in terms of these factors have been discussed by several writers [e.g. Herzberg (1950), Chamberlain (1961), Nicholls (1964a)] . These discussions refer specifically to electric dipole transitions so it is necessary to review the basic concepts briefly and apply them to transitions such as those of the LBH system.

The intensity of a molecular band, defined as the energy emitted per second by the transition $v' \rightarrow v''$ is given by

$$I_{v'v''} = N_{v'} h\nu A_{v'v''} . \qquad (5.1)$$

Here $N_{v'}$ is the number of molecules in the upper state, $h\nu$ is the energy of the radiated quantum and $A_{v'v''}$ is the Einstein A coefficient, the probability of spontaneous transition from state v' to v''.

The transition probability $A_{v'v''}$ may be expressed, in an analogous way to atomic transitions (Condon and Shortley (1935)) as

$$A^{E}_{v'v''} = \frac{64\pi^4}{3h} \frac{S^{E}_{v'v''}}{g_{v'} \lambda^{3}_{v'v''}} \quad \text{sec}^{-1} , \qquad (5.2a)$$

$$A^{M}_{v'v''} = \frac{64\pi^4}{3h} \frac{S^{M}_{v'v''}}{g_{v'} \lambda^{3}_{v'v''}} \quad \text{sec}^{-1} , \qquad (5.2b)$$

$$A^{Q}_{v'v''} = \frac{32\pi^6}{5h} \frac{S^{Q}_{v'v''}}{g_{v'} \lambda^{5}_{v'v''}} \quad \text{sec}^{-1} , \qquad (5.2c)$$

for electric dipole, magnetic dipole and electric quadrupole transitions respectively. In these and further equations the superscripts E, M and Q are used to specify these types of transitions while absence of superscripts denotes the general case.

In the above equations $S_{v'v''}$ is the band strength, $g_{v'}$ is the statistical weight of the upper level and $\lambda_{v'v''}$ is the wavelength of the emitted photon.

The band strength in the general case is defined as

$$S_{v'v''} = \left| \int \psi_{v'} R_e(r) \psi_{v''} dr \right|^2 , \qquad (5.3)$$

where $\psi_{v'}$ and $\psi_{v''}$ are the vibrational wave functions of the v' and v'' levels and r is the internuclear separation.

$R_e(r)$ is the electronic transition moment of the band system and is defined as follows for the three types of transitions:

$$R_e^E(r) = \int \psi^*_{e\,v'} \; P_e \; \psi_{e\,v''} \; d\tau \tag{5.4a}$$

$$R_e^M(r) = \int \psi_e^*{}_{v'} \; M \; \psi_{e\,v''} \; d\tau \tag{5.4b}$$

$$R_e^Q(r) = \int \psi_e^*{}_{v'} \; R \; \psi_{e\,v''} \; d\tau \tag{5.4c}$$

$\psi_{e\,v'}$ and $\psi_{e\,v''}$ are the molecular electronic wave functions and $d\tau$ is the element of configuration space. P_e, M and R are the electric dipole, magnetic dipole and electric quadrupole moments respectively.

The electronic transition moment R_e is usually a slowly varying function of r and if it has the same dependence on r for all bands being considered it can be expressed (Fraser (1954)) as $R_e(\bar{r}_{v'v''})$ where $\bar{r}_{v'v''}$, the r-centroid, is the mean internuclear distance involved in the transition and may be computed by

$$\bar{r}_{v'v''} = \int \psi_{v'} \; r \; \psi_{v''} \, dr \; / \int \psi_{v'} \; \psi_{v''} \; dr \; . \tag{5.5}$$

Thus from equation 5.3, the band strength may be written as

$$S_{v'v''} = R_e{}^2 \; (\bar{r}_{v'v''}) \; q_{v'v''} \; , \tag{5.6}$$

where

$$q_{v'v''} = \left| \int \psi_{v'} \; \psi_{v''} \; dr \right|^2 \tag{5.7}$$

the vibrational overlap integral square is called the Franck Condon factor of the band.

Thus equation 5.1 may be written, using equations 5.2 and 5.6

$$I^{E}_{v'v''} = C_1 N_{v'} \nu^4_{v'v''} R^{E\,2}_e(\bar{r}_{v'v''}) \quad q_{v'v''} , \tag{5.8a}$$

$$I^{M}_{v'v''} = C_2 N_{v'} \nu^4_{v'v''} R^{M\,2}_e(\bar{r}_{v'v''}) \quad q_{v'v''} , \tag{5.8b}$$

$$I^{Q}_{v'v''} = C_3 N_{v'} \nu^6_{v'v''} R^{Q\,2}_e(\bar{r}_{v'v''}) \quad q_{v'v''} , \tag{5.8c}$$

for the three types of transitions, where C_1, C_2 and C_3 are constants incorporating the constants of equation 5.2.

In the case of the bands of the LBH system their intensities can be written as a sum of equations 5.8b and 5.8c. That is,

$$\begin{aligned} I_{v'v''} &= I^{M}_{v'v''} + I^{Q}_{v'v''} \\ &= K N_{v'} \nu^4_{v'v''} \left[R^{M\,2}_e(\bar{r}_{v'v''}) + \alpha \nu^2 R^{Q\,2}_e(\bar{r}_{v'v''}) \right] q_{v'v''} \end{aligned} \tag{5.9}$$

where K and α are constants.

Inspection of this equation for the total intensity of a band of the LBH system shows that a complication arises due to the electric quadrupole transition moment term. It is necessary to consider its relative importance. As discussed in section 5.2.1 this term contributes some 13% to the total intensity, at the wavelength of the (2, 0) band at 1384 A (72267 cm^{-1}). Assuming for the moment that the dependence of R^{M}_e and R^{Q}_e on internuclear distance are of the same form, the contribution of the quadrupole transitions will vary from 14% at 1300 A to only 6% at 2000 A, due to the effect of the ν^2 term in equation 5.9.

It is thus possible to neglect this small factor and to consider a hypothetical resultant transition moment such that equation 5.9

reduces to

$$I_{v'v''} = K\, N_{v'}\, \nu^4_{v'v''}\, R_e^2\, (\bar{r}_{v'v''})\, q_{v'v''} \qquad (5.10)$$

It must be remembered however that this $R_e^2(\bar{r}_{v'v''})$ contains the two transition moment terms of equation 5.9, and thus is not strictly true. Lacking more knowledge of the quadrupole contribution across the band system however there is nothing to be gained by attempting a more rigorous interpretation.

The greatest influence over the intensity distribution, as seen in equations 5.9 and 5.10, is the Franck-Condon factor, $q_{v'v''}$, which can vary over several orders of magnitude across the band system. In recent years much work has been devoted to the calculation of arrays of these factors for molecular band systems. Most of these calculations have employed Morse potential curves to represent the upper and lower electronic states. More realistic types of potentials such as the Klein-Dunham and Klein-Dunham-Rees potentials are now being used to obtain somewhat more reliable Franck-Condon factors, especially for high vibrational quantum numbers. Franck-Condon factors for a number of electronic band systems of N_2 have recently been calculated using Klein-Dunham-Rees potentials by Zare et al (1965). These Franck-Condon factors for the LBH system are listed in Table 5.1.

While for many purposes relative band intensities themselves are of prime importance, use of equation 5.10 can yield other important information. A plot of $(I/q\,\nu^4)_{v'v''}$ vs $\bar{r}_{v'v''}$ for bands of a v" progression (v' = constant) expresses $N_{v'}\, R_e^2(\bar{r})$ as a function of internuclear separation. Due to the monotonic relation between $\bar{r}_{v'v''}$ and

Table 5.1

Franck-Condon factors for the N_2 Lyman-Birge-Hopfield ($a\ ^1\Pi_g - X\ ^1\Sigma_g^+$) gand system. (*) (Zare et al (1965))

v' / v''	0	1	2	3	4	5	6
0	4.43-2	1.18-1	1.73-1	1.85-1	1.60-1	1.20-1	8.08-2
1	1.51-1	1.90-1	9.44-2	1.15-2	6.67-3	4.75-2	8.52-2
2	2.50-1	8.02-2	3.30-3	7.51-2	9.62-2	4.70-2	4.94-3
3	2.53-1	5.84-4	1.08-1	6.81-2	4.43-4	3.47-2	7.32-2
4	1.73-1	9.22-2	8.41-2	4.39-3	7.81-2	5.51-2	2.37-3
5	8.61-2	1.91-1	3.19-4	9.76-2	3.47-2	9.80-3	6.39-2
6	3.22-2	1.76-1	7.30-2	6.18-2	2.05-2	7.84-2	1.24-2
7	9.17-3	9.93-2	1.73-1	1.17-3	9.90-2	5.16-3	4.47-2
8	1.99-3	3.87-2	1.60-1	9.17-2	2.93-2	5.50-2	5.01-2
9	3.37-4	1.10-2	8.76-2	1.71-1	1.64-2	8.17-2	5.19-3
10	4.75-5	2.33-3	3.23-2	1.38-1	1.25-1	3.08-3	8.54-2
11	5.64-6	3.82-4	8.50-3	6.71-2	1.66-1	5.56-2	4.09-2
12	3.93-7	4.90-5	1.65-3	2.19-2	1.09-1	1.55-1	7.44-3
13	8.72-9	4.29-6	2.37-4	5.03-3	4.45-2	1.46-1	1.09-1
14	2.46-9	1.85-7	2.43-5	8.35-4	1.22-2	7.55-2	1.63-1
15	5.58-10	1.80-8	1.62-6	9.86-5	2.34-3	2.50-2	1.11-1
16	2.66-10	6.22-9	1.17-7	7.93-6	3.17-4	5.62-3	4.52-2
17	2.83-11	5.41-10	1.31-8	5.57-7	3.09-5	8.94-4	1.22-2
18	4.25-11	3.25-10	5.71-10	6.06-8	2.71-6	1.08-4	2.35-3
19	1.42-10	4.86-10	8.40-15	1.68-9	3.47-7	1.27-5	3.66-4
20	3.40-11	1.24-13	1.66-9	6.11-10	4.10-8	2.03-6	5.69-5

(*) The negative number in each entry is the power of ten by which it is multiplied.

$\lambda_{v'v''}$, as discussed by Nicholls (1965), this information is obtained equally well by plotting $(I/q\upsilon^4)_{v'v''}$ against $\lambda_{v'v''}$. A rescaling of the plots for each v' to place them all on the same relative scale will them indicate how $R_e^2(\bar{r})$ changes with $\bar{r}_{v'v''}$ or $\lambda_{v'v''}$. The rescaling factors required to place all the v'' progressions on the same scale provide a measure of the relative populations of the upper vibrational levels $N_{v'}$.

Knowledge of relative populations can provide information on excitation conditions and vibrational temperature in the source while the electronic transition moment values, $R_e(r)$, can be used to calculate relative band strengths $S_{v'v''}$ from equation 5.6.

5.3 Experimental Technique

Much of the preliminary work directed towards the relative intensities of bands of the LBH system has been described in earlier chapters.

The LBH system was excited in the high voltage discharge described in section 3.2. The external spark gap was removed however to obtain a simple AC discharge. This had the advantage that it operated much more stably and thus was better suited to photoelectric measurements. The brightness of the discharge was decreased by about a factor of two when used in this way and while this made it unsatisfactory for photographic work it was still adequately bright for photoelectric measurements. A further advantage in using the source without the spark gap was that the N_2^+ Second Negative system was completely absent and the atomic lines were somewhat subdued.

Voltage was applied to the primary of the high voltage transformer through a variac and an ammeter was placed in the primary circuit. The current was maintained at 3.2 amperes. This gave a voltage of approximately 15000 volts from the secondary of the transformer and this was applied directly to the discharge tube electrodes. Current drawn by the discharge was thus about 23 milliamperes.

Prepurified tank nitrogen was flowed through the discharge tube after passing through a liquid air trap. The flow rate was kept constant and at a low rate to avoid self-absorption of radiation in the discharge or in the spectrometer. The operating pressure in the discharge was approximately 0.3 mm Hg and in the spectrometer 1.5×10^{-3} mm Hg. The discharge was operated several hours before intensity measurements were made, to allow time for impurities to be pumped out and for stabilization of the discharge.

The spectrum was scanned at a rate of 10 A/min from 2150 A to 1200 A. The amplifier sensitivity was changed during the scan over the range of 10^{-9} to 10^{-10} amperes per division deflection of the recorder as required to obtain adequate deflections for both the strong and weak bands of the LBH system.

The slit widths used were 0.1 mm (approximately 0.5 A resolution) so that the smoothed band profiles were obtained with the rotational structure unresolved. The area under each band profile was measured with a planimeter. Some of the extremely weak bands were rescanned using a 0.2 mm slit to obtain greater sensitivity; in these cases an appropriate conversion factor was applied to get the equivalent band area for a 0.1 mm slit.

A total of 4 scans was made over the complete band system, the band areas were measured and the results averaged. These measurements were made during the same period that the spectrometer calibration (described in section 4) was carried out, thus the spectral response of the spectrometer was as given in the graph in Figure 4.10.

The average area of each band was then divided by the relative sensitivity of the spectrometer at that wavelength to give the relative intensity of each band. These intensities were normalized to give an arbitrary value of 100 to the strongest band of the system (the 0-2 band at 1554 A).

The general method used in recording band areas may be inferred from Figure 5.2. This is a photoelectric recording of the LBH system from 1150 A to 2150 A made at a scanning rate of 40 A/min, 4 times the scanning speed used for area measurements. The recording gives a view of the predominant bands of the system. To avoid distortion of relative band intensities only one change of amplifier gain was made during the scan; the central portion of the scan, from 1400 to 1800 A, was covered with only $\frac{1}{2}$ the gain of the regions on either side where the bands were much weaker.

The main bands of the system are identified as well as a number of prominent atomic nitrogen multiplet lines. A rough estimate of the relative band intensities can be obtained by viewing the peak amplitudes of the bands and taking into account the gradual decrease in spectrometer sensitivity toward shorter wavelength; the sensitivity at 1200 A for this particular scan was approximately 1/7 the sensitivity at 2100 A.

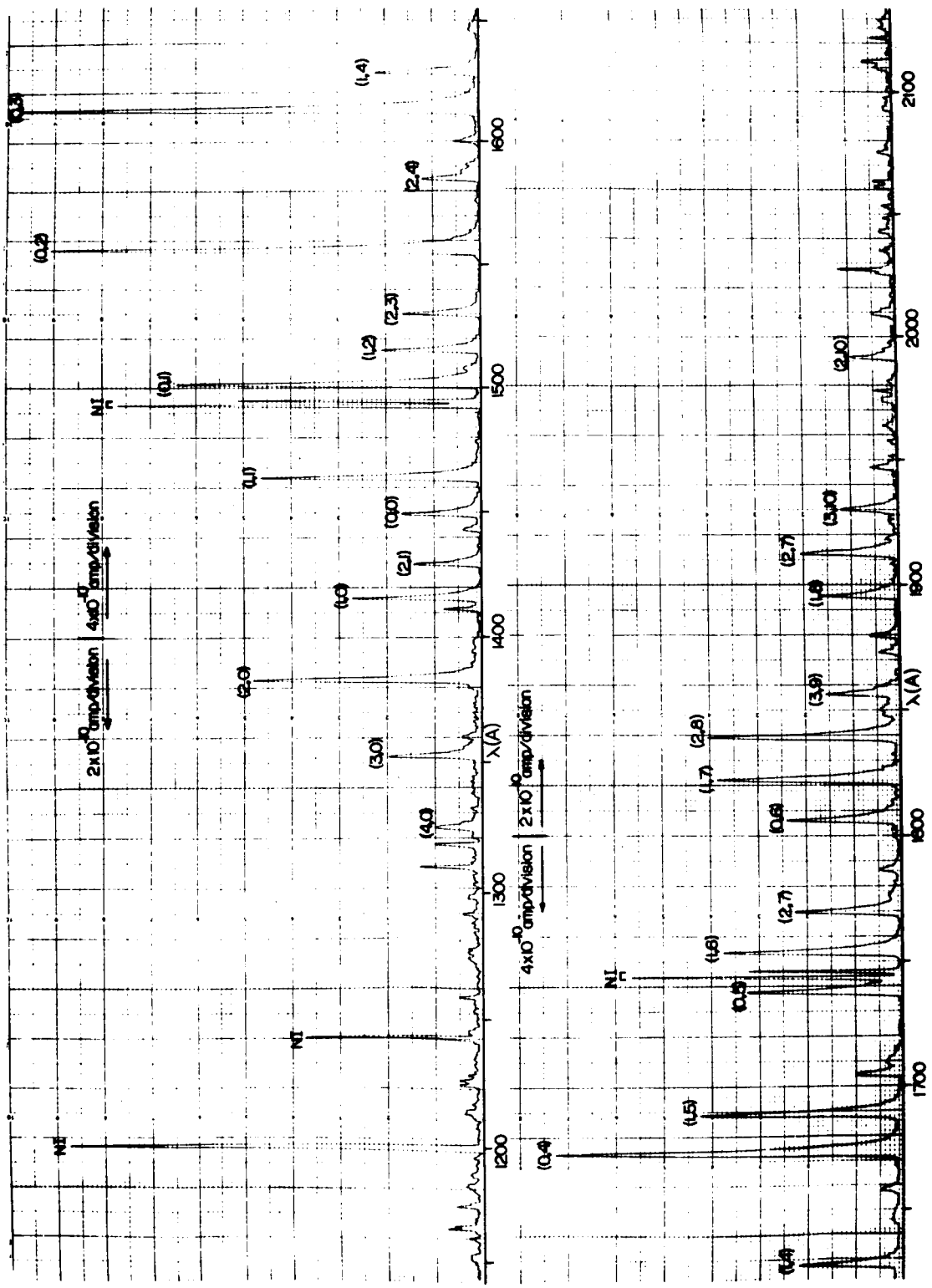

Figure 52 Spectrometer Scan of the Lyman-Birge-Hopfield System of Nitrogen

At a later date the intensities were remeasured to obtain a completely independent measure of relative band intensities. The experimental technique was improved somewhat by two modifications. A Sola constant voltage transformer was used to regulate the line voltage applied to the high voltage supply of the discharge tube, and instead of scanning over the whole LBH band system each v'' progression (v' = constant) was covered separately. That is, all the bands arising from a given upper level were recorded in turn. This was done by scanning over the first band in the progression then manually advancing the grating drive to the wavelength of the next band in that progression and scanning over it, and in this way covering every band in the progression.

These changes gave two advantages. The source was somewhat more stable as minor fluctuations in the voltage were removed, and since a given v'' progression could be covered in 10-15 minutes instead of the two hours required to scan over the complete band system the effect of long term changes in source brightness was much reduced. These scans gave band areas that were consistent to 2-3% for repeated scans with the same operating conditions.

The sodium salicylate surface on the photomultiplier had been renewed some two months prior to the second set of intensity measurements. This coating was inherently a superior one to the previous one, due to a better method of application, but because of aging effects its response below 1500 A was much poorer. The spectral response of the spectrometer was determined using the atomic line

intensity method described in section 4.3.4. The sensitivity above 1600 A was about 10% higher than during the first calibration, but only about $\frac{1}{2}$ the former values at 1215 A and 1085 A.

The band areas were divided by the sensitivity factors obtained by the second calibration and the resulting band intensities were normalized to 100 for the 0-2 band, as in the case of the first set of measurements.

5.4 Results

5.4.1 Relative Band Intensities

The two independent sets of measurements of band intensities obtained as described above for 50 bands of the LBH system were averaged. The results are listed in Table 5.2. These are all the bands of the system that could be measured with any degree of reliability over an intensity range of nearly three orders of magnitude.

A number of bands of reasonable intensity could not be measured due to presence of other features, or overlapping of other bands. Two examples of such bands are the (4,0) band at 1325 A which could not be separated from the (0,12) Birge Hopfield band at 1326 A, and the (4,2) at 1412 A which could not be separated from the stronger NI line at the same wavelength.

A number of bands in the region above 2000 A could be observed weakly but the presence of other features, including some second order NI lines, allowed measurement of only some of them. In general these bands were about two orders of magnitude weaker than the strongest bands of the system and thus do not contribute greatly to the system.

Table 5.2

Relative Band Intensities of the LBH System

v' \ v''	0	1	2	3	4	5	6	7	8	9	10	11	12
0	23.7	72.2	100	92.6	52.9	23.7	6.90	1.83	.31				
1	36.8	62.6	23.7		20.7	34.2	28.7	13.1	4.75	1.22			
2	40.4	20.3		19.4	13.7		6.93	15.3	12.7	6.68	2.75	.60	
3	17.2		5.55			4.86	3.07		2.83	4.99	4.30	1.95	.24
4					1.73						1.25	1.85	
5	3.14	1.24	1.21	.52	1.21		.80					.40	
6	2.27	1.32				.81							

These intensity measurements are considered accurate to within $\pm$20%, the degree of accuracy of the spectral response calibration of the spectrometer, over the full range of wavelengths from 1200 A to 2100 A. The accuracy of relative intensity values at any specific wavelength is naturally considerably better, of the order of $\pm$5%.

5.4.2 Relative Electronic Transition Moment $R_e(r)$

To investigate the variation of the electronic transition moment with internuclear separation, plots of $(I/q\nu^4)_{v'v''}$ vs $\bar{r}_{v'v''}$ were made for each of the four upper levels $v' = 0$ to 3 inclusive. An array of r-centroid values for the LBH system calculated by Nicholls (1964b) was used. This array is given in Table 5.3.

The resulting graphs are shown in Figure 5.3. It is seen that there is no significant variation in $(I/q\nu^4)_{v'v''}$ (which is proportional to $R_e^2(\bar{r}_{v'v''})$) with $\bar{r}_{v'v''}$.

To examine the data more carefully these plots were put on a common scale. This was done by determining an average $(I/q\nu^4)_{v'}$ value for each progression. These averages are proportional to the population factors $N_{v'}$ and it is therefore possible by dividing each $(I/q\nu^4)_{v'v''}$ value by the average for that progression to arrive at relative $\left(\frac{I}{N_{v'}q\nu^4}\right)_{v'v''}$ values with the population factor removed and thus all normalized to the same scale.

The square roots of these quantities, as seen by equation 5.10, are proportional to $R_e(\bar{r}_{v'v''})$, therefore it was advantageous to plot $(I/N_{v'}\, q\nu^4)^{\frac{1}{2}}_{v'v''}$ against $\bar{r}_{v'v''}$ as shown in Figure 5.4. This shows no significant change of $R_e(r)$ with internuclear separation. The degree of scatter of points about the mean value gives an indication

Table 5.3

Calculated r-Centroid Values (A) for the LBH System

(Nicholls (1964b))

v'' \ v'	0	1	2	3	4	5	6
0	1.157	1.141	1.126	1.110	1.096	1.082	1.069
1	1.180	1.163	1.146	1.127	1.123	1.105	1.090
2	1.204	1.185	1.180	1.156	1.138	1.122	1.103
3	1.228	1.244	1.194	1.175	1.133	1.148	1.131
4	1.254	1.237	1.216	1.212	1.184	1.166	1.140
5	1.280	1.261	1.213	1.224	1.203	1.198	1.175
6	1.307	1.287	1.270	1.246	1.237	1.213	1.191
7	1.336	1.314	1.295	1.355	1.255	1.227	1.223
8	1.366	1.343	1.322	1.304	1.277	1.265	1.242
9	1.398	1.373	1.350	1.329	1.319	1.287	1.293
10	1.432	1.405	1.380	1.358	1.338	1.302	1.296
11	1.468	1.439	1.412	1.388	1.366	1.348	1.318
12	1.506	1.475	1.446	1.419	1.395	1.374	1.383

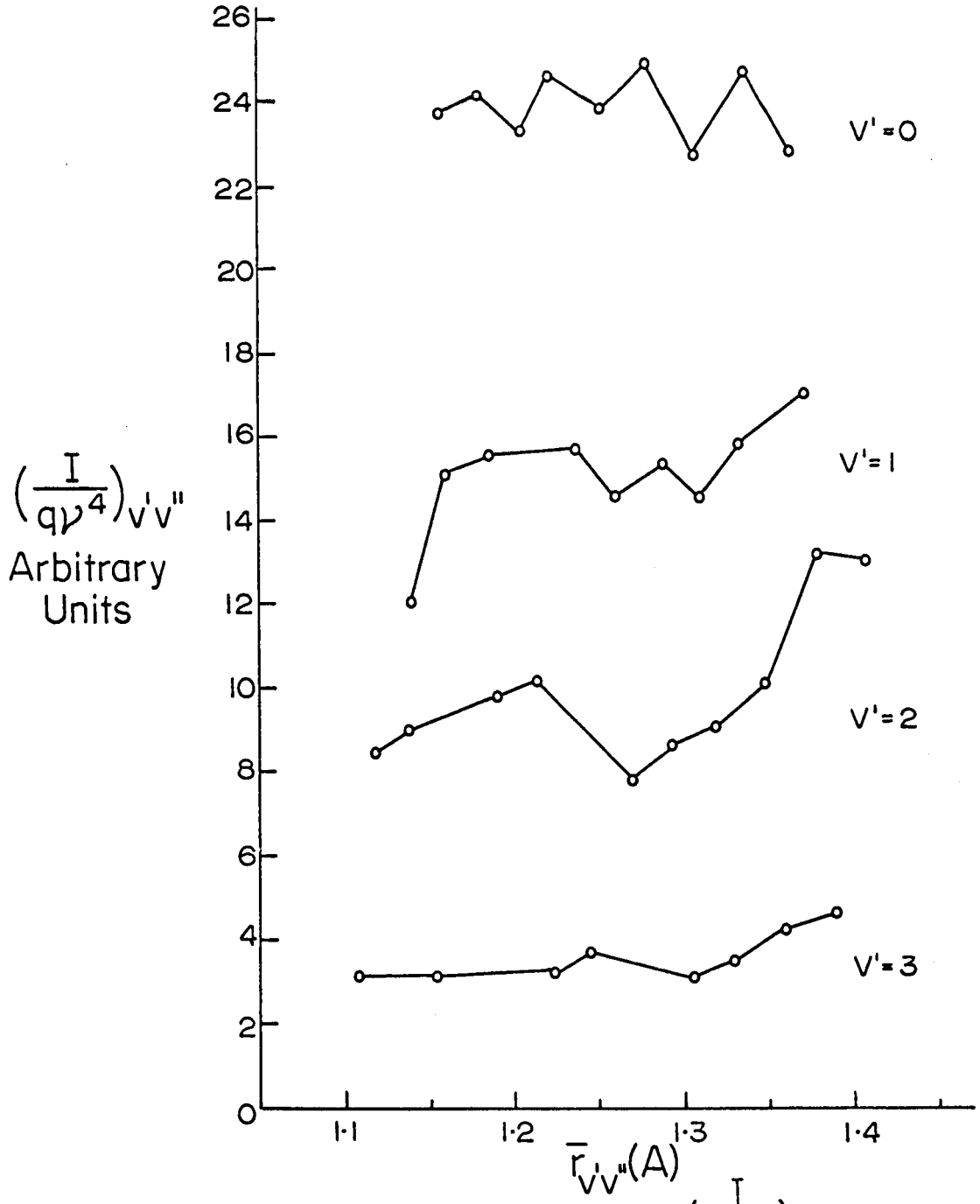

Figure 5·3 The Variation of $\left(\frac{I}{q\nu^4}\right)_{v'v''}$ with $\bar{r}_{v'v''}$ for v' Progressions 0 to 3

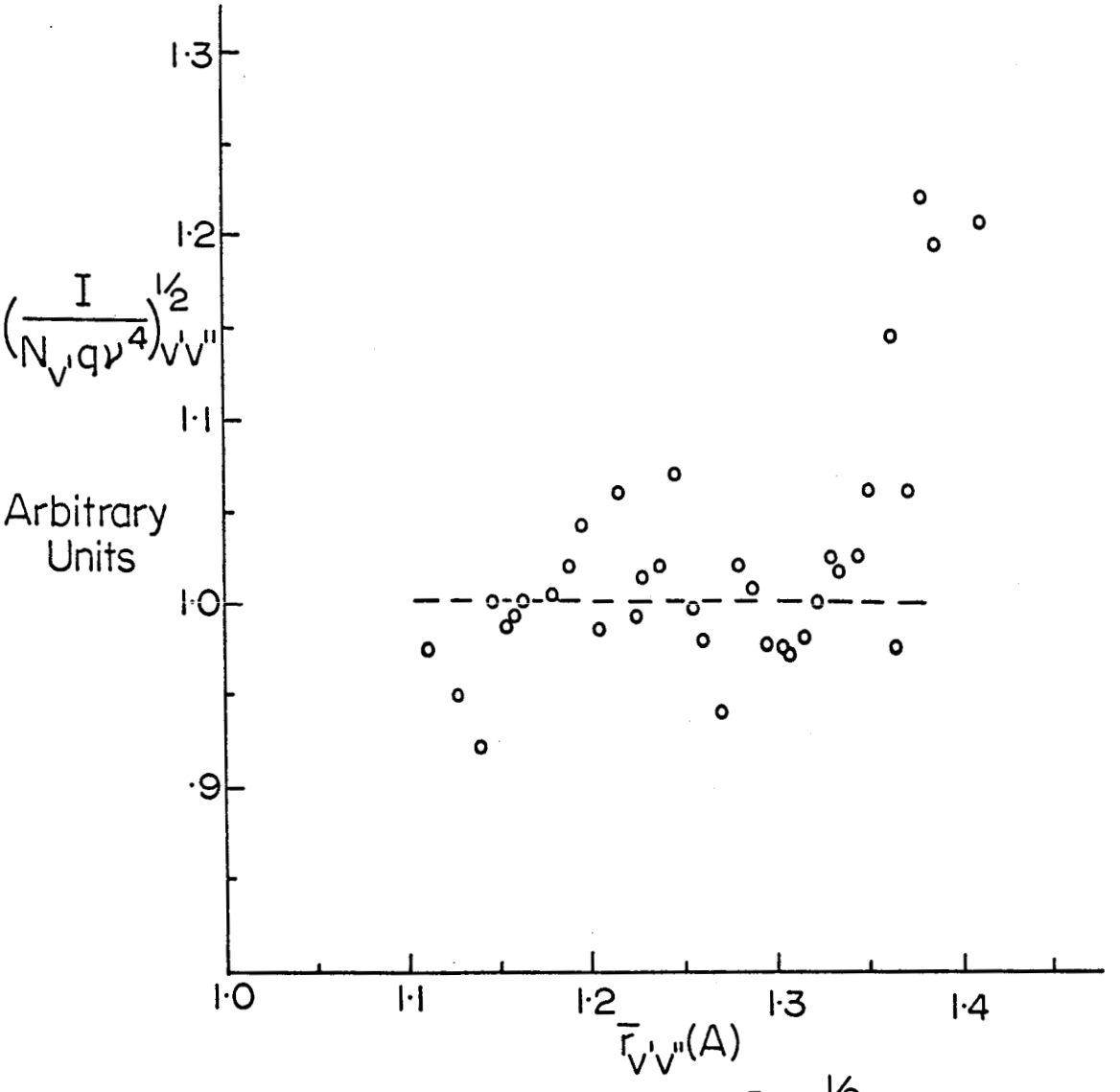

Figure 5·4 The Variation of $\left(\frac{I}{N_{v'}q\nu^4}\right)^{1/2}_{v'v''}$ with $\bar{r}_{v'v''}$

of the combined errors in the measured intensity and Franck Condon factor for each band. The majority of the points lie within 5% of the mean.

The four points lying far off the mean at internuclear separation of about 1.4 A are from the (1,9), (2,10), (2,11) and (3,11) bands all of wavelength in the vicinity of 2000 A. Their intensities are low, as seen in Table 5.2, of the order of 1/50 of that of the strongest bands of the system and it must be concluded that the intensity measurements for these bands are in error perhaps due to contamination by other radiation.

The conclusion drawn from this plot is that $R_e(r)$ is constant across the band system to within the estimated accuracy of the intensity measurements.

5.4.3 Relative Populations of the Upper State

As discussed in the previous section the average $(I/q\nu^4)$ value for each progression (v' = constant) is proportional to the population $N_{v'}$ of that upper level. The relative populations obtained in this way for the first four levels are given in Table 5.4; the relative populations for levels v' = 4, 5 and 6 were estimated from the few band intensities measured with those upper levels.

A semi-log plot of $N_{v'}/N_o$ against the vibrational term values $G(v')$, as shown in Figure 5.5, shows a near Boltzmanndistribution of population. A straight line was fitted by eye to these points and from the measured slope an effective vibrational temperature of 3100 $\pm$ 200 ^oK was determined.

Table 5.4

Relative Populations of Upper State

v'	Relative Population
0	100
1	63
2	38
3	14
4	5.5
5	3.4
6	2.5

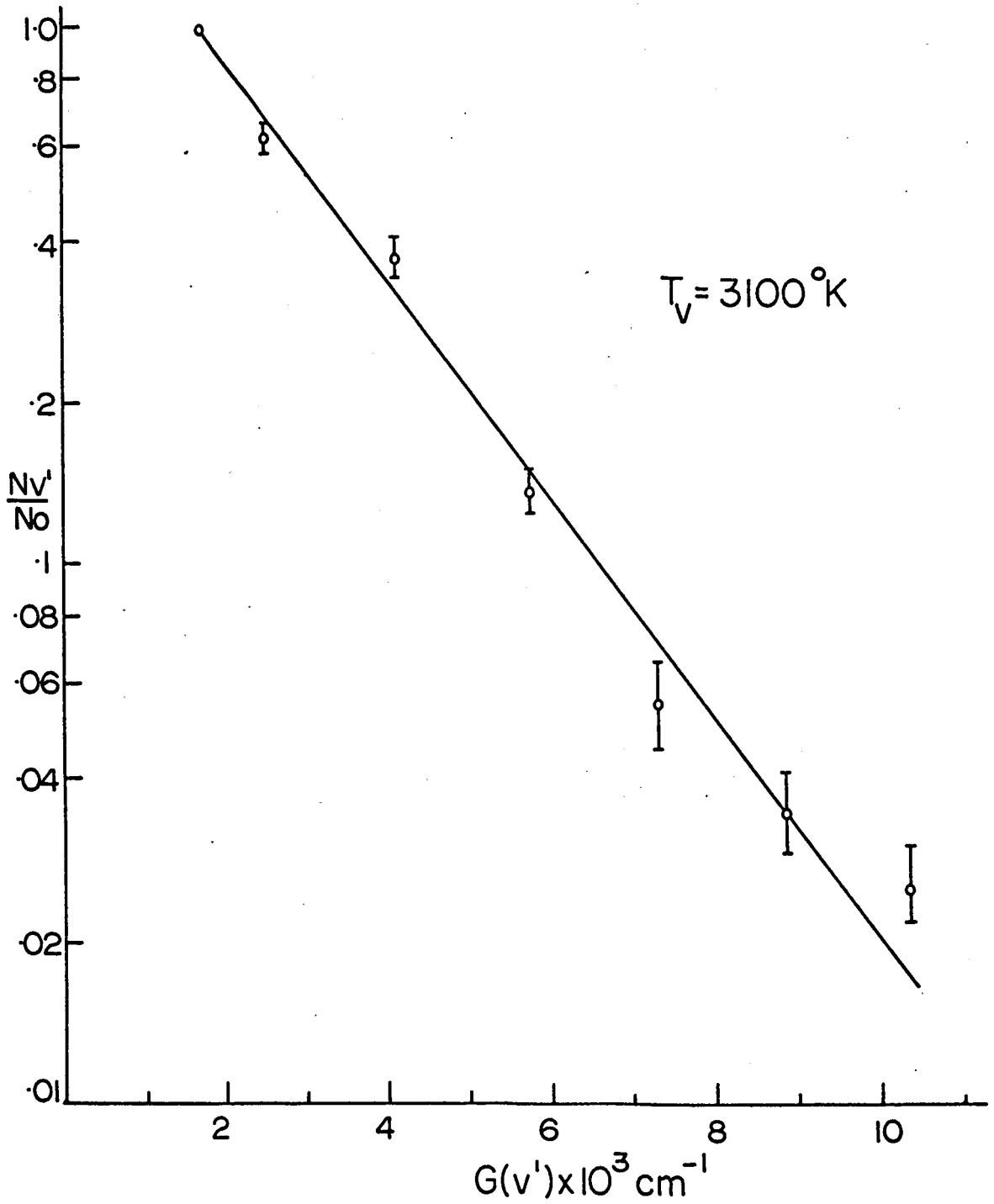

Figure 5·5 Effective Vibrational Temperature of N_2 Discharge

5.5 Discussion of Results

These are the first reliable measurements of intensity of the LBH system in emission. The only data which can be compared with these are the eye estimates of intensity by Birge and Hopfield (1928). A casual inspection of these in relation to the present measurements shows that their intensities at high wavelengths (1800 - 2000 A) are roughly 5 times too large compared with their estimated intensities at shorter wavelengths (1500 - 1300 A). This is easily explained of course by the failure to take into account the rapidly decreasing sensitivity of their spectrograph below 2000 A; the decrease in reflectivity with wavelength of the aluminum surface of their grating itself would account for most of the discrepancy. This is certainly no reflection on their reported intensities; the fact that they have been cited for the past thirty-five years as typical of the LBH system and no better ones were available shows they have served their purpose well. Indeed, by judicious interpretation of them Nicholls (1960) was able to conclude that $R_e(r)$ was probably constant for the system.

Zare et al (1965) have concluded from a study of the N_2 First and Second Positive systems that there is no significant variation of $R_e^2(r)$ for these band systems and that it may be essentially constant for many other band systems. On the hypothesis that $R_e^2(r)$ was constant for the LBH system they have calculated relative intensities expected for the LBH system. In this simplifying case, as may be seen from equation 5.10, the intensity of any band is directly proportional to $q\nu^4$, the product of the Franck Condon factor and the frequency term, aside from population factors.

The present results show there is in fact no measurable variation of $R_e(r)$ across the band system and thus their predicted intensities are in good agreement (within 5% in general) with the band intensities measured in this study.

Observation of some bands of the LBH system in aurora have been reported by Crosswhite et al (1962). These spectra were obtained with a photoelectric spectrometer carried aloft into an aurora by an Aerobee rocket in the only experiment of its kind reported to date.

Because of the significance of this data in relation to the intensities reported in the present study it is of interest to re-examine the rocket data. A copy of one of their spectra (obtained through the courtesy of Mr. W. Fastie, John Hopkins University) is shown in Figure 5.6. It is a photoelectric recording of the auroral spectrum from 1200 A to 3400 A. The sensitivity of the spectrometer below 1800 A was estimated at 1/15 the sensitivity above 1800 A (due to the particular type of detector used). Since no filter was used the spectral features from 1200 to 1700 A appeared also in second order, and to sort out their contribution the observed spectrum from 2400 to 3400 A is sketched in above the spectrum of the first order.

The authors have ascribed the total auroral spectrum in the region 1800 to 2200 A to the LBH system - mainly the $\Delta v = 6$ to $\Delta v = 9$ sequences, and have identified the (6,0), (3,0), (2,0) and (1,0) bands at 1273, 1353, 1383 and 1415 A respectively. They report roughly equal intensities for these four bands of about 30 kilorayleighs (to within a factor of two either way).

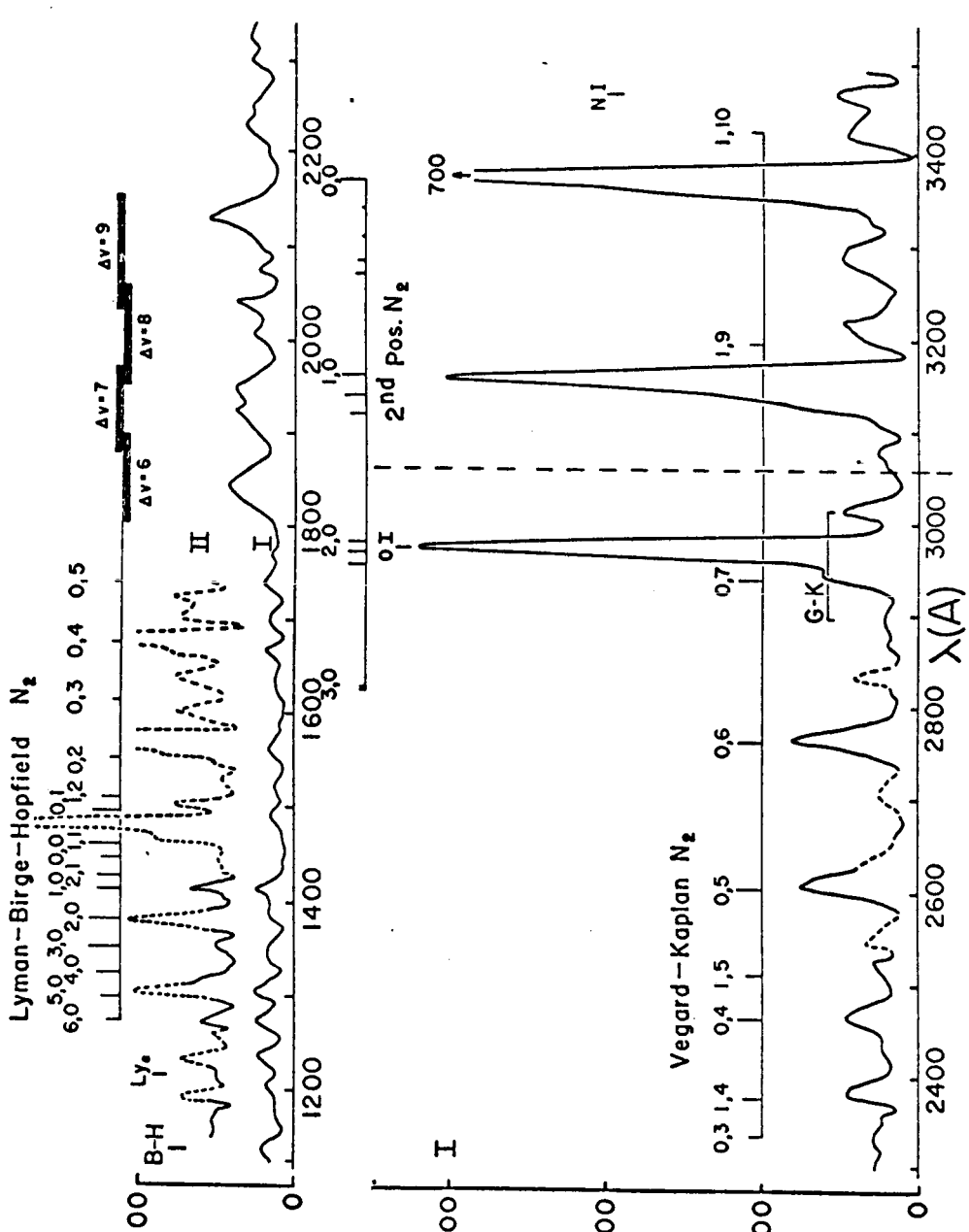

Figure 5·6 Auroral Spectrum in Region 1100-3500A (Courtesy of W·Fastie)

The rayleigh is a unit of photon flux defined as $\frac{10^6}{4\pi}$ quanta/cm^2 sec sterad and must be clearly distinguished from the relative intensity units of energy/cm^2 sec sterad used exclusively in this thesis.

Ground based measurements of auroral brightness at the time indicated that the 3914 A N_2^+ (0,0) band, the strongest band in the visible region, was approximately 10 kr.

The first conclusion drawn, if these intensities are reliable, is that the strongest LBH bands, the (0,2) and (0,3) at 1554 and 1611 A must have been of the order of 100 kr for this aurora. This is 25 times as intense as the 3914 A band, taking into account the difference in energy of quanta at the two wavelengths, and would suggest that the major part of the radiation emitted by the aurora is in the vacuum ultraviolet region.

A more detailed study of the spectrum and reported intensities in relation to the laboratory measurements of relative band intensities of the LBH system suggests that the distribution of populations in the upper state is markedly different from that of the laboratory discharge - a distribution such that the vibrational temperature in the auroral spectrum is greatly in excess of the 3100°K effective vibrational temperature of the laboratory discharge. This however is inconsistent with vibrational temperatures measured in auroral spectra for several other nitrogen band systems; they are in general considerably lower than 3000°K.

Further investigations of the auroral spectrum in the region 1000 - 2000 A are necessary before one can unreservedly accept these two

findings - the very high intensity of the LBH system relative to other N_2 and N_2^+ systems, and the unusually high vibrational temperature.

CHAPTER VI

SUMMARY AND GENERAL DISCUSSION

6.1 Summary

The research described in this thesis has been directed towards the measurement of relative intensities of one of the important band systems of nitrogen, the Lyman-Birge-Hopfield system. Since this band system lies in the vacuum ultraviolet region of the spectrum where there are as yet no completely satisfactory intensity standards a major part of the work of the thesis was the development of instrumentation and the devising of techniques by which intensity calibrations could be carried out.

The first part of this involved the modification of a 3 meter vacuum spectrograph by the addition of a grating drive assembly and an exit slit plate so the instrument could be used as a scanning spectrometer. A photomultiplier mount was built and mounted behind the exit slit. A sodium salicylate surface added to the photomultiplier window provided a detector which was sensitive to ultraviolet radiation of any wavelength. The instrument thus modified was shown to be satisfactory for making intensity measurements and superior to using photographic techniques. A number of spectral sources were designed and built to mount on the entrance flange of the modified spectrograph.

The second main part of the project involved the development and utilization of techniques for calibrating the spectrometer to determine its spectral response as a function of wavelength. The first method investigated was the use of Cerenkov radiation, whose spectral distribution could be calculated, as an intensity standard; this proved fruitless due to the lack of a medium which would transmit the radiation generated.

Three other methods were investigated. The first and simplest was the observation of short wavelength spectral lines in a number of higher diffraction orders and determination of grating efficiency from these; this was shown to be a useful method above 1200 A. Next considered was the use of radiation emitted from a carbon arc, which was of value down to 1900 A when used with some discretion. The most involved method and the one which holds the most promise as an eventual practical solution as a calibration standard was the use of a number of pairs of atomic lines originating from the same excited level and whose relative intensities could be calculated. This permitted calibration points at specific wavelengths through the vacuum region and above.

The combined use of these three techniques provided a reliable spectral response calibration for the spectrometer that covered the spectral region from 3000 to 1000 A.

Prior to proceeding to the third stage of the research project, the measurement of relative band intensities, a photographic survey was made of the LBH system and a number of other band systems in the vacuum ultraviolet region to investigate suitable methods of excitation

and to become familiarized with the band systems. In the course of this work a number of new bands previously unreported were observed in the LBH system and in the CO Fourth Positive system.

Finally, the relative intensities of 50 of the stronger bands of the LBH system were measured using the instrumentation and the calibration techniques developed for the purpose. These represent the first reliable measurements of intensities of spectral features in emission over any extended portion of the vacuum region.

The band intensities measured show that over the band system the electronic transition moment (combined magnetic dipole and electric quadrupole) was constant to within the accuracy of the intensity measurements. The band strengths of the LBH system are therefore directly proportional to the calculated Franck-Condon factors.

6.2 General Discussion

The work described in this thesis was somewhat hampered by the lack of a grating of reasonable quality; the installation of a new grating, recently obtained, with a blaze wavelength at 1500 A and with a MgF_2 coating should increase the sensitivity of the spectrograph by a factor of 10 or more through the vacuum region. This will make the instrument much more useful for both observations and intensity measurements of weaker spectral features than are now observable. This will also facilitate calibration of the instrument, as a number of atomic lines useful for calibration are relatively weak.

The development of usable techniques for calibration purposes means that quantitative measurements of emission band intensities can now be carried out in the vacuum ultraviolet region. There are many band systems of astrophysical importance in this spectral region and undoubtedly intensity measurements will be made on a number of these in the near future.

A number of workers are currently investigating absolute intensity standards in the vacuum region and it is certain that as time goes on more complete and more accurate calibration methods will become available.

With specific reference to the LBH system of N_2, there is now a need for absolute measurements of absorption intensities so that the present relative band strengths can be placed on an absolute scale. The major contribution of the LBH system to the auroral spectrum, as indicated by the limited information available, points out the need for further examination of the vacuum ultraviolet spectrum of the aurora by rocket instrumentation.

BIBLIOGRAPHY

Allen, C.W. 1963. Astrophysical Quantities, 2nd edition (Athlone Press, London).

Allison, R., Burns, J., and Tuzzolino, A.J. 1964. J. Appl. Opt. 1, 727.

Appleyard, E.T.S. 1932. Phys. Rev. 41, 254.

Baer, P. and Meischer, E. 1952. Nature, 169, 581.

Baum, W.A., Johnson, F.S., Oberly, J.J., Rockwood, C.C., Strain, C.V., and Tousey, R. 1946. Phys. Rev. 70, 781.

Bethe, H.A. and Salpeter, E.E. 1957. Hand. der Phys. 35, 88.

Birge, R.T. 1926. Nature, 117, 229.

Birge, R.T. and Hopfield, J.J. 1928. Ap. J. 68, 257.

Boyce, J.C. 1941. Revs. Modern Phys. 13, 1.

Carroll, P.K. 1959. Can. J. Phys. 37, 880.

Chamberlain, J.W. 1961. Physics of the Aurora and Airglow (Academic Press, New York).

Condon, E.U. and Shortley, G.H. 1935. The Theory of Atomic Spectra (Cambridge University Press, London).

Crosswhite, H.M., Zipf, E.C., and Fastie, W.G. 1962. J. Opt. Soc. Am. 52, 643.

Delbecq, C.J. and Pringsheim, P. 1953. J. Chem. Phys. 21, 794.

Deslandres, H. 1888. Comptus Rendus, 106, 842.

Douglas, A.E. 1952. Can. J. Phys. 30, 302.

Douglas, A.E. and Potter, J.G. 1962. J. Appl. Opt. 1, 727.

Douglas, A.E. and Rao, K.S. 1958. Can. J. Phys. 36, 565.

Edlen, B. 1942. Z. Astrophys. 20, 30.

Estey, R.S. 1930. Phys. Rev. 35, 309.

Fellgett, P. 1958. Monthly Not. Roy. Astron. Soc. 118, 224.

Fraser, P.A. 1954. Can. J. Phys. 32, 515.

Greenfield, M.A., Norman, A., Dowdy, A.H., and Kratz, P.M. 1953. J. Opt. Soc. Am. 43, 42.

Griffin, W.G. and McWhirter, R.W.P. 1963. Proceedings of the Conference on Optical Instruments and Techniques, London, 1961 (Wiley and Sons, London).

Hass, G. and Tousey, R. 1959. J. Opt. Soc. Am. 49, 593.

Headrick, L.B. and Fox, G.W. 1930. Phys. Rev. 35, 1033.

Heddle, D.W.O., Jennings, R.E., and Parsons, A.S.L. 1963. J. Opt. Soc. Am. 53, 840.

Herman, R. and Herman, L. 1942. Ann. d'Astrophys. 5, 71.

Herzburg, G. 1946. Phys. Rev. 69, 362.

Herzburg, G. 1950. Spectra of Diatomic Molecules (van Nostrand, New York).

Hinnov, E. 1964. Private communication.

Hinnov, E. and Hofmann, F.W. 1963. J. Opt. Soc. Am. 53, 1259.

Hirschberg, J.G., Hinnov, E., and Hofmann, F.W. 1963. Sixth Int. Conf. on Ionization Phenomena In Gases, Paris.

Hopfield, J.J. 1930. Phys. Rev. 36, 789.

James, H.M. and Coolidge, A.S. 1938. Ap. J. 87, 438.

Jelley, J.V. 1958. Cerenkov Radiation and its Applications (Pergamon Press, London).

Johnson, F.S. 1956. J. Opt. Soc. Am. 46, 103.

Johnson, F.S., Watanabe, K. and Tousey, R. 1951. J. Opt. Soc. Am. 41, 702.

Knapp, R.A. 1964. J. Appl. Opt. 2, 1334.

Knapp, R.A. and Smith, A.M. 1964. J. Appl. Opt. 3, 637.

Kristianpoller, N. 1964. J. Opt. Soc. Am. 54, 1285.

Kristianpoller, N. and Knapp, R.A. 1964. J. Appl. Opt. 3, 915.

Loftus, A. 1956. Can. J. Phys. 34, 780.

Loftus, A. 1960. Spectroscopic Report No. 2, Univ. of Oslo.

Lyman, T. 1906. Ap. J. 23, 181.

Lyman, T. 1911. Ap. J. 38, 98.

Lyman, T. 1928. The Spectroscopy of the Extreme Ultraviolet, 2nd edition (Longmans Green and Co., New York).

Macpherson, H.G. 1940. J. Opt. Soc. Am. 30, 189.

Madden, R.P. 1964. Private communication.

Madden, R.P. and Codling, K. 1964. J. Opt. Soc. Am. 54, 268.

Nadeau, J.S. and Johnston, W.S. 1963. Chemical and Engineering News, April 22, p. 48.

Nicholls, R.W. 1960. Nature, 186, 958.

Nicholls, R.W. 1964a. Ann. Geophys. 20, 144.

Nicholls, R.W. 1964b. Private communication.

Nicholls, R.W. 1965. Proc. Phys. Soc. In press.

Null, M.R. and Lozier, W.W. 1962. J. Opt. Soc. Am. 52, 1156.

Osgood, T.H. 1927. Phys. Rev. 30, 567.

Patterson, D.A. and Vaughan, W.H. 1963. J. Opt. Soc. Am. 53, 851.

Pivovonsky, M. and Nagel, M.R. 1961. Tables of Blackbody Radiation Functions (Macmillan Company, New York).

Price, W.C. 1951. Rep. Prog. Phys. 14, 1.

Pringsheim, P. and Yuster, P. 1950. Phys. Rev. 78, 293.

Read, D.N. 1934. Phys. Rev. 46, 571.

Rich, J.A., Slovacek, R.E., and Studer, F.J. 1953. J. Opt. Soc. Am. 43, 750.

Richardson, D. 1964. Private communication.

Samson, J.A.R. 1964. J. Opt. Soc. Am. 54, 6.

Setlow, R.B. 1948. Phys. Rev. 74, 153.

Schneider, E.G. 1936. Phys. Rev. 79, 341.

Schoen, A.L. and Hodge, E.S. 1950. J. Opt. Soc. Am. 40, 23.

Schumann, V. 1893. Akad. Wiss. Wien. 102, 2A, 994.

Spinks, J.W.T. 1942. Can. J. Res. 20, 1.

Tanaka, Y., Jursa, A.S., and LeBlanc, F. 1957. J. Chem. Phys. 26, 862.

Tanaka, Y., Namioka, T., and Jursa, A.S. 1961. Can. J. Phys. 39, 1138.

Tomboulian, D.H. and Hartman, P.L. 1956. Phys. Rev. 102, 1423.

Tousey, R. 1961. J. Opt. Soc. Am. 51, 384.

Tousey, R. 1962. J. Appl. Opt. 1, 679.

Watanabe, K. and Inn, E.C.Y. 1953. J. Opt. Soc. Am. 43, 32.

Watson, W.W. and Kuntz, P.G. 1934. Phys. Rev. 46, 32.

Wilkinson, P.G. 1956. Can. J. Phys. 34, 250.

Wilkinson, P.G. 1957. Ap. J. 126, 1.

Wilkinson, P.G. 1957a. J. Mol. Spectroscopy 1, 288.

Wilkinson, P.G. 1961. J. Mol. Spectroscopy 6, 1.

Wilkinson, P.G. and Angel, D.W. 1962. J. Opt. Soc. Am. 52, 1120.

Wilkinson, P.G. and Houk, N.B. 1956. J. Chem. Phys. 24, 528.

Wilkinson, P.G. and Mulliken, R.S. 1957. Ap. J. 126, 10.

Zare, R.N., Larsson, E.O., and Berg, R.A. 1965. J. Chem. Phys. In press.

VITA

NAME: Donald James McEwen

BORN: Riverhurst, Saskatchewan, 1930.

EDUCATED:

Public: Boldenhurst School District,
Riverhurst, Saskatchewan,
1935 - 1944.

High: Riverhurst High School,
Riverhurst, Saskatchewan,
1945 - 1947.

University: University of Saskatchewan,
Saskatoon, Saskatchewan,
1949 - 1950, 1952 - 1957.

University of Western Ontario,
London, Ontario,
1961 - 1965.

Courses: Education, Physics,
B.Ed., May, 1954.
B.A., May, 1955.
M.A., November, 1958.

APPOINTMENTS:

Teacher: Davidson School Unit,
1947 - 1948.

Outlook School Unit,
1948 - 1949.

Weyburn School Unit,
1950 - 1952.

Research Associate:	Physics Department, University of Saskatchewan, 1956 - 1958.
Research Officer:	Defence Research Board, 1958 - present.

PUBLICATIONS:

McEwen, D.J. and Montalbetti, R., Parallactic Measurements on Aurorae over Churchill, Canada, Can. J. Phys. 36, 1593 (1958).

Montalbetti, R. and McEwen, D.J., Hydrogen Emissions During the Period November 9-16, 1960, Can. J. Phys. 39, 617 (1961).

Montalbetti, R. and McEwen, D.J., Hydrogen Emissions and Sporadic E Layer Behaviour, J. Phys. Soc. Japan 17, Suppl. A-1, 212 (1962).

PAPERS PRESENTED:

McEwen, D.J. and Montalbetti, R., Upper Atmosphere Temperatures Measured from Auroral Nitrogen Bands, C.A.P. Annual Congress, Saskatoon, June, 1959.

Montalbetti, R. and McEwen, D.J., Studies of Hydrogen Emissions in Aurorae and Airglow, Midwest Cosmic Ray Conference, Iowa City, October, 1959.

McEwen, D.J. and Montalbetti, R., Motion and Form of Auroral Arcs, C.A.P. Annual Congress, Kingston, June, 1960.